UNIVERSIDADE DE LISBOA

Faculdade de Medicina Veterinária

PRELIMINARY INVESTIGATION INTO FIXATION OF THE DISTAL TIBIAL TUBEROSITY IN THE MODIFIED MAQUET PROCEDURE

PEDRO ALEXANDRE PALHAIS ALVES

CONSTITUIÇÃO DO JÚRI

Doutor António José de Almeida Ferreira

Doutor João José Martins Afonso

Doutor Luís Miguel Alves Carreira

ORIENTADOR

Dr. Malcolm Graham Ness

CO-ORIENTADOR

Doutor Luís Miguel Alves Carreira

2014

LISBOA

UNIVERSIDADE DE LISBOA

Faculdade de Medicina Veterinária

PRELIMINARY INVESTIGATION INTO FIXATION OF THE DISTAL TIBIAL TUBEROSITY IN THE MODIFIED MAQUET PROCEDURE

PEDRO ALEXANDRE PALHAIS ALVES

DISSERTAÇÃO DE MESTRADO INTEGRADO EM MEDICINA VETERINÁRIA

CONSTITUIÇÃO DO JÚRI

Doutor António José de Almeida Ferreira

Doutor João José Martins Afonso

Doutor Luís Miguel Alves Carreira

ORIENTADOR

Dr. Malcolm Graham Ness

CO-ORIENTADOR

Doutor Luís Miguel Alves Carreira

2014

LISBOA

To my parents…

Acknowledgements

Firstly, I would like to thank Malcolm Ness, my supervisor, for accepting me as a trainee, for his enthusiasm and dedication towards the profession, for the constant availability and support, and his help and efforts to carry this project out successfully. A mentor and an inspiration, without whom this project would not have happened.

I would also like to thank Prof. Dr. Miguel Carreira, my co-supervisor, for his support and availability throughout the last part of the degree, including his help with this thesis. His attitude, dedication, and professionalism make him an example to follow.

To Orthomed UK Ltd. for supplying the blocks, wires, and staples, without which this study would have been impossible.

To Prof. Dr. Leigh Fleming and the University of Huddersfield for the testing facility, and Mr. Chris Dawson for the assistance with the testing machine.

To the amazing staff at Croft. I cannot be more grateful to Malcolm Ness and Judith Joyce for accepting me as a trainee at Croft, allowing me to be part of the Croft team and have one the most important experiences of my life. To Joanne Jobling for her constant availability and support. To Carol Thompson and the nurse team for their help and support during my stay; their skills, dedication, and professionalism would make many vets blush. To the outstanding vet team for their remarkable help and untiring patience with me, with a special reference to Dani McCready, Mark Gosling, Rieke Hettrick, and Sean Henney.

To Hugo Martins, faculty colleague, co-worker, housemate, and above all, friend, to whom I am truly grateful for all the help and advice before, during, and after my stay in the UK.

To all my friends from FMV. Especially to Nuno Milharadas, Pedro Silveira, and Rafael Gomes, my friends and companions during the course of the degree, for the support during the good and bad times throughout this chapter of my life, I cannot imagine going through it without you by my side.

To all my friends from my hometown Amadora, with a special reference to João Cheira and André Sousa, for their valuable friendship and incessant support for the last decade.

Finally, to my parents, for a humble education and for giving me the opportunities they never had, even with all the obstacles that came up in the way. I am proud of you, I hope to make you proud of me.

Abstract

PRELIMINARY INVESTIGATION INTO FIXATION OF THE DISTAL TIBIAL TUBEROSITY IN THE MODIFIED MAQUET PROCEDURE

Cranial cruciate ligament rupture is one of the most common causes of lameness in the dog, having a significant impact in Veterinary Medicine. From the plethora of available options, it has yet to be found the perfect treatment for this condition. The Modified Maquet Procedure (MMP) for the advancement of the tibial tuberosity (TT) provides a surgical alternative to existing techniques. In the MMP, stabilization of the distal TT is supported by the placement of an orthopaedic staple or orthopaedic wire in a figure-of-eight pattern. In this *in vitro* mechanical study, we tested the behaviour of different types of implants used in the stabilization of the distal TT, when submitted to an acute monotonic unidirectional axial load. Three sizes of wire (0.8, 1.0, 1.2 mm diameter) and two sizes of staple (1.6 mm, 2.0 mm width) were used. A specimen consisted of two rigid foam polyurethane blocks, linked up by an orthopaedic staple or orthopaedic wire in a figure-of-eight pattern. There were 50 samples in total, organized in 10-sample groups according to implant type. Testing was performed in a universal materials testing machine, with each sample submitted to 20 N preload and distracted at 5 mm/min until failure of the construct. The recorded parameters were: displacement at 100 N (D_{100}), 200 N (D_{200}), and failure (D_{FAIL}), load to failure (LTF), stiffness (STIF), yield load (YL), and mode of failure. Mean D_{100} was highest in group 0.8, and no significant differences were shown between groups 1.2, 1.6 and 2.0. The highest mean D_{200} was seen in group 0.8, with no significant differences between groups 1.6 and 2.0. Regarding D_{FAIL}, all groups were significantly different from each other ($p < 0.05$), with group 1.0 showing the highest mean. Results failed to show a significant difference in mean LTF between groups 1.0, 1.6, and 2.0, with the highest values being observed in group 1.2. Mean STIF was highest for the 2.0 group, and no significant differences were seen between groups 0.8, 1.0 and 1.2. Results failed to show a significant difference in mean YL between groups 1.6 and 2.0, with group 1.2 showing the highest YL values. All the specimens failed by knot untwisting in groups 0.8 and 1.0, and by block breakage in the remaining groups. Based on our results the 2.0 width orthopaedic staple proved to be the most advantageous option. Given the poorer performance we would not recommend using the 0.8 mm and 1.0 mm wire.

Keywords: Orthopaedic wire, Orthopaedic staple, Modified Maquet Procedure, fixation, mechanical testing.

Resumo

ESTUDO PRELIMINAR SOBRE A FIXAÇÃO DA TUBEROSIDADE TIBIAL DISTAL NO *MODIFIED MAQUET PROCEDURE*

A ruptura do ligamento cruzado cranial é uma das causas mais frequentes de claudicação em cães, tendo um impacto significativo em Medicina Veterinária. Apesar de haver uma miríade de tratamentos, ainda não há um superior aos restantes. O *Modified Maquet Procedure* (MMP) para o avanço da tuberosidade tibial (TT) é uma alternativa cirúrgica às técnicas já existentes. No MMP utiliza-se arame ortopédico em figura-de-oito ou um agrafo ortopédico como suporte à estabilização da TT distal. Neste estudo mecânico *in vitro*, testou-se o comportamento de diferentes tipos de implantes usados na estabilização da TT distal, quando submetidos a uma carga axial, unidireccional e monotónica. Usou-se arame de três diâmetros diferentes (0.8, 1.0, e 1.2 mm) e agrafos de duas espessuras diferentes (1.6 e 2.0 mm). Cada espécimen foi consituído por dois blocos de poliuretano de espuma rígida unidos por um agrafo ortopédico ou arame ortopédico em figura-de-oito. No total testaram-se 50 amostras, organizadas em grupos de 10, de acordo com o tipo de implante. As amostras foram testadas numa máquina de teste de materiais universal, e cada uma delas submetida a 20 N de pré-carga e a uma velocidade de distracção de 5 mm/min ate colapsarem. Os parâmetros registados foram: deformação aos 100 N (D_{100}), 200 N (D_{200}), e à ruptura (D_{FAIL}), tensão à ruptura (LTF), rigidez (STIF), tensão de limite elástico (YL) e modo de ruptura. D_{100} médio foi mais alto no grupo 0.8, sem se observar diferenças significativas (DF) entre os grupos 1.2, 1.6 e 2.0. No grupo 0.8 observou-se o D_{200} médio mais elevado e ausência de DF entre os grupos 1.6 e 2.0. No que toca ao D_{FAIL}, todos os grupos foram significativamente diferentes ($p < 0.05$), com o grupo 1.0 a obter a média mais alta. Não se registaram DF entre os grupos 1.0, 1.6 e 2.0 no que toca a LTF, tendo o grupo 1.2 a média mais alta. O grupo 2.0 registou a STIF média mais elevada, sem se observar DF entre os grupos 0.8, 1.0 e 1.2. Não se observou DF na YL média entre os grupos 1.6 e 2.0, tendo-se observado os valores mais altos no grupo 1.2. Nos grupos 0.8 e 1.0 todas as amostras colapsaram devido ao desenrolamento do arame. Nos restantes grupos as amostras colapsaram todas por quebra dos blocos. Com base nestes resultados, o agrafo ortopédico com 2.0 mm de espessura parece ser o tipo de implante mais vantajoso. Dada a pior performance das amostras com arame de 0.8 e 1.0 mm de espessura, não se recomenda o seu uso.

Palavras-chave: Arame ortopédico, agrafo ortopédico, *Modified Maquet Procedure*, fixação, teste mecânico.

Table of contents

List of Figures

List of Abbreviations and Symbols

CLB – Caudolateral band

CMB – Craniomedial band

CT – Computed tomography

CTWO – Cranial tibial wedge osteotomy

CaCL – Caudal cruciate ligament

CrCL – Cranial cruciate ligament

D_{100} – Displacement at 100 N

D_{200} – Displacement at 200 N

D_{FAIL} – Displacement at failure

ECM – Extracellular matrix

g/cm^3 – Grams per cubic centimetre

ICN – Intercondylar notch

Kg – Kilogram

LCL – Lateral collateral ligament

LTF – Load to failure

MCL – Medial collateral ligament

MMP – Modified Maquet Procedure

MMT – Modified Maquet technique

MRI – Magnetic resonance imaging

mm – Millimeters

N – Newton

NSAID – Nonsteroidal anti-inflammatory drug

p – p-value

SD – Standard deviation

STIF – Stiffness variable

TPA – Tibial plateau angle

TPLO – Tibial plateau levelling osteotomy

TT – Tibial tuberosity

TTA – Tibial tuberosity advancement

UK – United Kingdom

USA – United States of America

YL – Yield load

YP – Yield point

^{O} – Degrees

Internship report

To fulfill the requirements of the Integrated Masters in Veterinary Medicine from the Faculty of Veterinary Medicine, University of Lisbon, I completed a 6-month training at Croft Veterinary Surgeons A&E Hospital, UK, between 7th October 2013 and 11th April 2014, in a total of approximately 1200 hours.

During that time I was deeply involved in the Hospital's routine, assisting and participating, under supervision, in several procedures englobing different areas of referral and first opinion small animal Veterinary Medicine. Overall I was able to put my knowledge to practice and to develop my clinical case solving skills. In terms of Anaesthesia, I was able to assist and practice procedures such as induction, intubation, and general anaesthetic monitoring. In terms of Surgery, I was able to assist the surgeons during soft-tissue, orthopaedic, and spinal surgeries. Some of these included total ear canal ablation, portosystemic shunt resolution, lung lobectomy, Modified Maquet Procedure for tibial tuberosity advancement, total hip replacement, shoulder arthroscopy, hemilaminectomy, and ventral slot. With respect to Internal Medicine, I was mainly involved in clinical solving and participating in diagnostic tests. I was able to collect blood, catheterize and collect urine, and run several laboratory tests such as haematology, biochemistry, and urinalysis. In terms of Diagnostic Imaging, I was able to assist and practice patient positioning during radiographies and computerized tomography scans. In addition, I assisted the responsible surgeon during ultrasonography, endoscopy and MRI scans. After these procedures I was taught to interpret the results and relate them with the clinical case. I was also able to practice, under supervision of senior surgeons, basic surgical procedures such as castrations (dogs, cats, and rabbits), ovariohisterectomies (cats), and dentistry procedures such as teeth scaling.

In addition, I have participated in other veterinary-related activities. During my stay I attended several in-house lectures given by the senior surgeons, on subjects such as Orthopaedics, Dermatology, and Rabbit Medicine. In the beginning of April 2014 I have also attended all days of the BSAVA congress in Birmingham. Furthermore, I have also attended Orthomed UK's Modified Maquet Procedure course given by Malcolm Ness, being a fundamental starting point for the study from which this thesis resulted.

From February 2014 to April 2014 the study was designed and developed. However, it was only possible to successfully perform the mechanical testing in June 2014.

I. Introduction

Since it was first described in 1926, canine cranial cruciate ligament (CrCL) rupture has been a focus of scientific research and generated a plenitude of literature. Albeit rare in the feline species, CrCL rupture is one of the most common causes of lameness in the dog, therefore, this dissertation shall focus mainly on canine CrCL failure. CrCL rupture has a marked clinical and economic relevance in small animal practice. A decade ago, pet owners in the USA spent approximately 1.32 billion dollars for treatment of this condition (Wilke, Robinson, Evans, Rothschild, & Conzemius, 2005). As research moves forward, the complex physiopathology is gradually clarified and the continuous pursuit for a superior treatment is far from its ending. At the time, proximal tibial osteotomies seem to be the most popular treatment, either by levelling of the tibial plateau or advancement of the tibial tuberosity (TT). Thus far, no technique has proven to surpass the other and further investigation is invariably warranted. The Modified Maquet Procedure is an alternative method of advancing the TT with its origins in human medicine, and offers a different surgical option for veterinary patients. However, the literature on this procedure is but scarce and further research becomes necessary.

1. Cranial cruciate ligament morphology and function

1.1. General anatomy

The canine stifle is a complex condylar synovial joint involving the femur, patella, and tibia (Evans & Lahunta, 2013a). It has two interdependent articulating components, the femoropatellar and femorotibial joints. The space between the convex femoral and tibial articulating surfaces is occupied by two wedge-shaped fibrocartilaginous structures, the medial and lateral menisci. Distally to the patella, within the fibrous layer of the capsule, lies the infrapatellar fat pad (Evans & Lahunta, 2013a). In addition to the patella, there are three more sesamoid bones in the stifle. The lateral and medial fabellae, caudal to the stifle on the lateral and medial femoral condyle, respectively, and a sesamoid in the tendon of origin of the popliteus muscle (Evans & Lahunta, 2013b). The joint capsule of the stifle joint is the largest in the body, forming three intercommunicable sacs: medial and lateral femorotibial, and femoropatellar sacs. The femoropatellar is considerably larger than the femorotibial sacs (Evans & Lahunta, 2013a).

Within each femorotibial sac lies a meniscus. The menisci are developments of the fibrous layer of the joint capsule and are covered by synovial membrane. However, the lateral meniscus has lost his attachment to the joint capsule (Evans & Lahunta, 2013a). Each meniscus is attached to the tibia by a cranial and a caudal meniscotibial ligament, and to each other by the transverse ligament (Fig. 1). The lateral meniscus is connected to the femur by the meniscofemoral ligament (Evans & Lahunta, 2013a). The lateral meniscus is smaller and more circular than the medial one (Pozzi & Cook, 2011). They are semilunar, wedge-shaped fibrocartilaginous discs, with a sharp concave axial, and thick convex abaxial borders (Evans & Lahunta, 2013a). The menisci are highly efficient shock absorbers that contribute to joint stability and stifle kinematics by enhancing congruity between the tibial plateau and the femoral condyles. In addition, by being consecutively submitted to loading-unloading cycles, they induce synovial fluid circulation, promoting joint nutrition and lubrication (Pozzi & Cook, 2011).

Figure 1: Ligaments and menisci of the stifle joint. (Left) Ligaments of the left stifle. (From: Evans, H. E., & Lahunta, A. de. Arthrology. Miller's Anatomy of the Dog, 4th ed., 2013, p 178. Saint Louis: Elsevier Health Sciences). (Right) Dorsal view of the ligaments and menisci of the right stifle. MM, Medial meniscus; LM, lateral meniscus. (From: Kowaleski, M. P., Boudrieau, R. J., & Pozzi, A. Stifle Joint. In Tobias, K. M. & Johnston, S. A., editors: Veterinary Surgery: Small Animal, 2012, p. 907. Saint Louis: Elsevier Saunders.)

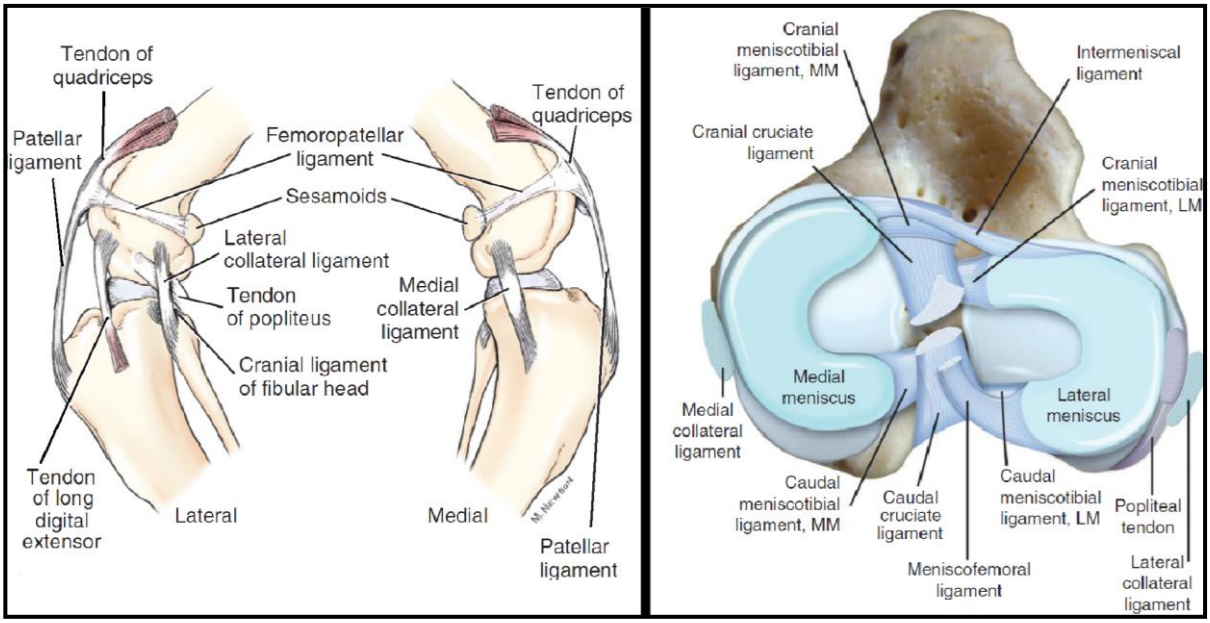

Apart from the meniscal ligaments, there are four other main ligaments in the stifle joint: the medial and lateral collateral ligaments, and the caudal and cranial cruciate ligaments (Fig. 1). However, the portion of the tendon of the quadriceps femoris muscle between the patella and the tibial tuberosity is also commonly referred to as "patellar ligament" (Evans & Lahunta, 2013a). The medial collateral ligament (MCL) is proximally attached to an oval area on the medial epicondyle of the femur and distally to a rectangular area on the medial proximal tibia (Fig. 1). As the MCL passes along the joint capsule it blends with it and fuses with the medial meniscus (Vasseur & Arnoczky, 1981). The lateral collateral ligament (LCL) attaches proximally to an oval area on the lateral femoral epicondyle, courses caudodistally, and inserts on the fibular head (Fig. 1). The LCL has a superficial band that arises from the lateral femorofabellar ligament area, merges with the major component as it crosses the joint surface, and dispersedly inserts on the fascia of the *fibularis longus* muscle. Contrarily to what happens on the medial side of the joint, the LCL is loosely attached to the joint capsule and does not fuse with the lateral meniscus (Vasseur & Arnoczky, 1981).

The caudal cruciate ligament (CaCL) is attached proximally to a fossa in the ventral aspect of the lateral side of the medial femoral condyle, courses caudodistally, and inserts on the medial aspect of the popliteal notch (Fig. 1). It has two components that function independently of one another in flexion and extension, the cranial and caudal bands. Although it is not attached to the menisci, in some cases its femoral attachment may contain fibers of the femoromeniscal ligament (Arnoczky & Marshall, 1977). The CaCL crosses the CrCL medially at their proximal ends in the intercondylar fossa, and is slightly longer and broader than the CrCL (Arnoczky & Marshall, 1977; Heffron & Campbell, 1978; Evans & Lahunta, 2013a).

The CrCL is attached proximally to a fossa on the caudal portion of the medial side of the lateral femoral condyle, courses cranio-medio-distally, and attaches distally on the cranial intercondyloid area of the tibia, caudally to the cranial meniscotibial ligament of the medial meniscus and cranially to the cranial meniscotibial ligament of the lateral meniscus (Fig. 1; Arnoczky & Marshall, 1977; Heffron & Campbell, 1978). Due to the orientation of its femoral and tibial attachments it also presents a proximal-to-distal outward spiral of approximately 90 degrees (Arnoczky & Marshall, 1977). The CrCL has two components, the craniomedial (CMB) and caudolateral (CLB) bands, which are more individualized than those of the CaCL, and named according to their relative tibial attachment (Arnoczky & Marshall, 1977; Heffron & Campbell, 1978). The CLB is shorter and straighter than the spiral CMB (Heffron & Campbell, 1978). The CrCL has its narrowest portion at its middle and fans out

proximally and distally, and its length is directly proportional with body weight (Heffron & Campbell, 1978; Vasseur, Pool, Arnoczky, & Lau, 1985).

1.2. Microanatomy and neurovascular supply

The CrCL is mainly constituted by mostly parallel bundles of longitudinally oriented collagen fibers intercalated with fibroblasts (Heffron & Campbell, 1978). These collagen fibers are organized in sub-fascicles, which, in turn, are organized in fascicles (Yahia & Drouin, 1989). These fascicles have variable diameters as they can be composed of 1 to 10 sub-fascicles (Yahia & Drouin, 1989). Blood vessels, adipocytes, and elastin occupy the space between these subfascicles (Yahia & Drouin, 1989).

The cruciate ligaments are covered by a fold of synovial membrane that incompletely divides the joint in the sagittal plane, being absent only on the surface of contact between CrCL and CaCL (Arnoczky, Rubin, & Marshall, 1979; Vasseur et al., 1985). That synovial membrane is constituted by dense connective tissue and fibroblasts, being more cellular than the rest of the ligaments (Heffron & Campbell, 1978), and has many small holes that are thought to play a role in ligament nutrition (Kobayashi et al., 2006).

The major vascular contribution to the center of the stifle joint occurs from the genicular branches, which arise from the popliteal artery (Evans & Lahunta, 2013c). The blood supply to both cruciate ligaments is predominantly of soft tissue origin (Arnoczky et al., 1979), with the most important sources of vessels being the infrapatellar fat pad and the richly vascularized synovial membranes that ensheat the cruciate ligaments (Arnoczky et al., 1979; Kobayashi et al., 2006). The intraligamentous vessels are less abundant in the central part of the mid portion of both cruciates (Arnoczky et al., 1979; Vasseur et al., 1985). The CaCL appears to be better vascularized than the CrCL, having a greater density of periligamentous and synovial vessels than the CrCL (Tirgari, 1978; Arnoczky et al., 1979).

The main articular nerves of the stifle are the medial articular nerve, which branches from the saphenous nerve, the lateral articular nerve, which branches from the common peroneal nerve, and the caudal articular nerve, which branches directly from the tibial nerve or from one of its muscular branches (O'Connor & Woodbury, 1982). The first is the largest supplier to the stifle joint and the third is sometimes absent in dogs (O'Connor & Woodbury, 1982). There are axons that penetrate the centre of the cruciate ligaments branching from the nerves in the enveloping ligament synovium (Yahia, Newman, & St-Georges, 1992). Within the CrCL

there are proprioceptors and mechanoreceptors that can induce quadriceps and hamstring muscle activity (Yahia et al., 1992; Miyatsu, Atsuta, & Watakabe, 1993). Their number is highest in the proximal third of the ligament (Arcand, Rhalmi, & Rivard, 2000), but there are fewer than in the CaCL (Yahia et al., 1992).

1.3. Functional anatomy

In general, the bulk of the CrCL remains taut in extension and becomes relaxed in flexion, as opposed to the bulk of the CaCL which remains relaxed in extension and becomes taut in flexion (Arnoczky & Marshall, 1977). Each component of a ligament functions independently of the other during flexion and extension (Arnoczky & Marshall, 1977). In extension, the CMB and the CLB of the CrCL are taut; with flexion, the CMB curves and twists around the CLB, and there is a shift in tension from the CLB, which becomes relatively relaxed, to the CMB, which remains taut (Arnoczky & Marshall, 1977; Heffron & Campbell, 1978). With flexion, both the CrCL and the CaCL become twisted, albeit to a lesser extent in the latter (Arnoczky & Marshall, 1977). In the CaCL, the cranial part is loose in extension and becomes taut in flexion, with the opposite occurring on the caudal part (Arnoczky & Marshall, 1977).

1.4. Biomechanics of the cranial cruciate ligament-intact stifle

The stifle allows motion in three planes, which is characterized by a combination of three rotations during the swing phase and a pure flexion-extension motion during the stance phase of gait (Korvick, Pijanowski, & Schaeffer, 1994; Pozzi & Kim, 2011). In Labrador Retrievers, the flexion-extension range-of-motion varies between approximately 160° in full extension and 40° in full flexion (Jaegger, Marcellin-Little, & Levine, 2002; Mostafa, Griffon, Thomas, & Constable, 2010). However, the stifle does not work as a pure hinge joint, as the flexion-extension movement results from a combination of rolling and gliding of the femur on the tibia (Pozzi & Kim, 2011). With flexion, LCL becomes more relaxed and allows the lateral condyle to move further caudally, resulting in internal rotation of the tibia (Vasseur & Arnoczky, 1981). This rotation occurring over a range-of-motion has been named the "screw-home" mechanism (Pozzi & Kim, 2011). Albeit to a much lesser extent, there is also internal-external and varus-valgus rotational movement occurring at the stifle joint during the swing phase of the walking gait (Korvick et al., 1994). Translation motion is absent during the stance phase (Korvick et al., 1994).

Given the peculiar congruence between the femoral condyles and the tibial plateau, the stifle relies on dynamic and passive stabilizers to provide adequate joint stability (Pozzi & Kim, 2011; Hayes, Granger, Langley-Hobbs, & Jeffery, 2013). Dynamic stabilization of the stifle is

mainly provided by the quadriceps, hamstrings, and gastrocnemius muscles (Hayes et al., 2013). It is a result of simultaneous contraction (co-contraction) of different muscles (Pozzi & Kim, 2011). Their activation and accurate coordination is mediated by the nervous system, and is fundamental for joint stability (Miyatsu et al., 1993; Hayes et al., 2013). Passive stabilization is provided by the soft tissues surrounding or within the joint (Pozzi & Kim, 2011). The femorotibial ligaments, the menisci, and the joint capsule all contribute for passive joint stabilization (Pozzi & Kim, 2011; Hayes et al., 2013). The menisci generally act as secondary stabilizers, with their role depending on the integrity of the primary stabilizers, particularly the CrCL (Pozzi et al., 2006). In extension, both bands of the CrCL are in tension and prevent cranial tibial translation relative to the femur (Arnoczky & Marshall, 1977; Heffron & Campbell, 1978). However, the primary restrain against cranial tibial translation is the CMB, with the CLB being the secondary (Arnoczky & Marshall, 1977). The CaCL, on the other hand, is the primary check against caudal tibial translation (Arnoczky & Marshall, 1977). Because they twist on themselves, the CrCL and the CaCL are the primary check against internal rotation of the tibia (Arnoczky & Marshall, 1977; Vasseur & Arnoczky, 1981). However, in extension, work as the secondary restraint, as the MCL and the LCL constitute the primary restraint against internal rotation of the tibia (Vasseur & Arnoczky, 1981). The collateral ligaments are also responsible for prevention of external rotation of the tibia during both extension and flexion (Vasseur & Arnoczky, 1981). The CrCL is also the primary check against hyperextension, with the CaCL being the secondary (Arnoczky & Marshall, 1977). Regarding flexion, the role of the cruciates is not that well defined, but it is believed that they contribute to limiting flexion (Arnoczky & Marshall, 1977). The collateral ligaments are the primary check against varus or valgus angulation, but, should they fail, stability is provided by the cruciate ligaments, as they constitute the secondary restraint against that type of movement (Vasseur & Arnoczky, 1981).

2. Cranial cruciate ligament failure

2.1. Pathogenesis

Failure of the CrCL can occur by avulsion or rupture of the ligament. The former is rare, usually traumatic, and occurs in skeletally immature dogs as a result of the higher strength of the ligament compared with that of the bone itself (Gielen, Saunders, Ryssen, & Bree, 2011; Kowaleski, Boudrieau, & Pozzi, 2012). Acute rupture is also rare and is commonly characterized by tearing of the mid-portion of the ligament secondary to a traumatic event (Kowaleski et al., 2012). The majority of CrCL ruptures occur as a result of chronic degenerative changes within the ligament (Vasseur et al., 1985; Griffon, 2010). These changes include a decrease in ligament fibroblast cellularity, chondroid metaplasia of remaining ligament fibroblasts, loss of the normal architecture of the extracellular matrix (ECM) of collagen, and proliferation of the epiligamentous tissue (Vasseur et al., 1985; Hayashi et al., 2003). In spite of the proliferative epiligamentous repair response, there is no effective spontaneous bridging scar formation (Vasseur et al., 1985; Hayashi et al., 2003). These changes progress with age and are associated with the progressive partial or complete failure of the CrCL (Vasseur et al., 1985; Hayashi et al., 2003).

Despite the plenitude of published studies, the exact aetiopathogenesis of CrCL rupture remains incompletely understood (Cook, 2010; Griffon, 2010; Comerford, Smith, & Hayashi, 2011). It is believed to be influenced by multiple factors that lead to a vicious cycle of abnormal mechanics and abnormal biology, osteoarthritis progression, and overall failure of the stifle joint (Cook, 2010; Griffon, 2010; Comerford et al., 2011). Thus far, it is not known if the cascade of pathological processes is initiated by abnormal biomechanics (leading to biological changes), by abnormal biology (resulting in altered biomechanics), or by a mixture of both, but it is generally agreed that both factors play an important role in the progression of the disease (Cook, 2010; Griffon, 2010; Comerford et al., 2011).

Because antibodies to type I and type II collagen were found in the serum and synovial fluid of dogs with spontaneous CrCL rupture, it has been suggested that there may be an immune-mediated component in CrCL rupture (Niebauer, Wolf, Bashey, & Newton, 1987). However, further studies have showed that the synovial anti-collagen autoantibodies are not specific for CrCL disease and are unlikely to play a role in the initiation of CrCL damage (de Rooster, Cox, & Bree, 2000; de Bruin, de Rooster, van Bree, & Cox, 2007).

Causal factors related to the CrCL itself include cellular apoptosis and ECM metabolism. Some studies have suggested apoptosis may have a role in CrCL rupture rather than being simply a consequence of it (Gyger et al., 2007; Krayer et al., 2008). Comerford and colleagues (2005) observed that higher ECM turnover in the CrCL of dogs predisposed to rupture was related to greater stifle laxity and lower ultimate tensile strength. It has also been suggested that rupture may be influenced by the development of cellular ischemia resulting from the poor CrCL blood supply, particularly in the mid-portion of the ligament (Vasseur et al., 1985; Hayashi et al., 2003).

Hindlimb conformational abnormalities have been a focus of research. Distal femoral conformation has been investigated as a risk factor for CrCL, particularly the intercondylar notch (ICN; Comerford, Tarlton, Avery, Bailey, & Innes, 2006; Lewis, Allen, Henrikson, & Lehenbauer, 2008). It has been observed that dogs with uni or bilateral CrCL rupture have a narrower ICN when compared with normal dogs, and that dogs of high-risk breeds (such as Labrador and Golden Retrievers) have a narrower ICN than dogs of a low-risk breed (Greyhounds; Comerford et al., 2006; Lewis et al., 2008). These findings suggest that the CrCL impingement by the narrower ICN may cause biochemical changes within the ECM of the ligament, leading to a reduced CrCL structural integrity and predisposing it to increased laxity, thus leading to CrCL degeneration (Comerford et al., 2006; Comerford, 2011). Medial patellar luxation, with the associated genu varum and misalignment of the quadriceps mechanism, has been suggested to contribute to CrCL rupture by increasing stress on the ligament (Comerford, 2011). An increased tibial plateau angle (TPA) has also been suggested to predispose to CrCL rupture by leading to higher stresses loading to the ligament (Morris & Lipowitz, 2001). Although Morris and Lipowitz (2001) have observed that dogs with CrCL injuries has significantly greater TPA than normal dogs, the effect of TPA on CrCL is still controversial as further studies have failed to substantiate those findings (Wilke, Conzemius, Besancon, Evans, & Ritter, 2002 ; Reif & Probst, 2003; Guastella, Fox, & Cook, 2008). The angle between the patellar tendon and the tibial plateau as also been suggested to influence CrCL and was found to be marginally greater in stifles affected by partial rupture than in intact joints (Dennler, Kipfer, Tepic, Hassig, & Montavon, 2006; Schwandt et al., 2006). Cranial angulation of the proximal tibia has been described and suggested to be a risk factor for CrCL rupture (Read & Robins, 1982). In a study with Labrador Retrievers, this angulation has been shown to be greater in affected and predisposed (contralateral) limbs than in normal ones (Mostafa, Griffon, Thomas, & Constable, 2009). Inauen, Koch, Bass, and Haessig (2009) have identified TT width as a risk factor for CrCl rupture. In that study they suggested

that smaller TT widths would lead to a larger cranial tibial thrust, resulting in faster CrCL degeneration and therefore rupture in a younger population of dogs. In a study analyzing the morphometric characteristics of Labrador retrievers, Mostafa et al. (2009) observed that cranial angulation of the proximal tibia, excessive TPA, and distal femoral torsion appear more likely to contribute to the pathogenesis of CrCL disease than femoral angulation, increased inclination of the patellar ligament, ICN stenosis, and tibial torsion.

Hayes and colleagues (2013) have used electromyography to compare hamstring reflex of normal and CrCL-deficient dogs. They observed that the response of one of the components of the hamstring reflex is delayed in dogs with naturally occurring CrCL rupture. In dogs with unilateral rupture of the CrCL the response was altered in the contralateral stifle as well, suggesting that a delayed response could be a sign of chronic impairment of the dynamic stabilizers of stifle, which would then predispose to CrCL rupture (Hayes et al., 2013).

Obesity is considered to be a factor implicated in CrCL as higher bodyweight increases the loading forces occurring on the joint and, consequently, the strain on the ligament (Vasseur et al., 1985; Griffon, 2010). In addition, it can exacerbate dynamic imbalance caused by conformational abnormalities (Griffon, 2010). It also appears to exist a link between CrCL rupture and breed or neutering status, with some breeds and neutered dogs (regardless of gender) having a higher prevalence of disease (Whitehair, Vasseur, & Willits, 1993; Witsberger, Villamil, Schultz, Hahn, & Cook, 2008). Epidemiology is further discussed in "I.2.2. Epidemiology". The higher prevalence of CrCL rupture in certain breeds may be due to genetic predisposition. In fact, a study with Newfoundlands has shown a possibly recessive mode of inheritance and heritability of 0.27, suggesting that, in that group, CrCL rupture could be attributed to genetics to a certain extent (Wilke et al., 2006).

2.2. Epidemiology

Rupture of the CrCL can affect dogs of any age or breed, and its prevalence has been increasing since the mid-sixties (Witsberger et al., 2008). Nevertheless, it appears that dogs older than 4 years of age are more likely to be diagnosed with CrCL rupture, with the highest prevalence occurring between 7 and 10 years (Whitehair et al., 1993; Witsberger et al., 2008). In addition, a study has identified Newfoundlands, Rottweilers, and Labrador Retrievers as breeds with higher odds of having CrCL disease (Witsberger et al., 2008). On the contrary, Miniature Dachshunds, Dachshunds, and Greyhounds appear to have a lower risk of suffering from CrCL disease (Witsberger et al., 2008). Whitehair and colleagues (1993) observed

higher prevalence of CrCL rupture in Rottweilers, Newfoundlands, and Staffordshire Terriers; and lower prevalence in Dachshunds, Basset Hounds, and Old English Sheepdogs. It has been shown that Rottweilers have less stifle stability and inferior CrCL structural and material properties than Greyhounds, which may explain to some extent the relative prevalence within each breed (Wingfield, Amis, Stead, & Law, 2000a; Wingfield, Amis, Stead, & Law, 2000b). Heavier dogs are more likely to suffer CrCL rupture, with higher prevalence being observed in patients weighting over 22 Kg (Whitehair et al., 1993; Duval, Budsberg, Flo, & Sammarco, 1999). In addition, Whitehair and colleagues (1993) observed that larger dogs ruptured their CrCL earlier in life, compared with smaller dogs. The results of these studies are consistent with the findings of Vasseur et al. (1985). In that study, they observed that in larger dogs, CrCL degeneration is more severe and has an earlier onset and faster progression. In one study, female dogs had higher prevalence of CrCL rupture than males (Whitehair et al., 1993). Neutered dogs have been shown to be more likely to have CrCL rupture than sexually intact dogs, regardless of gender (Whitehair et al., 1993; Duval et al., 1999; Witsberger et al., 2008). Bilateral rupture may be present on admission in approximately 11% to 17% of cases (Cabrera, Owen, Mueller, & Kass, 2008; Buote, Fusco, & Radasch, 2009). Moreover, in cases with unilateral CrCL loss, contralateral rupture may happen in 22% to 48% of patients (Moore & Read, 1995; de Bruin et al., 2007; Cabrera et al., 2008; Buote et al., 2009).

2.3. Biomechanics of the cranial cruciate ligament-deficient stifle

It is believed that the instability at the CrCL-deficient stifle joint, which translates in an increase in tangential shear forces and abnormal contact mechanics (Pozzi et al., 2006; Anderst & Tashman, 2009), has an important role in osteoarthritis progression (Pozzi & Kim, 2011). It has been shown that dogs with a CrCL-deficient stifle adapt to joint instability by decreasing the load on the affected limb and carrying it more flexed while walking and trotting (Korvick et al., 1994; DeCamp et al., 1996; Tashman, Anderst, Kolowich, Havstad, & Arnoczky, 2004; Ragetly, Griffon, Mostafa, Thomas, & Hsiao-Wecksler, 2010). These adapting mechanisms are believed to be a result of a neuromuscular response to the pain level induced by joint instability (Korvick et al., 1994; DeCamp et al., 1996; Ragetly et al., 2010). The majority of changes occurring after experimental transection of the CrCL are observed during the stance phase (Korvick et al., 1994; Tashman et al., 2004).

In vivo studies have identified that the loss of the CrCL consistently leads to a dramatic increase in cranial tibial translation, which can be of up to 10 mm on average (Korvick et al.,

1994; Tashman et al., 2004). However, tibial translation pattern changes in the long term, with cranial tibial translation decreasing at 2 years post-transection, as a result of a more persistent cranial tibial subluxation throughout the gait cycle rather than a return to normal kinematics (Tashman et al., 2004). Korvick et al. (1994) and Tashman et al. (2004) have suggested that quadriceps contraction is one of several factors that lead to cranial tibial translation during the stance phase. Because the flexion angles during the swing phase do not allow the quadriceps to induce cranial tibial luxation, it also suggested that the swing phase is CrCL-independent (Korvick et al., 1994; Tashman et al., 2004). As the findings of Korvick et al. (1994) and Tashman et al. (2004) are a result of experimental sectioning of the CrCL, Pozzi and Kim (2011) have suggested that cranial tibial translation in clinically occurring CrCL rupture may be less pronounced, as a result of periarticular fibrosis.

The existing concept of tibial instability in the CrCL-deficient stifle has been questioned. In a study by Böttcher and Rey (2010) using biplanar fluoroscopy, during the stance phase, caudal translation of the femur relative to the tibia was observed. In that study, the same motion pattern was observed even in chronic cases with periarticular fibrosis and apparent macroscopical stability. More recently, using uniplanar fluoroscopy, Rey, Fischer, and Böttcher (2014) assessed sagittal motion pattern of CrCL-deficient stifles, and their findings were consistent with those of Böttcher and Rey (2010). They observed that the femoro-tibial motion pattern was consistently characterized by a sudden caudal translation of the femur at early stance phase, with spontaneous repositioning at the end of the stance phase. In addition, no translational movement of the tibia was apparent during the stance phase (Rey et al., 2014). These findings appear to question the pre-existing concept of tibial instability in CrCL-deficient stifles and the validity of previous *in vitro* CrCL rupture models (Rey et al., 2014).

Although it has been shown to occur *in vitro* (Warzee, Dejardin, Arnoczky, & Perry, 2001; Kim, Pozzi, Banks, Conrad, & Lewis, 2009), Tashman and colleagues (2004) have failed to show internal tibial rotation after CrCL loss *in vivo*. They have suggested that gait does not generate internal torques high enough for the CrCL to act as a restraint, and therefore, it would only be the secondary check against that motion after bone geometry, muscle forces, and other soft tissues. In addition, it has been shown that the abduction-adduction range-of-motion is altered after CrCL transection, increasing over the first year and being kept at high values at least until 2 years post-transection (Tashman et al., 2004). In CrCL-deficient stifles, medio-lateral translation was higher only during the first year, suggesting that gradual stabilization was achieved, possibly due to joint capsule thickening and osteophyte formation (Tashman et al., 2004).

2.4. History and clinical signs

In the majority of cases, although patient history is suggestive of trauma, further analysis reveals that the onset of hindlimb lameness is either insidious or occurs after a minor trauma during an everyday activity (Muir, 2011). Lameness in affected dogs is usually more severe following exercise or after periods of rest, and its duration is highly variable (Muir, 2011; Kowaleski et al., 2012). Although it is frequently weight-bearing, its severity usually depends on the extent of ligament disruption (Muir, 2011; Kowaleski et al., 2012). In most cases of complete CrCL rupture, there is a period of several days of non-weight-bearing lameness, followed by moderate to severe weight-bearing lameness (Kowaleski et al., 2012). Stiffness after rest is frequently associated, especially after periods of exercise, and on occasion, audible clicking during walking may be present (Kowaleski et al., 2012). In cases of relatively stable partial tears, lameness is more subtle, commonly bilateral, and more easily identifiable following strenuous activity (Muir, 2011; Kowaleski et al., 2012). In these cases, lameness is generally continuous and relatively refractory to nonsteroidal anti-inflammatory drugs (NSAID; Muir, 2011). Less frequently, patients can be presented with a history of major trauma (e.g. road traffic accident) which is usually associated with traumatic avulsion fracture of a CrCL attachment site (Muir, 2011).

Physical examination of affected dogs typically reveals uni or bilateral weight-bearing hindlimb lameness, stifle pain upon flexion and extension, variable crepitus, and possible audible clicking during walking associated with a meniscal tear (Muir, 2011; Kowaleski et al., 2012). Physical examination is of great importance in cases where bilateral rupture occurs as clinical signs may mimic those of a neurological disease (Muir, 2011). When lameness is bilateral, dogs may also alter their stance by leaning forward, in an attempt to unload the pelvic limbs (Muir, 2011). When unilaterally affected, dogs will present external rotation of the affected limb while sitting (abnormal "sit test") and during walking (Muir, 2011; Kowaleski et al., 2012). In chronic cases, atrophy of pelvic limb musculature is evident, and periarticular fibrosis is most easily palpated on the medial side of the stifle (Muir, 2011; Kowaleski et al., 2012). This medial firm thickness is also referred to as "medial buttress" and is almost always indicative of CrCL rupture (Muir, 2011; Kowaleski et al., 2012). When a partial tear is present, full extension of the stifle usually elicits a pain response (Scavelli, Schrader, Matthiesen, & Skorup, 1990; Kowaleski et al., 2012). Joint effusion is typically found during examination of the stifle and is characterized by loss of definition of the medial and lateral borders of the patellar tendon (Muir, 2011; Kowaleski et al., 2012). In fact, it has

been shown that patellar tendon palpation presents the same sensitivity and specificity than radiography for CrCL disease detection (Carobbi & Ness, 2009).

Cranio-caudal tibiofemoral instability can be tested with the cranial drawer test or the tibial compression test. In the cranial drawer test the operator creates cranio-caudal tibial translation by applying a force to the tibia, while holding the femur stable (Kowaleski et al., 2012). In general, any resulting motion is considered abnormal; however, in immature dogs, a small degree of physiologic cranio-caudal instability of 1-3 millimeters may be present (Muir, 2011; Kowaleski et al., 2012). It is termed "puppy drawer" and is characterized by a sudden stop in tibiofemoral translation during the cranial drawer test, as opposed to the soft or spongy stop occurring with CrCL rupture (Muir, 2011; Kowaleski et al., 2012). Tibiofemoral sagittal instability should be assessed from nearly full extension to flexion (Kowaleski et al., 2012). In full extension the collateral ligaments become taut and partially or completely prevent cranial drawer (Kowaleski et al., 2012). In dogs affected with partial CrCL rupture, cranial drawer could not be elicited in half of the cases and the other half it was usually evident only when the joint was in flexion (Scavelli et al., 1990). When only the CMB is ruptured, cranial drawer is present in flexion only because the CLB is taut in extension; when rupture happened in the CLB, no cranial drawer is present because the CMB is taut throughout the whole range of motion (Arnoczky & Marshall, 1977). If CrCL rupture is suspected but cranial drawer cannot be elicited in a conscious dog even with the stifle in flexion, the test should be repeated under general anaesthesia (Scavelli et al., 1990).

In the tibial compression test (Henderson & Milton, 1978) the operator creates stifle joint compression by flexing and extending the tarsocrural joint, simulating the contraction of the gastrocnemius muscle (Kowaleski et al., 2012). Any cranial motion detected by monitoring the TT is considered abnormal and reflects CrCL impairment (Kowaleski et al., 2012).

While performing these tests, it is important to ensure appropriate placement of the examining fingers on the bony prominences, as failure to do so may allow interpretation of skin and soft tissue movement as tibiofemoral translation (Muir, 2011; Kowaleski et al., 2012). In dogs that are nervous or suffer from chronic arthritis with periarticular fibrosis, it may be particularly important to repeat these tests under sedation or general anaesthesia to ensure that even subtle instability is identified (Muir, 2011). Indeed, it has been shown that the sensitivity and specificity of these testes are far from ideal but greatly increased in anaesthetized patients (Carobbi & Ness, 2009).

2.5. Diagnostic imaging

Radiographic examination of the stifle should be performed in all cases to confirm stifle pathology, to verify osteoarthritis in routine cases, and to discard other differentials such as fracture or neoplasia (Kowaleski et al., 2012). Both stifles should be included for comparison (Vasseur, 2003). Stifle effusion is one of the earliest and most consistent findings, characterized by partial or complete replacement of the infrapatellar fat opacity by a soft tissue opacity in the lateral view (Kowaleski et al., 2012). Usually the fat-to-soft tissue opacity transition occurs at the cranial margin of the tibial condyle and courses proximo-caudally until it reaches the femoral condyle (Fig. 2). Any alteration to these limits is consistent with stifle effusion or infrapatellar fad pad oedema (Kowaleski et al., 2012). Other typical radiographic findings in CrCL disease are consistent with stifle osteoarthritis, including enthesiophytosis, osteophytosis, and subchondral sclerosis, and will depend on its degree (Kowaleski et al., 2012). Tibial compression stress radiography can be used to confirm or discard CrCL damage, particularly when cranial drawer is absent during physical examination (Bree, Rooster, & Gielen, 2011). It consists in performing two lateral views of the stifle in 90° of flexion, one in neutral position (no compression), followed by one while performing the tibial compression test (compression position) (Bree et al., 2011). Similar to what happens with a regular tibial compression test, cranial translation of the tibia in the second radiograph is considered abnormal. This is an easy, reliable, cheap technique that can detect partial and complete ruptures of the CrCL with high sensitivity and perfect specificity (Bree et al., 2011). In young dogs affected by avulsion of the CrCL, radiography may also help identify the avulsed bone fragment (Vasseur, 2003).

Figure 2: Mediolateral radiographic views of a normal stifle (Left) and one with partial rupture of the cranial cruciate ligament (Right). (From: Kowaleski, M. P., Boudrieau, R. J., & Pozzi, A. Stifle Joint. In Tobias, K. M. & Johnston, S. A., editors: Veterinary Surgery: Small Animal, 2012, p. 919. Saint Louis: Elsevier Saunders.)

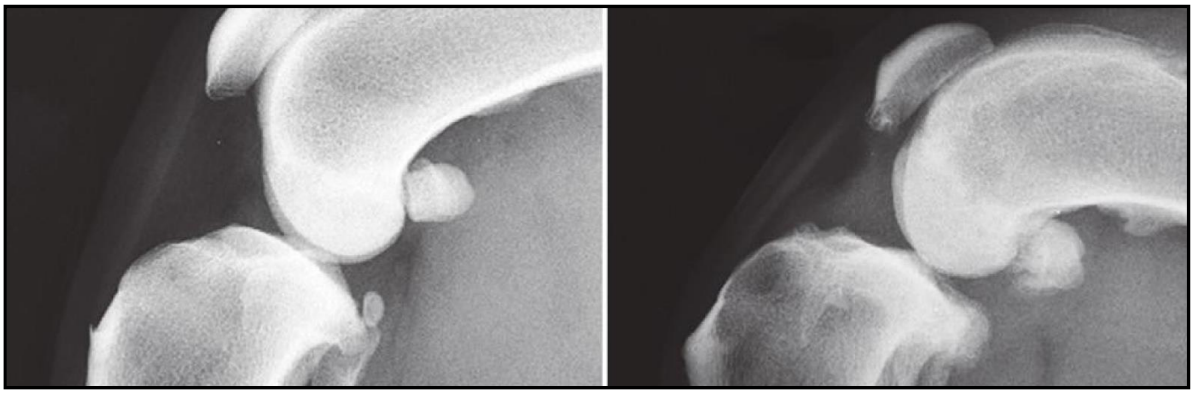

Computed tomography (CT) allows three-dimensional radiographic examination. It appears to be helpful when bone overlapping is to be avoided and detection of small bone fragments is important (Gielen et al., 2011). CT is, therefore, particularly useful for the confirmation and diagnosis of CrCL avulsion in young dogs (Gielen et al., 2011). However, it is not very useful to evaluate integrity of the cruciate ligaments or menisci (Gielen et al., 2011).

Single-plane fluoroscopy has been shown to be a highly repeatable and highly accurate non-invasive method of assessing stifle joint stability (Jones et al., 2014). It allows the analysis of dynamic motions that occur in conscious patients during regular daily activities (Jones et al., 2014). In patients with CrCL rupture, single-plane fluoroscopic analysis shows abnormal cranio-caudal tibiofemoral sagittal instability (Rey et al., 2014). Additionally, it can be used to evaluate the post-surgical stability and, consequently, the efficacy of dynamic stabilizing surgical procedures (Rey et al., 2014; Jones et al., 2014).

Ultrasonography is a reliable non-invasive imaging method that allows evaluation of intra and extra-articular soft tissues structures of the stifle joint (Cook, 2011). It can be particularly useful in the assessment of the menisci, quadriceps and long digital extensor tendons, collateral and patellar ligaments, and for the detection of osteochondritis dissecans and osteoarthritic changes, including joint effusion and synovitis (Gnudi & Bertoni, 2001; Arnault et al., 2009). However, its use as diagnostic method in CrCL rupture is limited, as it has been shown to identify CrCL rupture in approximately 15% to 20% of the cases only (Gnudi & Bertoni, 2001; Arnault et al., 2009). Rupture may be more difficult to identify if it is closer to the midsection or femoral attachment of the ligament (Cook, 2011). If it occurs nearer the tibial attachment it may be easier to identify, with the ligament appearing as a hypoechogenic structure surrounded by echogenic fat (Arnault et al., 2009; Cook, 2011). Effusion is usually mild to severe in acute cases (Cook, 2011). In chronic cases where identification of the ligament is possible, it may appear thickened, irregular, and with retracted rupture ends (Cook, 2011). Interstitial tears can be identified on occasion (Cook, 2011). Usage of ultrasound for the interpretation and diagnosis of stifle conditions is essentially dependent on the training and experience of the operator (Arnault et al., 2009; Cook, 2011).

Although the interest in magnetic resonance imaging (MRI) has been growing in Veterinary Medicine, it has yet to be shown that its cost-benefit ratio is superior to that of other existing diagnostic techniques (Scrivani, 2011). MRI is a non-invasive method that can be used to identify ligament rupture, but it appears to be most useful to diagnose pathologic changes in the menisci, subchondral bone, articular cartilage, or to identify a cause of lameness that may have passed undiagnosed by other methods (Scrivani, 2011).

2.6. Arthroscopy

Arthroscopy is presently considered the gold standard of joint evaluation (Kowaleski et al., 2012). It is a minimally invasive, highly accurate surgical technique with low intra and postoperative morbidity that provides a thorough evaluation and direct probing of the intra-articular structures, allowing the treatment of any existing lesions (Beale & Hulse, 2011; Kowaleski et al., 2012). Magnification of the cruciate ligaments, menisci, synovium, joint pouches, and tibial, femoral, and patellar cartilages allows a more accurate diagnosis of lesions and higher treatment precision (Beale & Hulse, 2011; Kowaleski et al., 2012). Arthroscopy is commonly used in the assessment and treatment of CrCL tears. The findings will depend on the stage of the disease and, in early partial tearing, include loss of the normal fiber pattern, ligament oedema, loss of ligament tension, and tearing of a portion of fibers (Kowaleski et al., 2012). The observed lesions will depend on the stage of the disease, with the proportion of torn fibers and ligament laxity gradually increasing (Kowaleski et al., 2012). In addition, with the progression of the disease, further osteoarthritis lesions can be found, such as synovitis, cartilage fibrillation and eburnation, or osteophytosis (Kowaleski et al., 2012). Arthroscopy is also very useful in the evaluation, diagnosis, and treatment of meniscal tears (Beale & Hulse, 2011; Kowaleski et al., 2012).

Arthroscopy-assisted arthrotomy consists in inserting an arthroscope in an arthrotomy incision. The advantages when compared with normal arthroscopy include the ability to use the arthrotomy incision for the placement of the arthroscopy instruments, a dramatic shortening of the arthroscopy learning curve, and a lesser probability of fluid extravasation within the surrounding soft tissues (Beale & Hulse, 2011). On the other hand, when compared with traditional arthrotomy, arthroscopy-assisted arthrotomy dramatically enhances visibility of the intra-articular structures, precision and accuracy of treatment, decreases pain, and allows an earlier return to function (Beale & Hulse, 2011).

3. Treatment of cranial cruciate ligament rupture

3.1. Conservative management

The main goals of conservative management are to minimize the clinical signs of osteoarthritis (particularly the associated pain), maintain or improve limb use, and, if possible, to slow disease progression (Jaegger & Budsberg, 2011). The use of a multimodal therapy allows a synergic effect of treatment acting in noncompeting modes of action (Jaegger & Budsberg, 2011). Multimodal therapy for the treatment of osteoarthritis incorporates the use of nonsteroidal anti-inflammatory drugs (NSAIDs), weight loss, and exercise modification (Jaegger & Budsberg, 2011; Vasseur, 2003). Other adjunctive analgesics, chondromodulating agents, nutraceuticals, and dietary supplements may also be added to therapy (Jaegger & Budsberg, 2011). In spite of the similar efficacies between different types of NSAIDs, some patients may show a different analgesic or adverse response to a determinate NSAID, thus it may be necessary to change NSAIDs until acceptable analgesia is achieved or the patient experiences an adverse response (Jaegger & Budsberg, 2011). Exercise modification passes by an initial exercise restriction and a controlled increase in activity (Vasseur, 2003). The rehabilitation program may include proprioceptive training, exercises of range-of-motion, and swimming (Vasseur, 2003; Arnoldy, 2011). Conservative management appears to be most suitable for dogs weighing less than 15 to 20 Kg (Pond & Campbell, 1972; Vasseur, 1984). Nevertheless, some authors still recommend surgical management in the majority of cases as a mean to minimize joint instability and disease progression (Vasseur, 1984; Piermattei, Flo, DeCamp, & Brinker, 2006a). Because osteoarthritis appears to have a different clinical impact between different dogs, and each patient responds differently to treatment, it is important to create and adjust the multimodal treatment according to a determinate patient's needs and response to treatment (Jaegger & Budsberg, 2011).

3.2. Surgical management

Numerous treatments have been described for the treatment of stifle joint instability with the aim of resolving the lameness caused by joint instability and provide adequate long-term function of the injured limb (Kim, Pozzi, Kowaleski, & Lewis, 2008). Overall they can be divided in three categories: intra-articular, extracapsular, and tibial osteotomies.

Intra-articular reconstruction of the ligament can be obtained by ligament repair or ligament replacement. Ligament repair by apposition of the free ends of the ligament has been shown

to be a rather unsuccessful technique due to the intrinsic poor healing mechanisms of the ligament and the influence of the constant loads to which it is submitted (O'donoghue, Charles a. Rockwood, Frank, Jack, & Kenyon, 1966). Many techniques for ligament replacement have been described using different types of materials: autografts, allografts, and prosthetics (Manley, 2011). The first surgical procedure for the management of CrCL deficiency was described by Paatsama in 1952 and consists in an intra-articular *fascia lata* autograft placement (Paatsama, 1988). The free end of the lateral fascial strip was passed through bone tunnels drilled in the femur and the tibia to simulate normal CrCL attachments and orientation (Paatsama, 1988). From then on, plenty of intra-articular autograft techniques were described. Dickinson and Nunamaker (1977) described a modification of Paatsama's technique in which only a femoral tunnel was drilled. In 1979, Arnoczky and colleagues described the over-the-top procedure, which consisted in passing the medial third of the patellar tendon proximally through the joint space, passing it over the top of the lateral femoral condyle, and securing it to the tissues on the lateral femoral condyle (Arnoczky, Tarvin, & Marshall, 1982). Later, Hulse, Michaelson, Johnson, and Abdelbaki (1980) described a modification of the over-the-top procedure using an autograft comprised of fascia lata, lateral retinacular fascia and the lateral third of the patellar tendon. Disadvantages of using these autografts include the need to undergo revascularization and the inability to replicate the mechanical properties of the CrCL (Arnoczky et al., 1982; Butler et al., 1983). More recently a study has shown that intra-articular stabilization with an autograft yields inferior results than extracapsular stabilization or levelling of the tibial plateau (Conzemius et al., 2005). In that study, dogs treated with the over-the-top procedure had worse limb function and a reduced chance of achieving a clinically substantial improvement than those treated with lateral suture stabilization or tibial plateau levelling osteotomy (Conzemius et al., 2005). The tissues more frequently used as allografts for CrCL replacement are the common calcaneal tendon and CrCL (Manley, 2011). Their use is not popular as they are associated with an increased immune-directed inflammatory response, difficulty of preservation, sub-optimal mechanical properties, and potential disease transmission (Manley, 2011). Prosthetics are synthetic grafts that can be used as primary replacement for the CrCL or as augmentation device for biologic graft protection, but, in spite of their apparent short-term success, long-term performance is impaired by wear and deterioration (Manley, 2011). Recently, the use of intra-articular scaffolds has gained some interest as they would have the advantage of performing like a prosthesis initially, but gradually allowing and promoting infiltration by soft tissue and undergo neoligamentization (Kowaleski et al., 2012). Despite the variety of intra-

articular techniques, the anatomical configuration and attachments of the CrCL are difficult to replicate with any type of graft, therefore, failure is frequently attributed to the inability to recreate these conditions rather than intrinsic graft mechanical properties (Manley, 2011). Due to the premature biological or mechanical failure of intra-articular grafts, extra-articular techniques are often the first choice of treatment (Manley, 2011).

There is a wide range of extracapsular stabilization techniques for the treatment of CrCL deficiency (Tonks, Lewis, & Pozzi, 2011). Extracapsular techniques are relatively simple procedures that do not require expensive highly technical equipment, and are associated with good outcomes, in terms of safety and efficiency, in CrCL-deficient patients (Cook, 2011). These are passive stabilizing techniques that rely on periarticular fibrosis for long-term stability, therefore, their goal is to provide adequate initial stability until adequate fibrosis is formed (Cook, 2011; Kowaleski et al., 2012). One of these procedures it the fibular head transposition that was first described by Smith and Torg (1985). It relies on the LCL to prevent cranial tibial translation and to minimize internal tibial rotation, by surgically moving the fibular head cranially (Smith & Torg, 1985). This technique appears to have become less popular due to the early and continued joint instability resulting from LCL elongation, and the frequent need for implant removal (Kowaleski et al., 2012). The lateral fabellotibial suture is a modification of the technique described by DeAngelis and Lau and is one of the most frequently used extracapsular procedures (DeAngelis & Lau, 1970; Cook, 2011; Kowaleski et al., 2012). It consists in passing a non-absorbable suture proximally around the lateral fabella and through a tunnel in the proximal tibial methaphysis (Kowaleski et al., 2012). Most of the complications associated with this technique result from failure of the stabilizing material due to inferior mechanical properties, inadequate placement, or fixation failure (Cook, 2011). However, this technique is appears to be superior to the fibular head transposition with regards to joint stability and limb function (Moore & Read, 1995). More recently a minimally invasive modification of the lateral fabellotibial suture has been described (TightRope CCL, Arthrex Inc., Naples, FL, USA) using a synthetic braided tape (FiberTape, Arthrex Inc., Naples, FL, USA) that is passed by a femoral and a tibial tunnel (Cook, Luther, Beetem, Karnes, & Cook, 2010). The tape is kept in place by two toggle buttons in a quasi-isometric position (Cook, Luther, et al., 2010). This technique is a viable alternative associated with good outcomes and a higher safety-to-efficacy ratio than tibial osteotomies (Christopher, Beetem, & Cook, 2013).

In 1984, Slocum and Devine described the cranial tibial wedge osteotomy (CTWO; Slocum & Devine, 1984). It was the first dynamic stabilizing technique to be described, as its main

objective was not to counteract but to eliminate the cranial tibial thrust (Slocum & Devine, 1984). It consists in removing a cranially based bone wedge from the proximal portion of the tibia, followed by apposition of the bone fragments, and stabilization with a medially applied plate according to the principles of internal fixation (Slocum & Devine, 1984; Kowaleski et al., 2012). In 1993, Slocum and Slocum described the tibial plateau levelling osteotomy (TPLO; Kim et al., 2008). The concept was the same as for CTWO, however, in the TPLO, only the tibial plateau was rotated (Kim et al., 2008). Slocum's model of the stifle and TPLO technique will be further discussed in "I.3.3 Tibial Plateau Levelling Osteotomy and Tibial Tuberosity Advancement". More recently, the tibial tuberosity advancement (TTA) was introduced (Montavon, Damur, & Tepic, 2002). Based on Tepic's model of the stifle, the objective of the TTA is to prevent cranial tibial thrust by advancing the tibial tuberosity (Tepic, Damur, & Montavon, 2002; Montavon et al., 2002). Tepic's model of the stifle and TTA technique will be further discussed in "I.3.3 Tibial Plateau Levelling Osteotomy and Tibial Tuberosity Advancement". Other osteotomies have also been developed and include the triple tibial osteotomy, chevron wedge tibial osteotomy, and PTIO (Kim et al., 2008).

At this time, extra-articular techniques are the most popular, however, despite the plenitude of surgical procedures, it is not possible to identify one technique as the superior treatment of CrCL insufficiency; an aspect that invariably reflects the complexity of the structure and function of the stifle joint (Lazar, Berry, Dehaan, Peck, & Correa, 2005; Conzemius et al., 2005; Aragon & Budsberg, 2005; Kim et al., 2008; Boudrieau, 2009; Au et al., 2010; Cook, Luther, et al., 2010; Christopher et al., 2013).

3.3. Tibial Plateau Levelling Osteotomy and Tibial Tuberosity Advancement

Slocum described the cranial tibial thrust as a cranially directed force that resulted from axial compression of the tibia and the slope of the tibial plateau (Slocum & Devine, 1983). According to Slocum's model of joint stability (Fig. 3A), in the absence of the CrCL, there is no restraint to the cranial tibial thrust and cranial translation of the tibia occurs (Slocum & Devine, 1983; Kim et al., 2008). Levelling of the tibial plateau neutralizes the cranial tibial thrust, restoring joint stability (Fig. 3B; Slocum & Devine, 1983; Reif, Hulse, & Hauptman, 2002). In the TPLO, that is achieved by performing a radial osteotomy of the proximal portion of the tibia, followed by rotation of that bone fragment until adequate levelling is achieved, and subsequent medial placement of a TPLO plate according to the principles of internal fixation (Kowaleski et al., 2012). It has been shown *in vitro* that cranial tibial thrust is

eliminated at a TPA of 6.5º, however, *in vivo*, final TPA of 0º to 14º did not seem to bear any relation to postoperative limb function (Warzee et al., 2001; Robinson, Mason, Evans, & Conzemius, 2006). TPLO complication rates vary from 18% to 28%, with cases of simultaneous bilateral surgery showing higher rates; however, most complications do not require surgical treatment (Pacchiana, Morris, Gillings, Jessen, & Lipowitz, 2003; Priddy, Tomlinson, Dodam, & Hornbostel, 2003; Stauffer, Tuttle, Elkins, Wehrenberg, & Character, 2006; Christopher et al., 2013). Some of these complications include tibial or fibular fractures, infection, implant failure, meniscal injury, and patellar swelling.

Figure 3: Slocum's model of the stifle joint. In a normal stifle (A), joint reaction force (magenta arrow) is parallel to the long axis of the tibia and can be divided in two components (yellow arrows): a cranially directed shear force approximately parallel to the tibial plateau (cranial tibial thrust), and a joint compression force perpendicular to the tibial plateau. With levelling of the tibial plateau (B), the cranial tibial thrust is eliminated and the resulting joint reaction force (magenta arrow) only has one component: a joint compression force (yellow arrow). (From: Kim SE, Pozzi A, Kowaleski MP, et al: Tibial osteotomies for cranial cruciate ligament insufficiency in dogs. Vet Surg 37:111, 2008.)

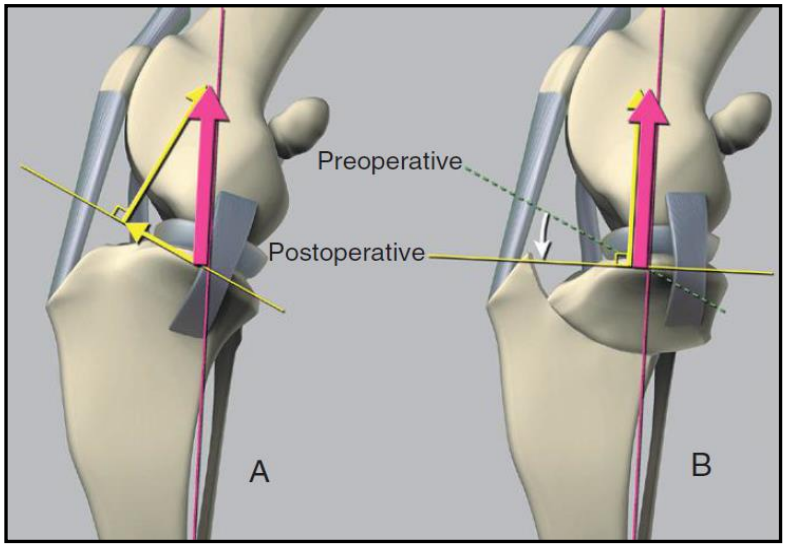

Tepic proposed an alternative model of the stifle (Fig. 4) wherein joint reaction force is parallel to the patellar tendon instead of the tibial axis (Tepic et al., 2002). Therefore, stability is achieved by advancing the TT at least until the angle between the patellar tendon and the tibial plateau reaches 90º (Fig. 4B; Tepic et al., 2002). In the standard TTA technique that is achieved by performing a frontal plane osteotomy of the TT (Lafaver, Miller, Stubbs, Taylor, & Boudrieau, 2007). Position of the TT relative to the tibia is maintained by a titanium cage

(Kyon, Zurich, Switzerland) on the most proximal aspect of the osteotomy gap and by a fork and plate system (Kyon, Zurich, Switzerland) fixating the TT to the tibial diaphysis (Lafaver et al., 2007). The technique's rationale has been validated *in vitro* (Apelt, Kowaleski, & Boudrieau, 2007).

Figure 4: Tepic's model of the stifle joint. In a normal stifle (A), joint reaction force (magenta arrow) is parallel to the patellar tendon and can be divided in two components (yellow arrows): a cranially directed shear force approximately parallel to the tibial plateau (cranial tibial thrust), and a joint compression force perpendicular to the tibial plateau. With advancement of the tibial tuberosity (B), the joint reaction force (magenta arrow) becomes perpendicular to the tibial plateau and the cranial tibial thrust is eliminated. The resulting joint reaction force only has one component: a joint compression force (yellow arrow). (From: Kim SE, Pozzi A, Kowaleski MP, et al: Tibial osteotomies for cranial cruciate ligament insufficiency in dogs. Vet Surg 37:111, 2008.)

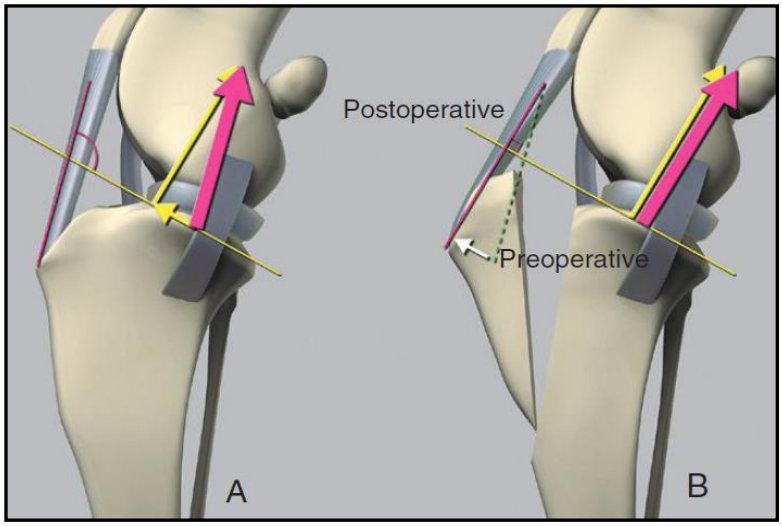

TTA complication rates vary from 20% to 61% (Hoffmann et al., 2006; Lafaver et al., 2007; Stein & Schmoekel, 2008; Christopher et al., 2013). Some of these complications include swelling, meniscal injury, infection, medial patellar luxation, tibial fractures, and implant failure.

Despite the methodical differences, the clinical similarities between TPLO and TTA lead to the suggestion that both would result in a patellar tendon-tibial plateau angle of approximately 90^{o} (Boudrieau, 2009). Later, that hypothesis was supported by a cadaveric study where Drygas and colleagues (2010) observed that TPLO to a TPA of 6^{o} reduced the patellar tendon-tibial plateau angle to approximately 90^{o}, consistent with the recommendations for TTA.

In some cases, there may be advantages or inconveniences of choosing one of these techniques instead of the other. When a low tibial insertion of the patellar tendon is present, TPLO may be more useful than TTA because the need for a smaller plate may leads to worse dispersion of forces throughout the plate and higher risk of TT failure (Boudrieau, 2011). Moreover, the size of the animal or the presence of an excessive TPA may be limitations to TTA because the available range of implant sizes may not be adequate (Boudrieau, 2011). In these cases, the need for a larger advancement of the TT may imply inadequate implant placement, therefore, TPLO may be considered, particularly in the cases with excessive TPA, as it can be combined with CTWO to achieve full correction (Talaat, Kowaleski, & Boudrieau, 2006; Boudrieau, 2011). In addition, TPLO may be more advantageous in cases where angular or torsional limb deformities need to be corrected (Boudrieau, 2011). In these cases, TPLO may exclude the need for a second osteotomy as the orientation of the proximal tibial segment of the tibia may be enough to achieve correction (Boudrieau, 2011). Furthermore, correction of deformities by TTA may warrant an additional plate on the medial side where TTA plate is already fixed, which is far from ideal (Boudrieau, 2011). In cases of patellar luxation, however, TTA may be the best option, as TT transposition may be combined with TTA by slightly overbending the plate (Boudrieau, 2011).

Recently, a study reported TTA and TPLO were associated with high long-term success, with TPLO having fewer complications and a better long-term outcome than TTA (Christopher et al., 2013). Overall both surgeries are comparable, with the election of either treatment usually depending on a patient's idiosyncrasies, and surgeon's experience and personal preference (Kim et al., 2008; Boudrieau, 2011).

3.4. Modified Maquet Procedure

Early in the 1960's, Maquet described a TTA technique for the treatment of human patellofemoral osteoarthritis and patellar chondromalacia (Maquet, 1976). Briefly, the surgery (Maquet, 1976) consists in performing a 150 mm long osteotomy parallel and posterior (7-8 mm) to the TT; followed by placement of a 20-30 mm thick iliac corticocancellous autograft between the TT and the tibial diaphysis, as proximal as possible; and lastly, by filling the created gap with additional iliac cancellous autograft (Fig. 5A). The rationale behind this procedure is that, by advancing the TT, quadriceps extensor mechanism efficiency is increased and quadriceps activation is decreased, ultimately resulting in reduction of the patellofemoral contact forces and stresses responsible for perpetuating the conditions

(Maquet, 1976). Studies have validated the technique's rationale (Maquet, 1979; Shirazi-Adl & Mesfar, 2007) and shown that the procedure consistently provides pain relief (Maquet, 1976; Mendes, Soudry, & Iusim, 1987), but due to the rate and type of complications, relative outcome unpredictability, and alternative treatments, it has become less frequently used (Herrenbruck, Mullen, & Parker, 2001; Fulkerson, 2002).

In 2010, Etchepareborde and colleagues hypothesised that, by keeping the TT distally attached in a standard TTA, it could be able to endure the forces acting on it in the absence of a fixation plate (Kyon, Zurich, Switzerland). A modification of the standard TTA (Lafaver et al., 2007) was designed based on Maquet's technique, and thus, it was named modified Maquet technique (MMT) (Fig. 5B). The MMT can be summarily described as follows (Etchepareborde et al., 2010; Etchepareborde, Brunel, Bollen, & Balligand, 2011). A 3.5 mm hole is drilled perpendicular to the sagittal plane, in a mediolateral direction, caudal to the cranial bone cortex, 10 mm distal to the distal end of the TT. A standard TTA osteotomy is performed so that it ends in the 3.5 mm hole, leaving a cortical bone bridge. A titanium cage (Kyon, Zurich, Switzerland) is fixed in the osteotomy gap after it has been slowly distracted with a spacer. Optionally, a figure-of-eight wire is then placed through the distal portion of the TT and the tibial diaphysis (distal to the 3.5 mm hole) to secure the bone bridge.

Figure 5: Two techniques for advancement of the tibial tuberosity. (A) Illustration of Maquet's technique for TTA. Note the portion of corticocancellous bone advancing the tibial tuberosity. (Modified from: Maquet P. Advancement of the tibial tuberosity. Clin Orthop Relat Res 1976; 115: 225–230). (B) Postoperative radiography of an MMT. Note the hole at the end of the osteotomy and the supporting figure-of-eight wire (From: Etchepareborde S, Barthelemy N, Mills J, et al. Mechanical testing of a modified stabilization method for tibial tuberosity advancement. Vet Comp Orthop Traumatol 2010; 23: 400–405.)

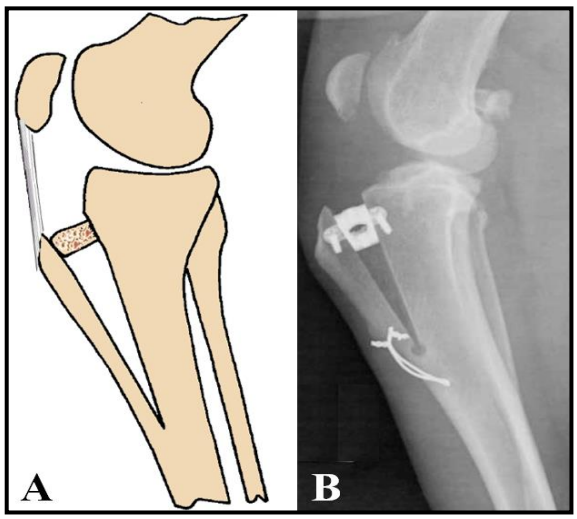

Given that the MMT is a relatively new procedure, it is not surprising that there are few reports available in the literature. The first study describing the technique also compared different methods of supporting the distal TT, highlighting the importance of leaving an intact bone bridge in TT stability, regardless of the addition of orthopaedic wire (Etchepareborde et al., 2010). In 2011, Etchepareborde and colleagues published the first report on the short-term outcome of the MMT. They observed rapid healing with 80% of the cases (16 out of 20) showing complete bone healing and a median lameness score of 0 by 12 weeks. Approximately 17% of the patients developed a subsequent meniscal tear (2 out of the 12 without meniscal tear at surgery), and, in one dog, TT fracture was an incidental radiographic finding. The rationale behind the hole at the end of the osteotomy is that it acts as a stress disperser (Etchepareborde et al., 2010). However, Brunel and colleagues (2013) experienced a significant frequency of intraoperatory bone bridge fissure and fractures, and hence designed an alternative osteotomy in an attempt to prevent that issue. A longer, distally curved osteotomy was developed and tested *in vitro*, and they found that it allowed adequate clinical advancement and resisted acute unidirectional loads of six times the body weight. Later, this osteotomy was used in a cadaveric biomechanical study comparing different types of implants to be placed in the osteotomy gap (Etchepareborde, Barthelemy, Brunel, Claeys, & Balligand, 2014). It was shown that a porous titanium wedge (OrthoFoam^{TM}, Orthomed UK Ltd., Huddersfield, UK) yielded biomechanical advantages over synthetic bone wedges. In 2014, Allan reported a case of feline CrCL rupture treated with an MMT. It was concluded that it is a feasible technique that provides a viable alternative to standard TTA in cats. In fact, he found that the absence of a plate and fork in the MMT is advantageous, because, given the feline poor tibial bone stock for implant, it excludes any problems related with their placement in the TT, namely the accuracy of placement, and the need for concomitant placement of plate and cage ear. More recently, Barthelemy and colleagues (2014) reported the risk factors, complications, and owner satisfaction associated with the MMT in 109 dogs. They observed 27% of complications (9% major, 18% minor) with subsequent meniscal tear being the most frequent major complication, and fracture of the distal tibial bone bridge the most frequent intraoperative and minor postoperative complication. High angle of opening and a drill hole distal to the osteotomy were identified as risk factors for intraoperative TT fracture, being recommended extending the osteotomy distally without drilling a hole. Thin cranio-caudal thickness of the bone bridge was identified as a risk factor for postoperative TT fracture. The overall outcome perceived by the owners was excellent in 82% of the cases and good in 13.1%.

In 2011, the Modified Maquet Procedure (MMP) (Orthomed UK Ltd., Hudersfield, UK) was made commercially available (Ness, 2011). In general, it is similar to the original MMT described by Etchepareborde et al. (2010), but features some differences (Fig. 6). The most notable difference is the addition of a porous titanium foam wedge (50% porosity, OrthoFoam^{TM}, Orthomed UK Ltd., Huddersfield, UK) to fill the osteotomy gap. Porous titanium foam is a biocompatible osteoconductive material (St-Pierre, Gauthier, Lefebvre, & Tabrizian, 2005; Cheung, Gauthier, Lefebvre, Dunbar, & Filiaggi, 2007; Rosa et al., 2009; Wazen, Lefebvre, Baril, & Nanci, 2010; Baril, Lefebvre, & Hacking, 2011; Lim, Bobyn, Bobyn, Lefebvre, & Tanzer, 2012) with mechanical properties similar to cortical bone when at 50% porosity (Imwinkelried, 2007). In fact, it has been shown that the wedge is biomechanically superior to its homologous synthetic bone alternatives (Etchepareborde et al., 2014). The other differences consist of passing a K-wire through the TT, wedge, and tibial diaphysis, and the recommended use of the figure-of-eight wire in every case (Ness, 2011).

Figure 6: MMP with wire support. (Left) 3D illustration. Note the porous titanium foam wedge filling the osteotomy gap. (Adapted from: Orthomed UK, 2011. MMP Surgical Technique [video]. Accessed September 2014. Available at: http://youtu.be/kc4MX1fRKNQ). (Right) Pre-suturing intraoperative photo. The arrow points cranially.

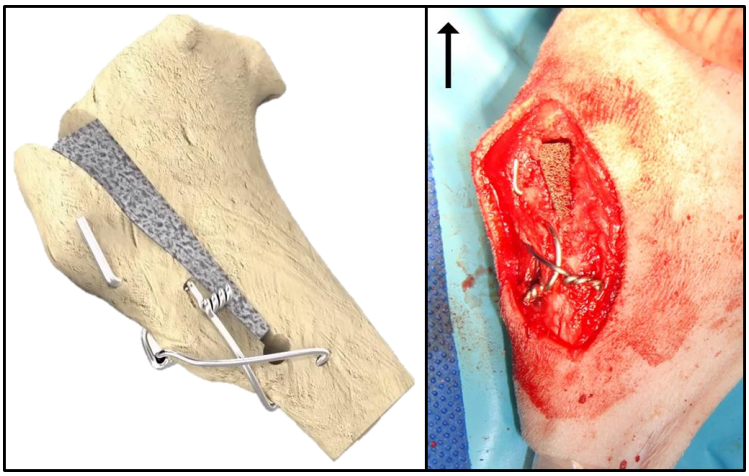

A method of assessing the advancement of the TT, based exclusively on tibial data points, was also introduced (Ness, 2011). There are still no published studies on the MMP. The only data available is provided by the manufacturing company (Ness, 2012). Considering the three "early-adopting" hospitals, it is reported an acceptable outcome (Cook, Evans, et al., 2010) at 8-week follow up in 98.5% of cases. Possible complications included loss of reduction of the TT, broken wedges, and tibial diaphyseal fractures. Indeed, TT avulsion fracture after MMP

has been reported in one dog, in a recent study on management of TTA complications (Lorenz & Pettitt, 2014).

In 2013 (Ness, 2013), the manufacturing company launched an alternative method to the figure-of-eight wire stabilization, a titanium orthopaedic staple (MMP Ti Staple, Orthomed UK Ltd., Huddersfield, UK) (Fig. 7). The staples are 1.6 mm width, and have several lengths and leg sizes to select for each patient. These implants aimed to provide an easy, simpler method to support the distal TT (Ness, 2013), but thus far no study has shown their advantage over the figure-of-eight wire.

Figure 7: MMP with staple support. (Left) 3D illustration. Note the porous titanium foam wedge filling the osteotomy gap. (Adapted from: Orthomed UK, 2013. MMP Surgical Technique - Staple method [video]. Accessed September 2014. Available at: http://youtu.be/BLTw_k0z8jY). (Right) Pre-suturing intraoperative photo. The arrow points cranially.

4. Objectives

The objective of this preliminary study was to compare the mechanical behaviour of 5 types of implant used for stabilization of the distal TT in the MMP. In addition, we intended to subjectively compare overall staple handleability and easiness of placement to the ones of orthopaedic wire.

II. Materials and Methods

1. Samples

Each specimen consisted of two solid foam polyurethane blocks (Sawbones Europe AB, Malmo, Sweden) with a density of 0.48 g/cm^3, linked together by either orthopaedic wire (316L stainless steel, Orthomed UK Ltd., Huddersfield, UK) or an orthopaedic staple (7 mm leg Standard MMP Ti Staple, Orthomed UK Ltd., Huddersfield, UK).

Three different diameters of orthopaedic wire (0.8 mm, 1.0 mm and 1.2 mm) and two widths of orthopaedic staple (1.6 mm and 2.0 mm) were used (Fig. 8A, 8B). The blocks had 60 mm length, 10 mm width, 15 mm height, and the two long edges of one of the 60 × 10 mm surfaces were round. To facilitate further reading, the aforementioned plane surface shall henceforth be referred to as “dorsal surface” (Fig. 8C).

Figure 8: Components of the samples. (A) Three examples of stainless steel orthopaedic wire with respective diameters. (B) Two examples of orthopaedic staples with respective dimensions. (C) Polyurethane block and respective dimensions. Note the rounded edges of the dorsal surface. Inset: Transversal view of a block. Note the foamy pattern and the rounded dorsal edges.

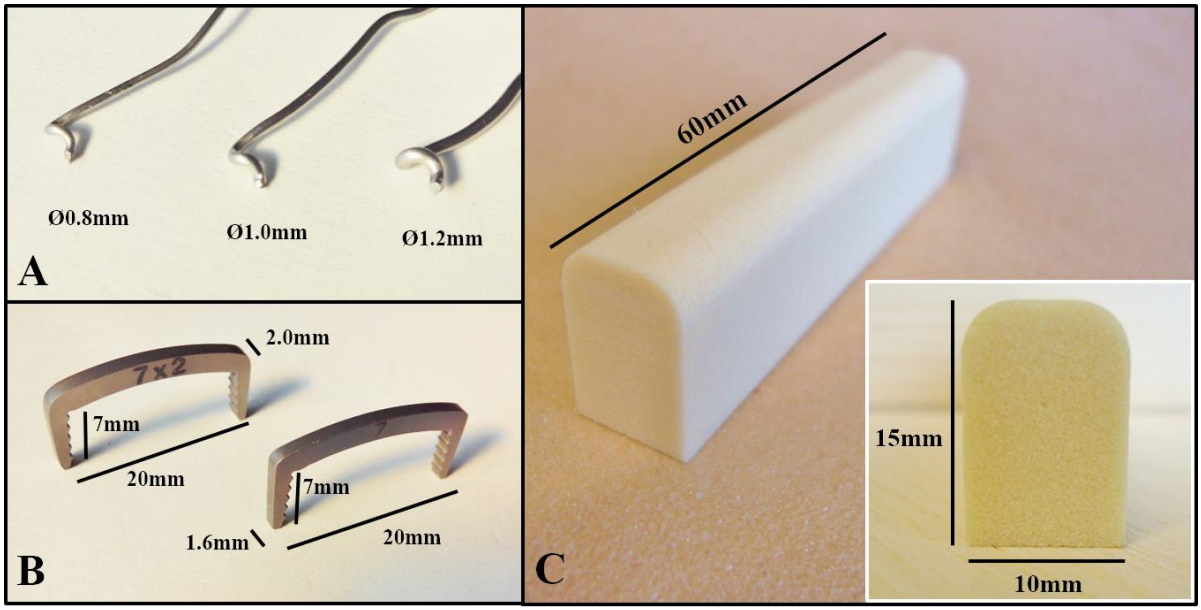

Sample structure aimed to resemble appropriate implant placement in a normal MMP. To assemble specimens within a group as similarly as possible, step-by-step, easily repeatable, reference guided methods were designed. In the end there were two different methods to be employed, one for the 3 wire groups and one for the 2 staple groups.

To first set up a wire specimen, a 2.0 mm diameter hole was drilled parallel to the dorsal surface and perpendicular to the long axis of each block. An orthopaedic staple was used as reference not only to ensure similar "hole-to-line of apposition" distance but also a "hole-to-hole" distance identical to the one in the staple specimens (Fig. 9A). Location was marked with a common mechanical pencil and the hole was drilled with the help of a drill guide (MMP Staple Drill Guide, Orthomed UK Ltd., Huddersfield, UK). The first block with correct hole location and direction was used as a drill guide in all the other blocks (Fig. 9B). The following step was to pass an approximately 100 mm long piece of wire by each of the blocks. The wires were positioned in a figure-of-eight pattern and each pair of wire ends was then tied with a twisting knot using a wire twister (Orthomed UK Ltd., Huddersfield, UK) (Ness, 2011). The twist was held under tension and perpendicular to the long axis of the loop to guarantee slack removal and appropriate wire wrapping on itself (Rooks, Tarvin, Pijanowski, & Daly, 1982; Roe, 1997; Piermattei, Flo, DeCamp, & Brinker, 2006b; Johnston, von Pfeil, Déjardin, Weh, & Roe, 2012) until a snug secure fit (rather than compression) and proper block apposition was achieved (Ness, 2011). The knot was then cut with common wire cutters leaving two twists, which were not bent. An example of a wire specimen can be seen in Figure 9C. These steps were repeated to assemble all the wire samples regardless of the diameter. If hole location or direction, twist-knots, or block-to-block apposition were perceived as unsatisfactory, the components were discarded and a new specimen was set up.

Figure 9: Wire sample assembling. (A) An orthopaedic staple was used as reference not only to ensure similar "hole-to-line of apposition" distance (so that α = α') but also a "hole-to-hole" distance (β) identical to the one in the staple specimens. The dashed circles represent ideal hole location. (B) Instant before drilling, with the guide block (GB) in place. (C) Orthopaedic wire sample labelled and ready to be tested. Note the slight block distraction "ventrally", caused by the figure-of-eight knot tension on the dorsal surface.

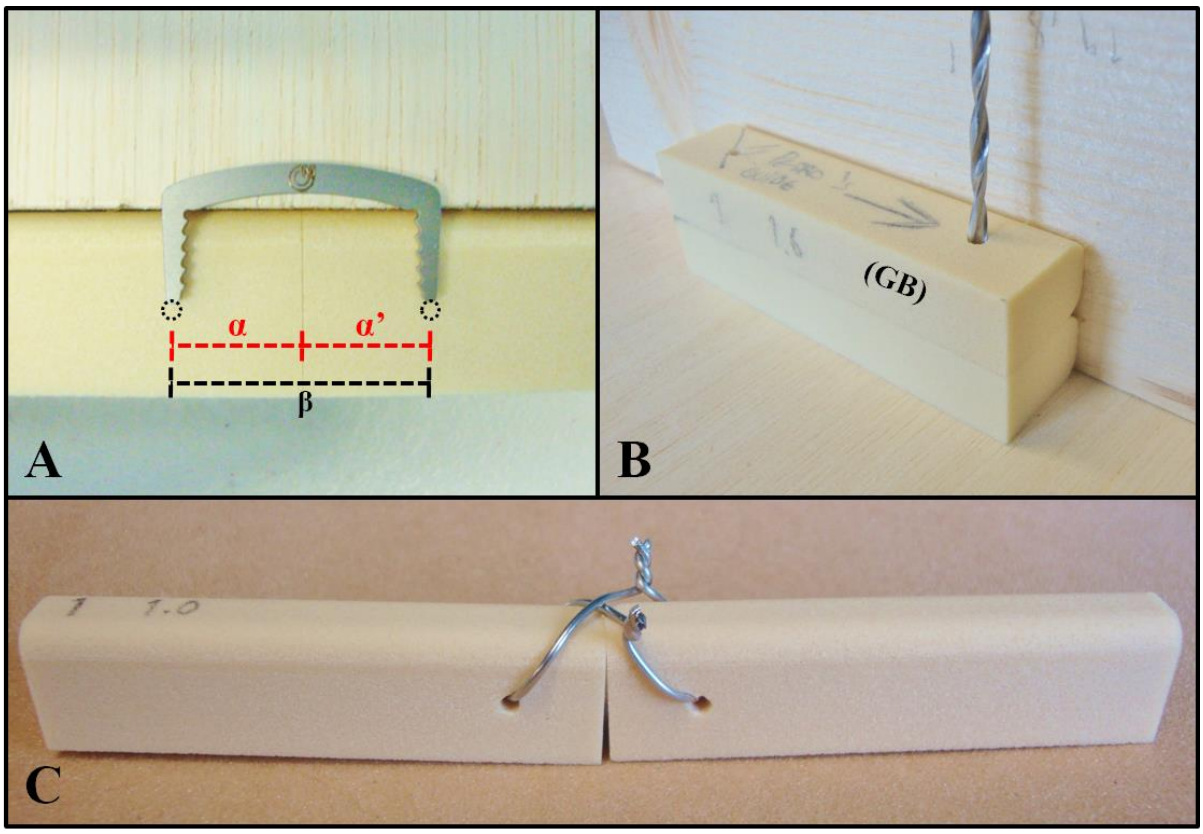

The first step to assemble a staple sample was to mark the 2.0 mm diameter drill bit. The marks provided a simple measurement of hole depth, which was intended to be the same length as the staple leg. The drill bit was marked in a manner that allowed the operator to easily assess the instant when ideal depth was achieved and drilling should be stopped (Fig. 10A). One 2.0 mm diameter hole was drilled (Ness, 2013) perpendicular to the long axis and the dorsal surface in each block. A drill guide (MMP Staple Drill Guide, Orthomed UK Ltd., Huddersfield, UK) was positioned in a way that allowed proper drilling direction and the holes to be equidistant from the line of apposition (Fig. 10B). Before drilling the second hole, a 2.0 mm diameter pin (MMP 2.0 mm Staple System Pin, Orthomed UK Ltd., Huddersfield, UK) was used to help securing the drill guide and the block in the same position (Fig. 10C). After the second hole was drilled, the staple was gently tapped into place with the drill guide

(Ness, 2013). Staple specimens were as seen in Figure 10D. These steps were carefully repeated to set up all the staple samples regardless of staple width. Similarly to what happened with the wire samples, if the location, direction or depth of the hole, or the block-to-block apposition were regarded as unsatisfactory, the components were discarded and a new specimen was set up.

Figure 10: Staple sample assembling. (A) Drill bit marks. The one on the bottom marks hole depth, the top one is a visual reference for the operator to know when to stop drilling. (B) The vertical stripes on the drill guide are equidistant from the "T". Appropriate positioning was achieved by aligning the "T" with the blocks' line of apposition, so that α = α'. (C) Instant before the second hole was drilled, note the pin on the right to help with positioning. (D) Staple sample labelled and ready to be tested. Note the perfect alignment (top), and block apposition (bottom).

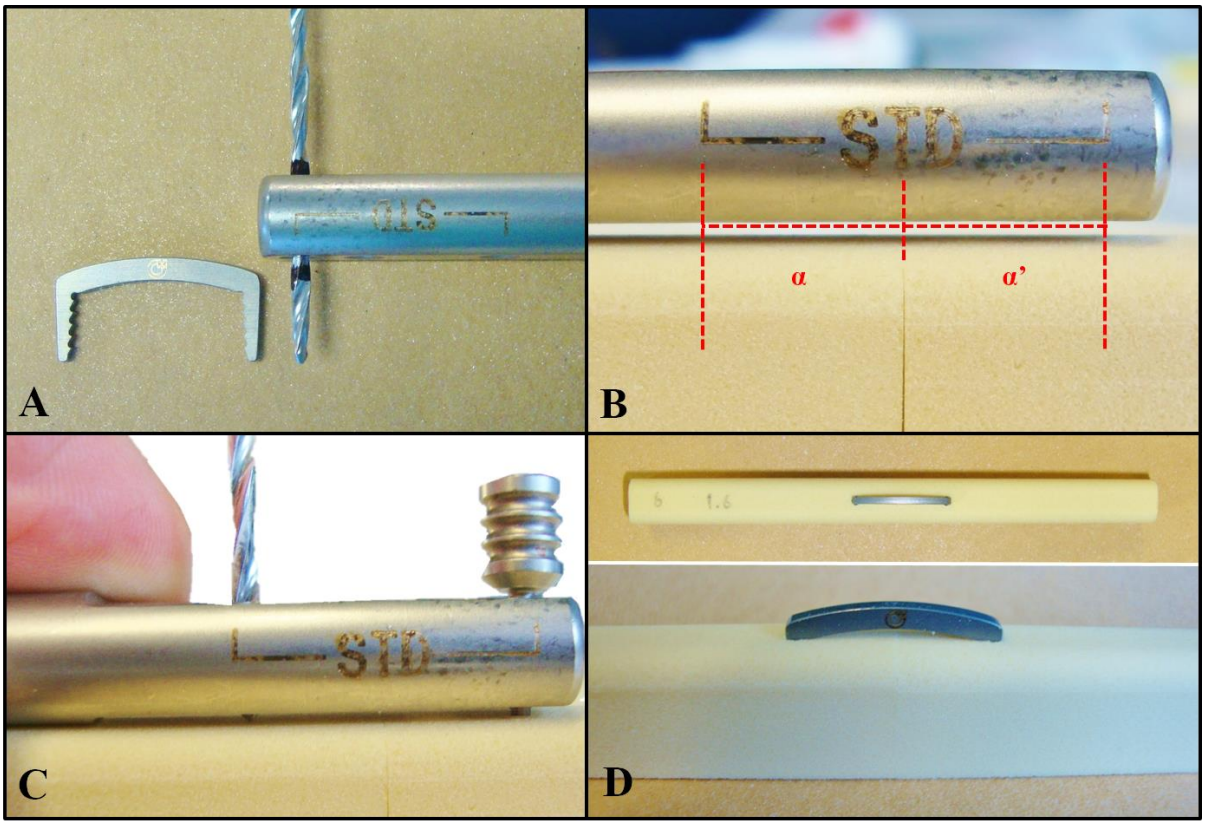

In total, 50 specimens were assembled, all by the same operator, and labelled according to the respective type of implant. Samples were numbered as *X_Y*, where *X* corresponded to the sample number (between 1 and 10) and *Y* to the implant group (0.8, 1.0 or 1.2 for the wire groups; and 1.6 or 2.0 for the staple groups), e.g. 5_1.2 would be sample number 5 from the 1.2 orthopaedic wire group (Fig. 11).

Figure 11: The 50 samples labelled and ready for testing.

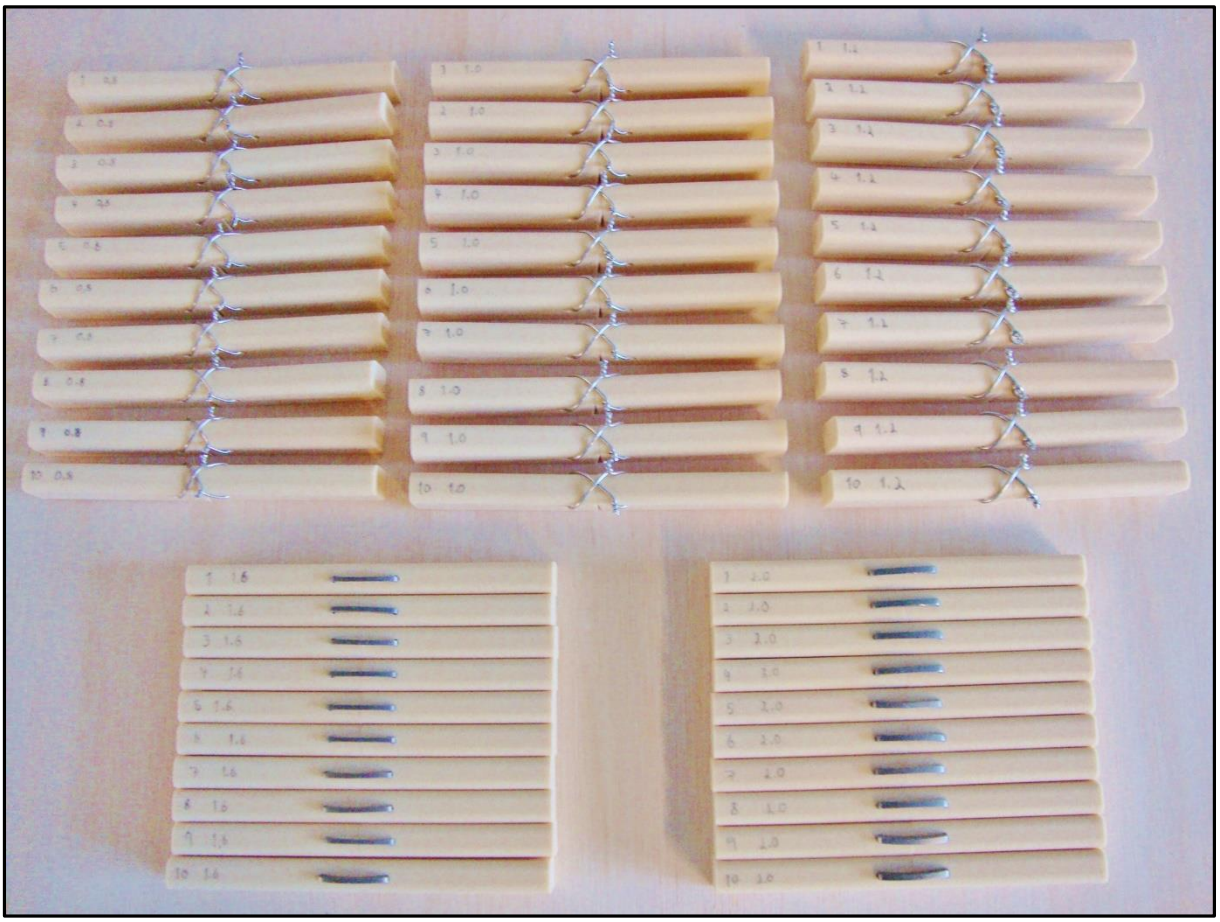

Three extra specimens (0.8 mm wire, 1.2 mm wire, 2.0 mm staple) were assembled, and labelled as T, to serve as test samples for setting up the tensioning machine.

2. Testing

All the tests were carried at the Mechanical Lab of the University of Huddersfield, on the 20th June 2014. Testing was performed on a universal materials testing machine (Model Number 3369, Instron, High Wycombe, UK). Specimen positioning was as shown in Figure 12. The machine's jaws clamped half of each block, the farthest from the implant. To ensure identical positioning of all the samples, one of the jaws was marked with a visual reference.

Figure 12: Samples ready for testing. Specimen 1_0.8 on the left and specimen 3_2.0 on the right. Blocks were clamped by the farthest half from the implant. Note the marker on the bottom jaws that served as a reference for sample positioning.

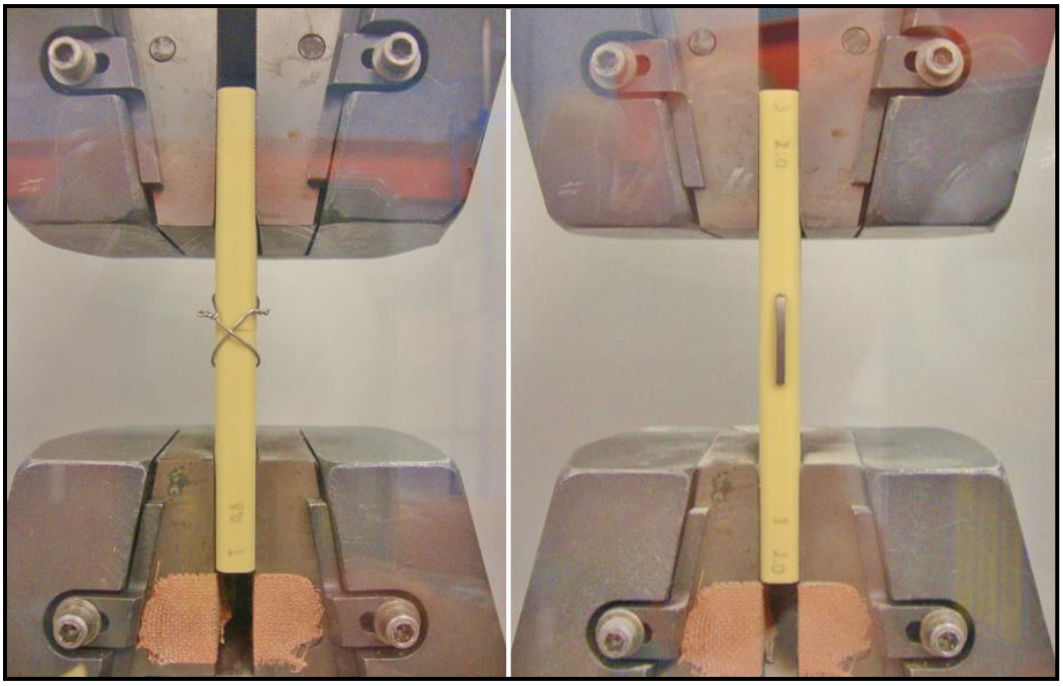

The three test specimens were used to assess ideal sample positioning on the machine and to help placing the visual markers. They also served to adjust and test the preload and distraction speed before testing any of the main fifty samples. The main fifty specimens were then submitted to a crosshead displacement rate of 1 mm/min until a preload of 20 N was reached, followed by testing at 5 mm/min until 0 N of resistance was recorded. For each sample, data regarding load and linear displacement was generated at 600 points per minute. A software (Bluehill®3, Instron, High Wycombe, UK) collected and compiled the data which was then stored in an electronic database (Excel® 2013, Microsoft, Redmond, WA, USA). Each specimen's mode of failure (MOF) was recorded as well.

3. Statistical analysis

Data processing was performed using a spreadsheet software (Excel® 2013, Microsoft, Redmond, WA, USA) and a statistical computing and graphics software (R i386 3.1.1, R Foundation for Statistical Computing, Vienna, Austria).

For each sample, the following parameters were registered:

- Displacement at 100 N (D_{100});
- Displacement at 200 N (D_{200});
- Displacement at Failure (D_{FAIL});
- Load to Failure (LTF);
- Stiffness (STIF);
- Yield Load (YL).

An example of a load-displacement curve and the mechanical variables interpreted in this study can be found in Figure 13.

Figure 13: Example of a load-displacement curve and the mechanical variables interpreted in this study. D_{100} – Displacement at 100 N; D_{200} – Displacement at 200 N; D_{FAIL} – Displacement at Failure; LTF – Load to Failure; STIF – Stiffness; YL – Yield Load. The red dot represents the yield point.

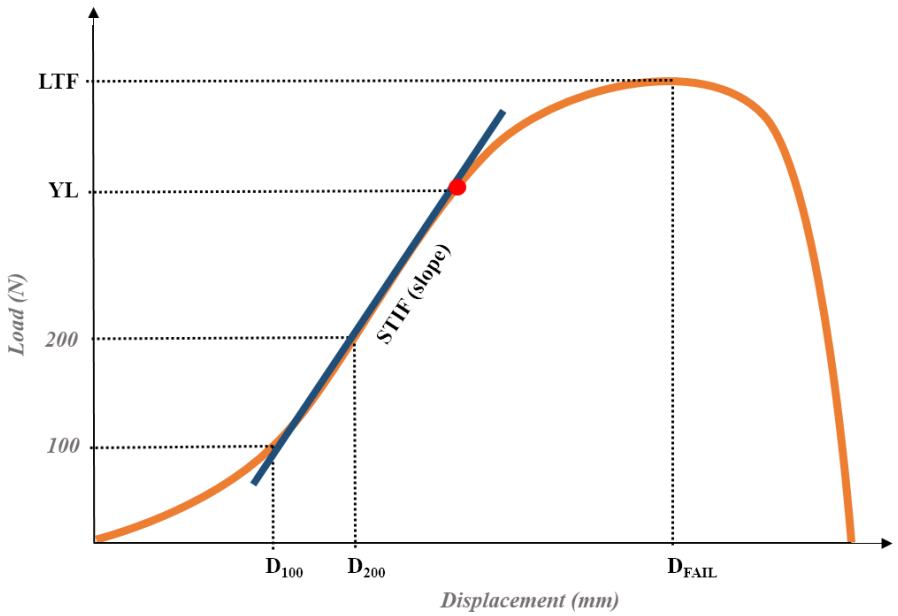

Displacement values D_{100}, D_{200} and D_{FAIL} represent a measure of distraction at 100 N load, 200 N load, and at failure, respectively. The displacement at failure measures the displacement at the point when catastrophic failure of the construct occurs (Cohen & Griffin, 2002). These values were obtained in millimeters (mm).

Load to Failure is the maximum force necessary to induce a catastrophic failure in the structure (Cohen & Griffin, 2002), it corresponds to the highest point in the curve and was obtained in Newtons (N).

Stiffness is represented by the slope of the linear portion of the load-displacement curve. (Noyes, Delucas, & Torvik, 1974; Butler et al., 1983; Cheng, Cameron, Warden, Fonger, & Gott, 1993; Roe, 1997; Cohen & Griffin, 2002; Sample, Vanderby, & Muir, 2011; Cross, 2012). It was calculated using the SLOPE function (Excel® 2013, Microsoft, Redmond, WA, USA) on a part of the linear portion of the curve and obtained in Newtons per millimeter (N/mm).

The point where the slope first changes and the curve becomes nonlinear is the yield point (Blass, Piermattei, Withrow, & Scott, 1986; Roe, 1997; Cohen & Griffin, 2002; Cross, 2012). The yield point was estimated by visual inspection (Roe, 1997) and the corresponding load was registered - the Yield Load. It was obtained in Newtons (N) and rounded to the nearest dozen (e.g. 217.23 N would be rounded to 220 N).

All the values are presented rounded to the nearest first decimal. Mean and standard deviation (SD) were found for each variable and are presented as Mean ± SD, unless otherwise stated. For each parameter, one-way analysis of variance (ANOVA) was used to detect differences between groups and results were corrected with a Bonferroni post-hoc adjustment. Values of $p < 0.05$ were considered significant.

III. Results

The overall behaviour of each group is graphically depicted in Figure 14. Examples of a load-displacement curve of a sample in each group are presented in Figure 15. Despite gross within-group similarity, obvious differences can be seen on the trace of the curve between samples from different groups.

Figure 14: Load-displacement curves of each group obtained by polynomial regression (bold lines). The faded lines represent each sample's load-displacement curve. All tests started at 20 N preload.

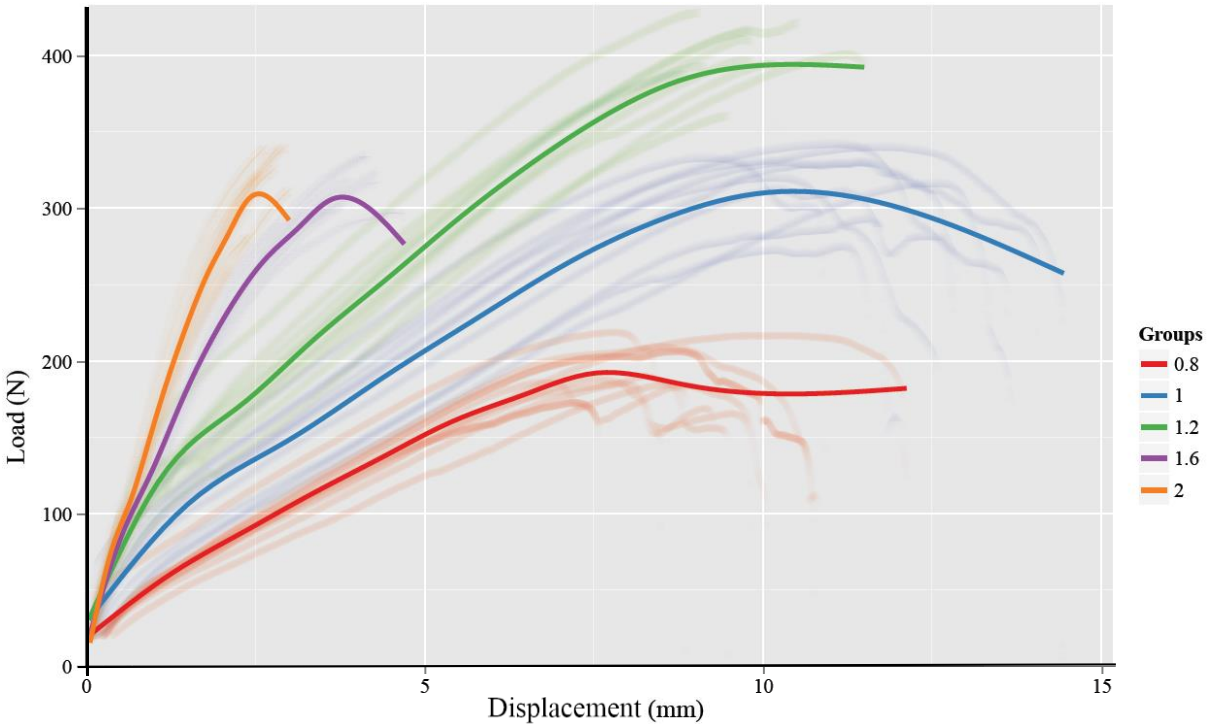

Figure 15: Examples of a typical load-displacement curve for each group. All tests started at 20 N preload.

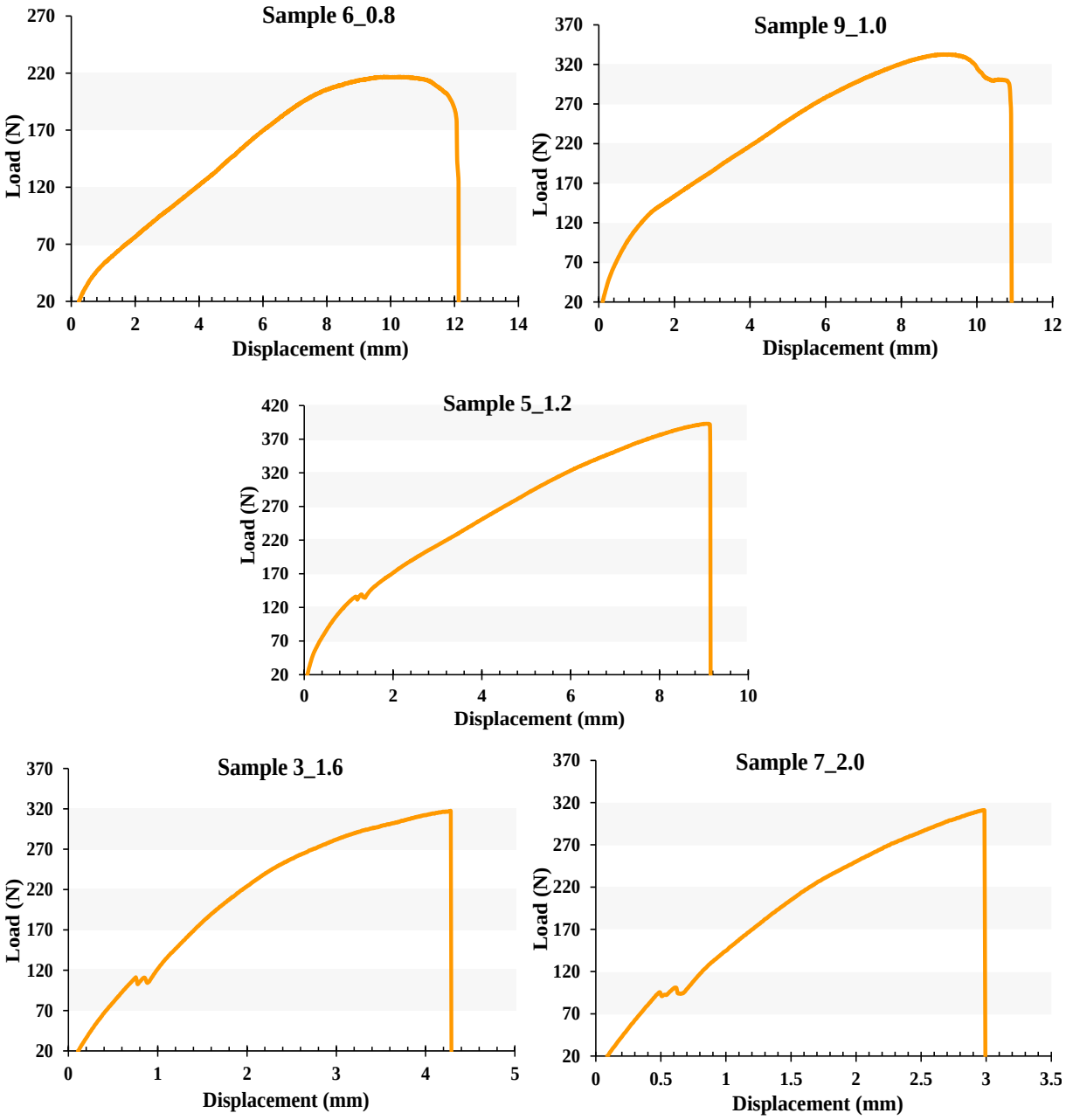

1. Displacement at 100 N

Mean results for D_{100} were 2.9 ± 0.5 mm, 1.4 ± 0.6 mm, 0.8 ± 0.2 mm, 0.7 ± 0.1 mm, and 0.6 ± 0.1 mm for the 0.8, 1.0, 1.2, 1.6, and 2.0 group, respectively. No significant differences were found between group 1.2, 1.6, and 2.0. These data are represented in Figure 16. Detailed statistical results for D_{100} can be found in Annex 1.

Figure 16: Comparison of mean and SD for Displacement at 100 N between groups. Columns marked with a letter (*a*) are not significantly different.

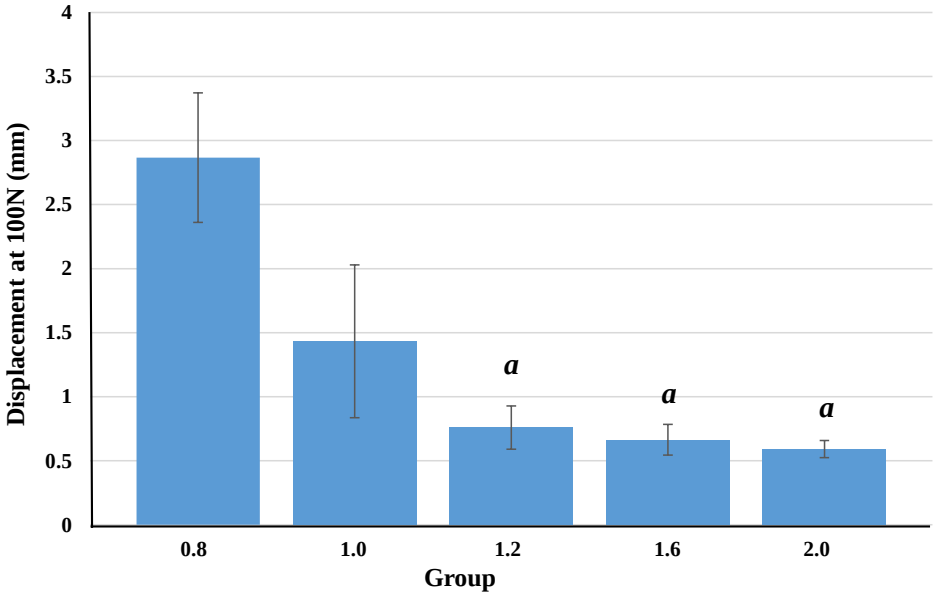

2. Displacement at 200 N

Mean results for D_{200} were 6.9 ± 0.7 mm, 4.9 ± 1.0 mm, 3.0 ± 0.6 mm, 1.7 ± 0.1 mm, and 1.3 ± 0.1 mm for the 0.8, 1.0, 1.2, 1.6, and 2.0 group, respectively. In group 0.8 only 4 samples reached 200 N. The resultant mean is, consequently, a reflection of only those specimens. There were no significant differences between group 1.6 and 2.0. These data are represented in Figure 17. See Annex 2 for the detailed statistical results regarding D_{200}.

Figure 17: Comparison of mean and SD for Displacement at 200 N between groups. Columns marked with a letter (*b*) are not significantly different. (*) Results for group 0.8 reflect only the 4 samples that reached 200 N of resistance.

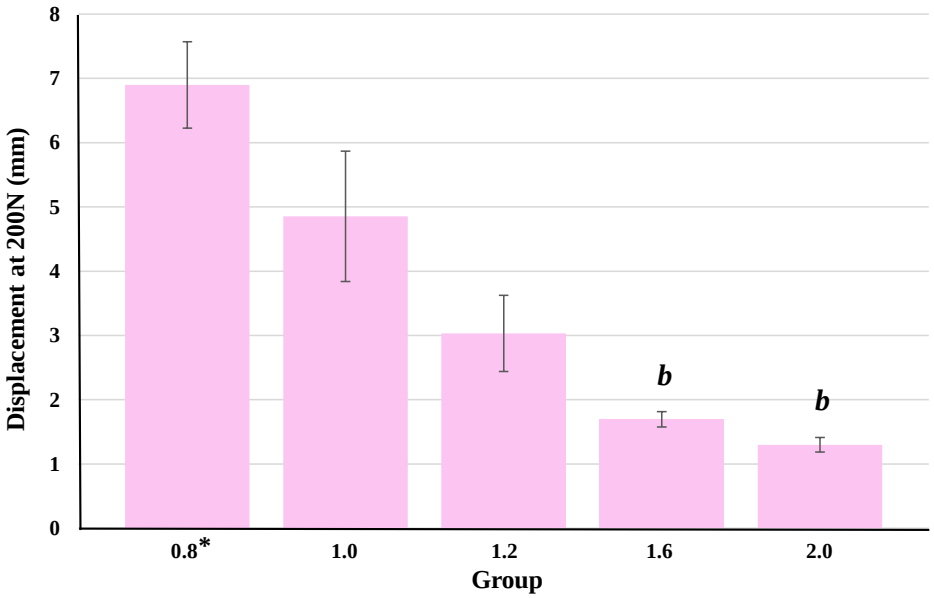

3. Displacement at Failure

Mean results for D_{FAIL} were 8.1 ± 0.9 mm, 10.9 ± 1.0 mm, 9.7 ± 0.7 mm, 3.9 ± 0.5 mm, and 2.6 ± 0.3 mm for the 0.8, 1.0, 1.2, 1.6, and 2.0 group, respectively. All the groups were significantly different from each other. These data are represented in Figure 18. Detailed statistical results for D_{FAIL} are shown in Annex 3.

Figure 18: Comparison of mean and SD for Displacement at Failure between groups. Statistically significant differences were found between all the groups.

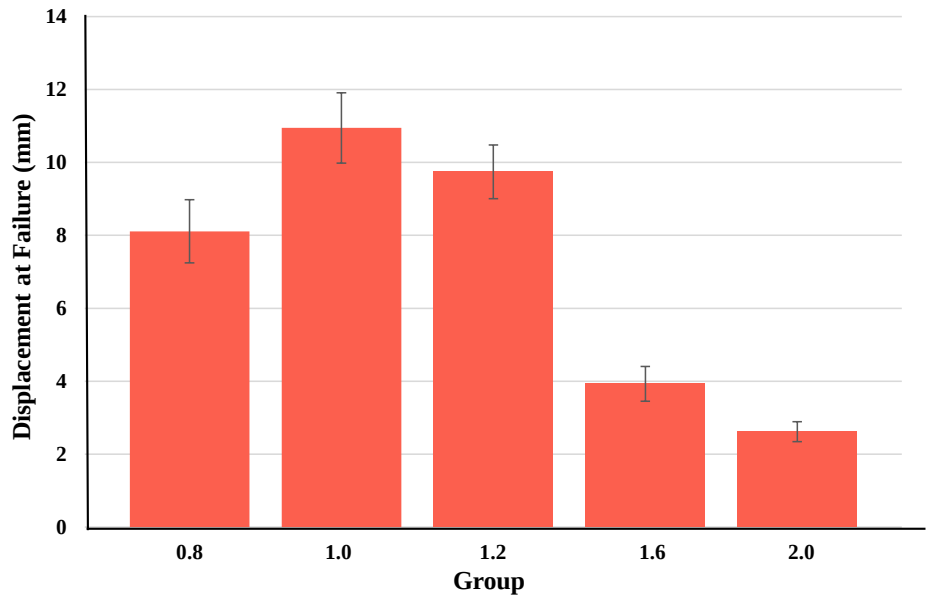

4. Load to Failure

Mean results for LTF were 195.9 ± 15.8 N, 319.2 ± 21.3 N, 401.1 ± 19.5 N, 312.4 ± 15.2 N, and 314.8 ± 26.3 N for the 0.8, 1.0, 1.2, 1.6, and 2.0 group, respectively. Groups 1.0, 1.6, and 2.0 showed no significant differences between each other. These data are represented in Figure 19. Load to Failure detailed statistical results can be found in Annex 4.

Figure 19: Comparison of mean and SD for Load to Failure between groups. Columns marked with a letter (*c*) are not significantly different.

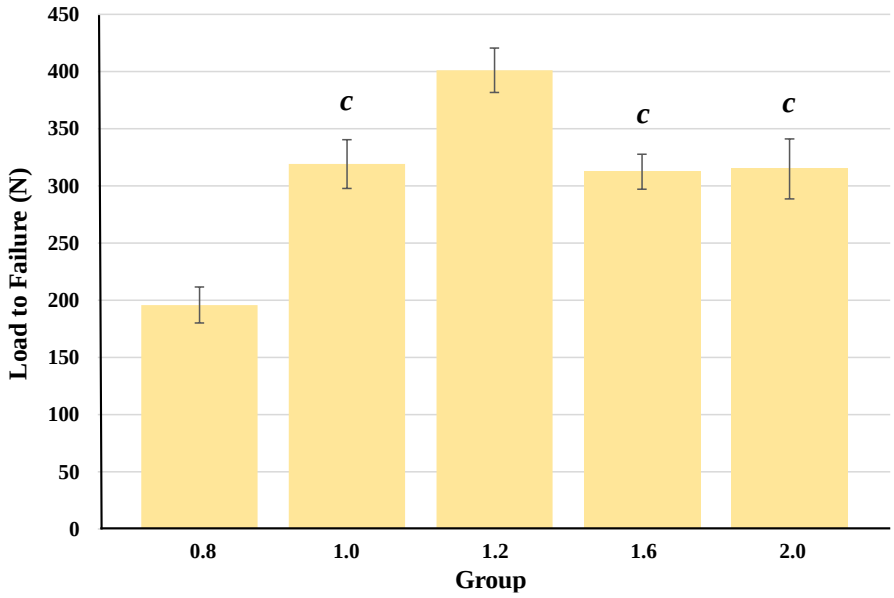

5. Stiffness

Mean results for STIF were 23.9 ± 2.1 N/mm, 28.8 ± 2.4 N/mm, 37.6 ± 2.0 N/mm, 98.3 ± 13.5 N/mm, and 142.2 ± 19.9 N/mm for the 0.8, 1.0, 1.2, 1.6, and 2.0 group, respectively. There were no significant differences between group 0.8, 1.0, and 1.2. These data are represented in Figure 20. See Annex 5 for the detailed statistical results regarding STIF.

Figure 20: Comparison of mean and SD for Stiffness between groups. Columns marked with a letter (*d*) are not significantly different.

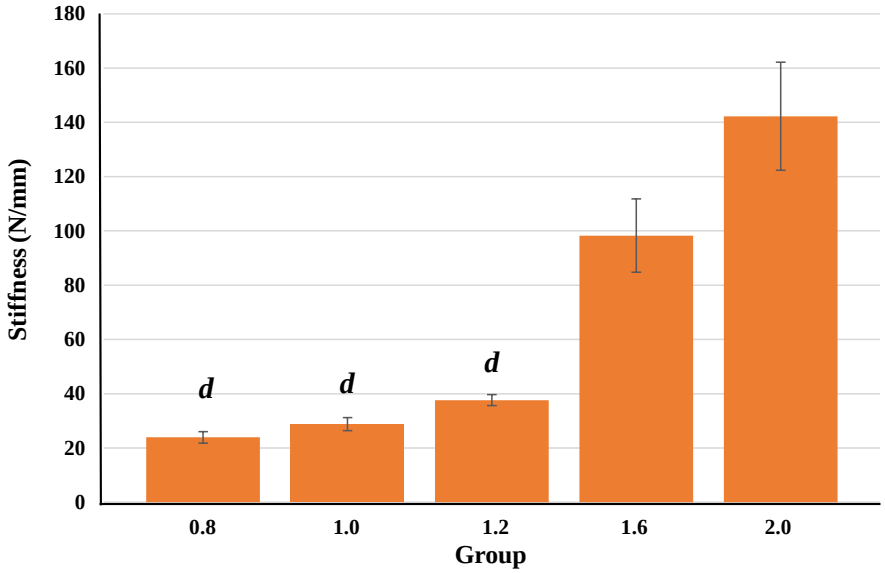

6. Yield Load

Mean results for YL were 158.0 ± 16.9 N, 264.0 ± 18.4 N, 324.0 ± 14.3 N, 213.0 ± 4.8 N, 216.0 ± 12.6 N for the 0.8, 1.0, 1.2, 1.6, and 2.0 group, respectively. No significant differences were found between groups 1.6 and 2.0. These data are represented in Figure 21. Detailed statistical results for YL can be found in Annex 6.

Figure 21: Comparison of mean and SD for Yield Load between groups. Columns marked with a letter (*e*) are not significantly different.

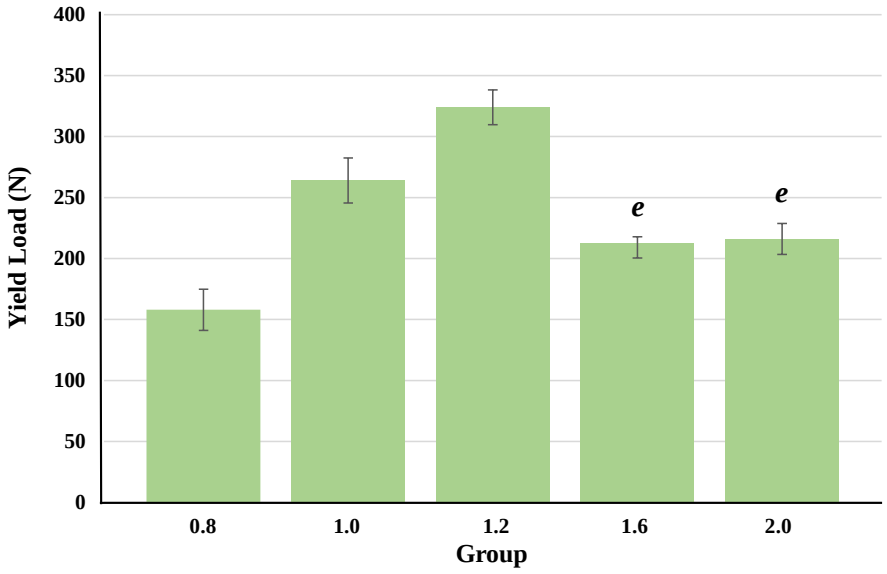

7. Mode of failure

In general, MOF can be divided in two types - implant failure or block failure. In groups 0.8 and 1.0, all specimens failed by implant failure, which occurred by untwisting of the knots (Fig. 22). In groups 1.2, 1.6, and 2.0, samples failed by block failure in every case. It was characterized by breakage of one of the blocks, in a plane approximately perpendicular to the long axis of the blocks, through the hole where the implant was placed (Fig. 23). Pictures of all the samples after the tests can be found in Annex 7.

Figure 22: Examples of implant failure by knot untwisting, in a 1.0 mm diameter wire sample (left) and 0.8 mm sample (right).

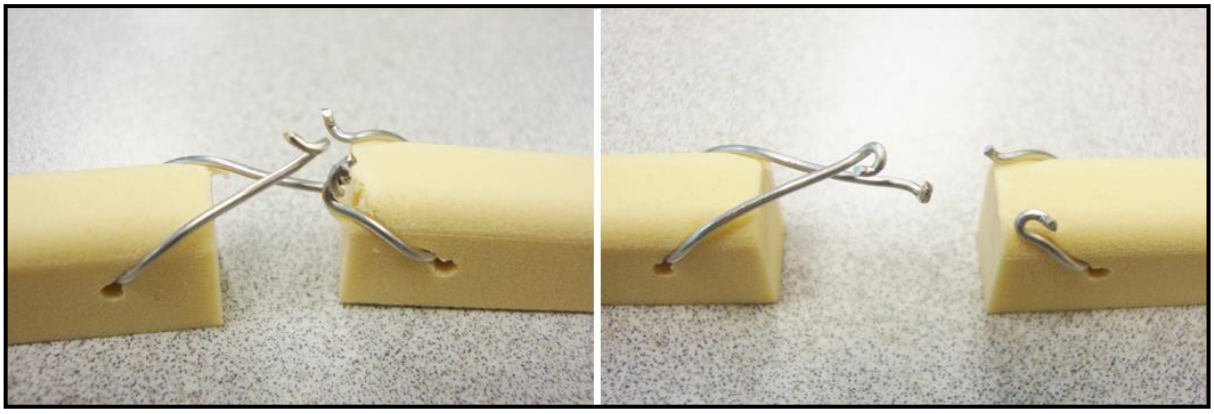

Figure 23: Examples of block failure, in a 1.2 mm diameter wire sample (left), and 2.0 mm width staple (right).

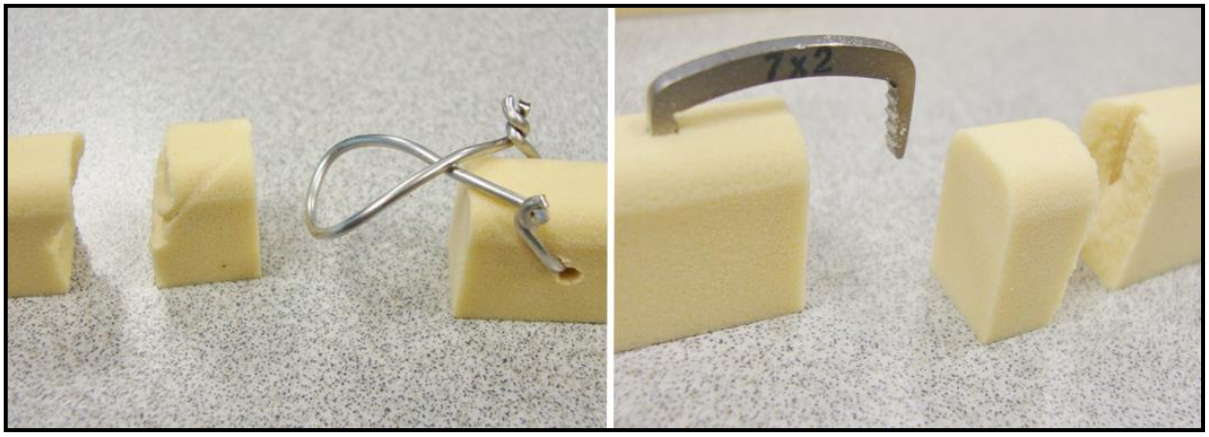

IV. Discussion

In this study, solid foam polyurethane blocks with a density of 0.48 g/cm^3 were used. Rigid foam polyurethane blocks are easy to handle and commercially available. Given their composition and production method, polyurethane blocks come in several shapes, sizes and densities (Szivek, Thomas, & Benjamin, 1993; Szivek, Thompson, & Benjamin, 1995; American Society for Testing and Materials, 2012). They have been widely used in biomechanical studies and had their mechanical properties vastly investigated, being shown that certain densities have mechanical properties comparable to human cancellous bone (Szivek et al., 1993; Szivek et al., 1995; Thompson, McCarthy, Lidgren, & Ryd, 2003; Palissery, Taylor, & Browne, 2004; Patel, Shepherd, & Hukins, 2008). However, solid polyurethane foam provides more consistent and repeatable mechanical properties, yielding lesser variability than human cancellous bone (Szivek et al., 1993; Szivek et al., 1995; Yakacki, Griffis, Poukalova, & Gall, 2009; Calvert, Trumble, Webster, & Kirkpatrick, 2010). Despite not having exactly the same features as a biological specimen, solid polyurethane foam serves as a consistent, uniform test medium for medical device testing (ASTM, 2012). Indeed, the ASTM (2012) considers it "the ideal material for comparative testing of bone screws and other medical devices and instruments". We believe that by using polyurethane blocks we were able to reduce block-related variability to a minimum and to exclude any individual, intra, or inter-breed related variability, while at the same time be able to choose block geometry that best suited our study design.

Final block geometry was chosen after a pilot assembling study where rectangular cuboid blocks were used. In that pilot study, we verified that, upon tightening of the knots, four stress points would rise on the edges of the surface where the figure-of-eight would lay, causing the wire to dent the edges of the blocks (Fig. 24). To prevent any damage to the blocks caused by these stress points before testing and any variability that could have possibly resulted from it, the blocks used in this experiment had two round edges.

Figure 24: Scheme of a sample from the pilot assembling test. Arrows mark the four stress points that rise when using sharp edge blocks. Inset: Real detail of the dent caused by wire tightening.

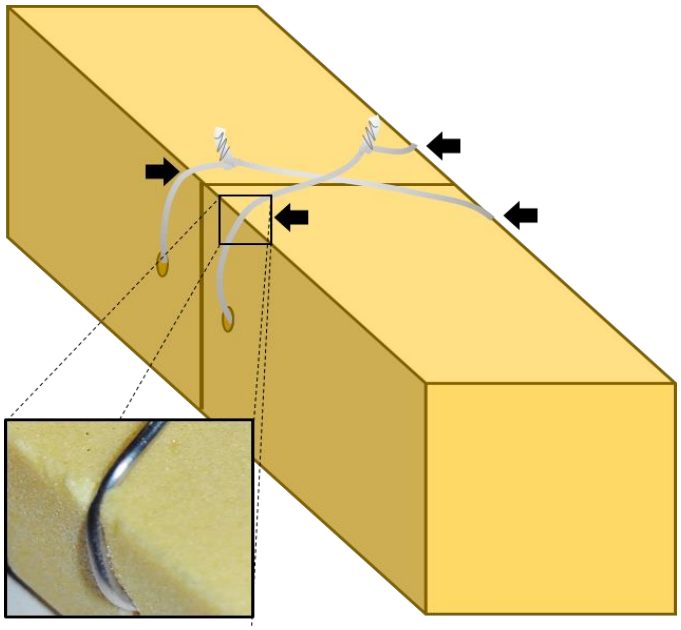

For this experiment we used 3 diameters of steel wire and 2 widths of orthopaedic staple. Generally, the only rule to follow when choosing wire size is to use the biggest diameter that appears clinically manageable and adequate to the strength and size of the bone in question (Schultz, Boger, & Dunn, 1985; Bostrom et al., 1994; Meyer, Ramseier, Lajtai, & Nötzli, 2003; Johnston et al., 2012). Based on the MMP guidelines, the implants used for distal TT fixation are 1.0 mm or 1.2 mm diameter wire (Ness, 2011), or 1.6 mm width staple (Ness, 2013). We also used two other types of implant, 0.8 mm diameter wire and 2.0 mm width orthopaedic staple. The former is the recommended wire size for the figure-of-eight knot in the MMT, in dogs weighting less than 20 Kg (Etchepareborde et al., 2011). It is also used in several other orthopaedic procedures, for instance, as cerclage or tension band for fracture repair in dogs under 20 Kg (Piermattei et al., 2006b; Johnston et al., 2012). However, it is not recommended in the MMP guidelines, which advocate the 1.0 mm diameter wire as the absolute minimum diameter to be used (Ness, 2011). Hence, we were interested in comparing its mechanical behavior with the one of the recommended sizes. On the other hand, the 2.0 mm staple, to the author's knowledge, is not commercially available and has never been used in other orthopaedic procedures, and this represents the first experimental study on its mechanical behaviour. With a sturdier appearance, we were interested to see the mechanical

repercussions of the slight increase in staple width. The mechanical differences between each type of implant will be discussed further ahead.

The author assembled all the specimens used in this experiment. Prior to assembling the 50 samples used in this study, the author was taught correct wire twisting and staple placing by the supervisor (MGN), and a 2-day period was spent practicing specimen set up until adequately assembled samples were consecutively achieved. It has been shown that operator experience is not associated with the ability to tie wire (Roe, 2002). By having one operator, we aimed to exclude inter-operator variability, and, to help keep intra-operator variability to a minimum, two systematic set up methods were designed and any unsatisfactory specimens were excluded from testing (see chapter II.1 "Samples").

The assembly methods were designed to be simple, systematic, easily repeatable, and, ultimately, to replicate the steps to achieve the correct final implant placement in an MMP. In general, these objectives were successfully achieved, but the assembly methods still yielded some differences from the actual surgical methodology. Drill hole diameter for orthopaedic wire passage is generally either 1.5 or 2.0 mm (Denny & Butterworth, 2000). In the MMP, recommended tibial drill hole diameter is 2.0 mm if a staple is to be placed, and 1.5 mm for orthopaedic wire (Ness, 2011). In spite of that fact, we opted by drilling a 2.0 mm diameter hole regardless of the type of the implant, with the objective of excluding any hole size influence, attributing the observed differences to the implant type solely. According to the guidelines, two figure-of-eight double-twist knots can be used in patients weighting over 25 Kg (Ness, 2011). In our experiment we opted for not testing that design and use a single figure-of-eight wire. The figure-of-eight double-twist knots used in our samples were indeed similar to the used in the MMP, yet not absolutely identical, as we did not bend the twist knots. It has been shown that the twist knot is stronger than other types of knots (Schultz et al., 1985; Wilson, Belloli, & Robbins, 1985) and that two twists are enough to reach maximal strength (Schultz et al., 1985; Guadagni & Drummond, 1986). Its properties have been widely investigated and depend on factors such as wire width, pre-twisting tension, pull force and direction, instrument used, post-twist knot cutting, and knot bending (Rooks et al., 1982; Schultz et al., 1985; Wilson et al., 1985; Guadagni & Drummond, 1986; Blass et al., 1986; Bostrom et al., 1994; Roe, 1997; Harnroongroj, 1998; Roe, 2002; Meyer et al., 2003; Wähnert, Lenz, Schlegel, Perren, & Windolf, 2011; Johnston et al., 2012). Work by Rooks and colleagues (1982) has demonstrated the effect of twist bending on knot tension in 1.0 mm diameter wire. They observed a reduction of approximately 33% of tension with the bending process. In another study, Meyer and colleagues (2003) also found that bending reduces knot

tension. For 1.0 mm diameter wire, the decrease of tension was dramatic, at 84%, and, for 1.2 mm wire, they observed 38% of loss. Wähnert et al. (2011) reported the same type of outcome. They observed a decrease of tension of 23% and 53%, for 1.0 mm and 1.2 mm wire, respectively, and that the amount of loss depends on the bending direction. Despite not being objectively quantified, tension loss was also observed by Roe (1997, 2002) and Johnston et al. (2012) during their experiments with orthopaedic wire. By leaving the knots unbent, we aimed to prevent loss of tension before testing and exclude any variability related with the bending process. However, this may account as a limitation, as in practice, given the scarce soft tissue covering of the medial TT, bending is an important step to prevent soft tissue trauma.

A recent study by Hayes et al. (2014) identified the use of orthopaedic wire as a risk factor for glove perforation during surgery. Indeed, the operator occasionally felt the traumatic effect of the sharp, recently cut wire while assembling these samples. Regarding this aspect, the staples appeared to have an advantage as they have a smooth surface without traumatic sharp edges. To best achieve a twist knot, it should be pre-tensed (Harnroongroj, 1998), kept in tension (Rooks et al., 1982; Roe, 2002; Wähnert et al., 2011), pulled perpendicular to the long axis of the loop (Rooks et al., 1982), and, if flattening is needed, it should be done by folding while twisting (Roe, 2002). As mentioned above, each of these steps influences the properties of a knot, and following them perfectly may, sometimes, be a challenge. Evidently, none of these steps, and their associated variability, apply to the staple. The staple assembly method seemed to be simple and intuitive, and the actual tapping of staple in place did not show to be a challenge. However, in practice, and particularly with the smaller small breed staples, holding the staple while tapping it into place may warrant additional care. In spite of the staple method's apparent advantages, these are subjective assessments made by one operator only, and should be interpreted as such. To draw any further conclusions, further objective studies on this subject would be necessary.

This study has no biological component, thus, the intrinsic differences between our study and clinical reality limit the transposition of our results to an *in vivo* scenario. In truth, the normal *in vivo* conditions are virtually impossible to replicate *in vitro*. For instance, our study ignores the stabilizing effect of the distal TT bone bridge and the bone-wedge mechanical interaction. The importance of the bone bridge has been highlighted by Etchepareborde and colleagues' (2010) cadaveric study, where, by pulling on the patellar tendon, they compared the strength of 3 types of distal TT support: intact bone bridge plus a 1.0 mm figure-of-eight wire, intact bone bridge solely, and broken bone bridge plus wire. They observed that, when 1.0 mm

figure-of-eight wire was added as support, samples with a broken bone bridge were only able to withstand half the maximal load of the ones with an intact bridge, and, moreover, when the bridge is intact, the addition of a 1.0 mm figure-of-eight wire has no significant increase in strength. On the other hand, it has been shown that the mechanical interaction between a porous titanium implant and the healing bone provides immediate postoperative mechanical stability (Simmons, Valiquette, & Pilliar, 1999). That interaction is mainly a consequence of the friction between the two surfaces, resulted from a tight intimate bone-implant fit (Simmons et al., 1999). In fact, it has been reported that the "bone-to-porous implant" interface stiffness after implantation is comparable to the one after osseointegration (Bragdon et al., 1996; Simmons et al., 1999). However, it should be noted that there is reduction of the bone-implant contact after that initial postoperative period, caused by the reabsorption of necrotic bone at the surgical site (Simmons et al., 1999), which may reduce stability at that time. Furthermore, it is suggested that the surrounding soft tissues and the K-wire that is inserted through the TT, wedge, and tibial diaphysis, have a stabilizing role as well (Ness, 2011). The importance of surrounding soft tissues in TT stability has been suggested by Etchepareborde et al. (2011) and seems to be supported by the absence of significant TT avulsion in MMP complications (Ness, 2012). In contrast, an *in vitro* study has questioned the necessity of K-wire placement, suggesting that the bone-wedge friction should be enough to keep the wedge in place (Etchepareborde et al., 2014). In that study, it was shown that, in the absence of K-wire or any other stabilizing implant, the porous titanium wedge was able to endure unidirectional fatigue testing for 200,000 cycles without migrating. However, the reduction in bone-implant contact that occurs postoperatively, caused by the reabsorption of necrotic bone (Simmons et al., 1999), was not taken into account. Therefore, further clinical studies are warranted to assess the true stabilizing role of the K-wire *in vivo*.

The complex forces acting on the surgery site, *in vivo,* are virtually impossible to reproduce. In our *in vitro* monotonic unidirectional study, we tried to simulate the distractive forces that act on the distal TT. Ideally, *in vivo,* the long axis of the implants should be parallel to the distraction force acting on the surgical site (Johnston et al., 2012). Thus, the distraction forces applied to the samples were parallel to the long axis of the implants. In the MMP, it is recommended that the long axis of the implants to be cranially directed, at 45º to the tibial long axis, to counteract the forces acting on that site (Ness, 2011; Ness, 2013). To the author's knowledge, the canine *in vivo* forces at that site have not been characterized thus far and there are no studies supporting that value. However, it has been suggested that the forces leading to distal tibial avulsion are a consequence of an enhancement of mainly the caudally (Ness,

2013) or the vertically (Etchepareborde et al., 2010) directed component of the quadriceps pull force applied to the TT.

It should also be noted that our study neglects the cyclical loading withstood by the TT during the postoperative period. This, together with the aforementioned limitations, emphasizes the fact that drawing any clinical transpositions based on our results should be done with great care.

After a porous implant has been left *in situ*, the physiological response of the organism is similar to the healing cascade of a cancellous defect, with the pores of the implant being filled with the newly formed tissue (Kienapfel, Sprey, Wilke, & Griss, 1999). The void space is filled with blood that forms a haematoma, then followed by infiltration of mesenchymal cells, ending up being replaced by woven bone. Shortly after, lamellar bone remodeling occurs, together with bone marrow reestablishment (Kienapfel et al., 1999). There is no fibrocartilagenous phase, resembling primary fracture healing (Kienapfel et al., 1999), where stability is of utmost importance for optimal osteosynthesis (Cross, 2012). Therefore, the eventual clinical success of porous implant fixation, by osseointegration and bone ingrowth, relies on the stability of the implant-bone interface (Kienapfel et al., 1999). Osseointegration refers to the intimate, rigid, stable implant-bone anchorage (Simmons et al., 1999; Kienapfel et al., 1999; Albrektsson & Johansson, 2001), and bone ingrowth can be defined as the formation of osseous tissue within a porous implant (Kienapfel et al., 1999). Several studies have shown that an impaired interface stability results in poor osseointegration and suboptimal bone ingrowth. In the early 1970's, Cameron, Pilliar, & Macnab (1973) reported the absence of bone ingrowth in the porous-coated surface of a metal implant subjected to macromovement, and suggested it would occur in the presence of micromovement. In a study by Ducheyne and colleagues (1977), bone ingrowth was not found in the dynamically loaded porous-surfaced metal implants, but was evident in the statically loaded. In addition, they observed periosteal reaction and peri-implant osteolysis in the dynamically loaded implants. Bone growth at the implant-bone interface has been documented to happen under micromovement, as Cameron et al. (1973) suggested, but its presence and histological properties depend on the extent of that motion. Pilliar, Lee, & Maniatopoulos (1986) observed stable bone growth with up to 28 μm of movement, in porous-coated metal implants. Bragdon and colleagues (1996) reported stable overall osseous continuity with 20 μm of motion, in porous titanium implants. However, at 40 μm, osseous continuity at the interface became irregular, and bone tissue was intercalated with fibrocallus. Jasty, Bragdon, Zalenski, et al. (1997), on the other hand, observed interface bone growth with axial and rotational

micromovement up to 42 μm and 56 μm, respectively, in canine porous-coated titanium femoral stem prostheses. In spite of that, the majority of the prostheses with bone growth presented motions of less than 10 μm. In a different study by Jasty, Bragdon, Burke, et al. (1997), using porous-coated titanium implants, the findings were similar to those of Bragdon and colleagues (1996), with formation of stable bone happening at 20 μm of motion, and a mixture of bone and fibrous or fibrocartilaginous tissue at 40 μm of micromovement. The micromovement threshold that dictates absence of bone growth at the implant-bone interface has been widely investigated. Several studies have shown that, from 150 μm of relative motion between the surfaces, bone growth at the interface does not occur (Pilliar et al., 1986; Søballe, Hansen, Brockstedt-Rasmussen, Jørgensen, & Bünger, 1992; Søballe, Brockstedt-Rasmussen, Hansen, & Bünger, 1992; Bragdon et al., 1996; Jasty, Bragdon, Burke, et al., 1997). Instead, interface stability is kept by the presence of well-organized fibrous and fibrocartilagenous tissue (Pilliar et al., 1986; Søballe, Hansen, et al., 1992; Søballe, Brockstedt-Rasmussen, et al., 1992; Bragdon et al., 1996; Jasty, Bragdon, Burke, et al., 1997). Furthermore, Bragdon et al. (1996) and Jasty, Bragdon, Burke, et al. (1997) found stable bone ingrowth in their porous titanium implants, suggesting that this degree of micromovement affects bone healing at the interface but not within the implant. It has also been shown that the initial instability will affect the mechanical properties of the interface, with the amount of micromovement being inversely related with interface stiffness (Bragdon et al., 1996; Jasty, Bragdon, Burke, et al., 1997).

Even though the goal of the implants placed at the distal TT in the MMP is mainly providing additional support to the TT instead of absolute wedge-bone fixation, it seems sensible to admit that the ideal implant for that function would still be the one that gathers the best mechanical properties which allow maximal stability.

Our displacement findings showed that, despite the lack of significant differences between groups 1.2, 1.6, and 2.0 regarding D_{100}, the differences gradually increased with increasing loads, until D_{FAIL} became significantly different between all the groups. That can be explained by the stiffness of each type of implant. A stiffer construct allows less displacement at each load (Cheng et al., 1993), hence, given the stiffness results for these groups (1.6 being stiffer than 1.2, and 2.0 stiffer than 1.6), the progressive increase in displacement differences is not a surprise. Regarding groups 0.8 and 1.0, displacement was already significantly different between each other and the remaining groups at only 100 N, suggesting that these implants will allow more movement than the remaining groups at low loads. In fact, group 0.8's D_{100} (2.9 ± 0.5 mm) was bigger than 2.0's D_{FAIL} (2.6 ± 0.3 mm), and group 1.0's D_{100} (1.4 ± 0.6

mm) registered more than half of 2.0's D_{FAIL} (2.9 ± 0.5 mm). Mean D_{200} for group 0.8 is a result of only 4 samples because the remaining 6 failed before reaching 200 N, as suggested by the mean LTF of the group (i.e. 195.9 ± 15.8 N). This aspect may help to clarify why group 0.8 allowed significantly larger displacements than group 1.0 at 100 N and 200 N, but, at failure, the larger displacements were observed in group 1.0 instead. An explanation may rely on the fact that, in group 0.8, the loads applied for D_{FAIL} were similar to the ones for D_{200} and, therefore, resulted in comparable displacements. Displacement can also depend on the amount of wire used for the twist (Meyer et al., 2003). We believe, however, that the observed differences were not influenced by this factor because all the twists were cut at the same size. The increase in displacement from D_{200} to D_{FAIL} in group 0.8 may be explained by a lower stiffness of the 6 samples that did not reach 200 N, as they would allow more displacement before failing. Increasing displacement leads to an increase in relative motion and consequent instability. Hence, the ideal implant would be the one that allows the least displacement. Our results demonstrated that the staples generally allowed less displacement than the wire, being therefore more advantageous. From the two types of staple, the 2.0 mm staple was the implant that allowed less displacement with increasing loads, with a D_{100} of 0.6 ± 0.1 mm, D_{200} of 1.3 ± 0.1 mm and D_{FAIL} of 2.6 ± 0.3 mm.

In our study, MOF was characterized as either implant or block failure. Implant failure occurred in groups 0.8 and 1.0 only, and resulted from failure of the figure-of-eight wire. Clinical failure of orthopaedic wire occurs by single high load fracture, fatigue fracture, or loosening without fracture, with fatigue fracture being the most frequent MOF (Bostrom et al., 1994). *In vitro*, the pattern appears to be different, with plenty of studies documenting untwisting as the typical MOF of unbent twist knots (Wilson et al., 1985; Guadagni & Drummond, 1986; Bostrom et al., 1994; Roe, 1997; Meyer et al., 2003). Our findings agree with the ones in the literature, with untwisting being the cause of implant failure in all samples from groups 0.8 and 1.0. In 2010, Etchepareborde and colleagues have also reported wire breakage as MOF, in addition to knot untwisting. The fact that all the specimens within a group failed in the same way, suggests that we may have been able to achieve minimal inter-specimen variability, supporting our assembly methods. Groups 1.2, 1.6, and 2.0, on the other hand, failed by block breakage. In these groups, the block was the portion of the construct to collapse, meaning that failure ultimately resulted from the properties of the blocks rather than the implants. This finding alone suggests that the implants from these three groups are stronger than those of the 0.8 and 1.0 groups, explaining therefore why samples from group 1.2 did not fail by untwisting as occurred in the remaining wire groups. A connection can be

established between the observed MOF and the trace of the load-displacement curves. In the 0.8 and 1.0 wire groups, there is a gradual decrease in post-failure resistance, which reflects the gradual untwisting of the knot, as opposed to the drastic reduction in post-failure resistance observed in the other groups, reflecting the sudden breakage of a block.

Our findings showed that samples in group 1.2 were able to withstand the highest loads (401.1 ± 19.5 N), as opposed to group 0.8 which registered the lowest LTF values (195.9 ± 15.8 N). Groups 1.0, 1.6, and 2.0 were in between, reaching 319.2 ± 21.3 N, 312.4 ± 15.2 N, and 314.8 ± 26.3 N, respectively, where no significant difference was found in their LTF values. Several studies have shown that an increase in wire diameter results in higher LTF values (Wilson et al., 1985; Guadagni & Drummond, 1986; Bostrom et al., 1994; Meyer et al., 2003; Wähnert et al., 2011). Indeed, it has been reported that the tensile strength of 1.2 mm and 0.8 mm diameter wire is 1.4 and 0.64 times that of 1.0 mm wire, respectively (Roe, 2003). Increasing resistance is related with the structural properties of the wire. Tensile strength is related to the cross-sectional area ($\pi \times \text{radius}^2$), therefore, it increases considerably with small increases in diameter (Johnston et al., 2012). Besides, increasing diameter results in a larger contact area and higher friction between the two wire surfaces of the knot, thus leading to a higher resistance (Wilson et al., 1985). In fact, Wilson et al. (1985) and Meyer et al. (2003) observed that a 50% increase in wire diameter resulted in an increase in LTF of approximately 128%, and up to 169%, respectively. Our findings are similar to those documented in the literature, as we have observed an increase in LTF with increasing wire diameter. Values of LTF, and corresponding wire size and knot features from several biomechanical studies using unbent twist knots can be found in Annex 8. In a study by Roe (1997) using 1.0 mm wire, it was observed that the ultimate load that reduced twist knot tension below 30 N (the value considered to correspond to failure) was of 259.8 N. Our results regarding wire LTF appear to be lower than those observed in other studies, particularly with the one with the most similar design (Etchepareborde et al., 2010). Differences may be explained by variations in study design, such as the number of knots used, initial knot tension, cut-related variability, and the testing of a construct rather than solely a knot. When compared with the two studies that used two knots, our findings seem to be comparable with those of Guadagni and Drummond (1986) only. In that study, it was shown that the addition of the second knot reduces LTF in 25%, hence, comparison with studies using a single knot may be limited. Interestingly, when applying Guadagni and Drummond's (1986) observations to the LTF obtained in the studies using single knots (i.e. multiplying LTF values by 0.75), the results are more comparable with ours, suggesting then that the

number of knots may have had some influence in the differences observed (Annex 8). Meyer et al. (2003) have shown the effect of knot tension on ultimate LTF in twist knots, using 1.0 and 1.2 diameter wire. In their study, they observed an increase in LTF values with increasing pre-testing tension. In our experiment, the knots were twisted until a snug fit of the blocks was obtained, rather than true compression, which means that maximal knot tension may not have been achieved. Hence, a lower knot tension may have led to lower LTF values than those of other studies. Because pre-testing knot tension was not measured in this study, its true effect on LTF could not be quantified. According to Meyer and colleagues (2003), it seems reasonable to conclude that any disturbance to knot tension is expected to negatively affect LTF. Several studies have investigated the effect of post-twisting knot manipulation, particularly the effects of bending and cutting. As previously discussed in this dissertation, by keeping the knots unbent, we believe we were able to rule out the detrimental effects of bending on the knot's mechanical properties, including knot tension. However, we did cut the knots after twisting, which has been shown to reduce knot tension (Rooks et al., 1982; Roe, 2002; Wähnert et al., 2011; Johnston et al., 2012). Cutting induces loosening of the twist and a decrease in friction, ultimately resulting in lower knot tension (Rooks et al., 1982). Rooks and colleagues (1982) observed a 12% decrease in tension following cutting. A study by Roe (2002) showed that cutting causes a loss of 20% in tension. More recently, it has been shown that the loss of tension depends on the place where the cut is performed. In that study, Wähnert et al., (2011) observed that cutting the wire within the twist causes 44% loss in tension, and cutting the protrusions causes 12% loss. Hence, with its associated variability, cutting the twist may have had some influence in the differences observed regarding LTF between other studies and ours. Another aspect that may have contributed to our lower LTF values when compared to those of other studies, specifically the values observed in group 1.2, is the fact that we tested constructs instead of just an implant. The constructs in that group failed by block breakage, suggesting that the implant might have been able to withstand higher loads and, consequently, that the observed LTF values do not reflect its actual strength. The relation between LTF and MOF for groups 1.0, 1.6, and 2.0 is noteworthy as well. Although there were no significant differences in LTF between those groups, samples in group 1.0 failed by untwisting while ones in groups 1.6 and 2.0 failed by block breakage, also suggesting that the actual ultimate strength of the staples was not reached. In spite of sharing the same MOF (block breakage), group 1.2's LTF was significantly higher than that of the staple groups. Because the blocks have the same properties, one would expect them to fail at similar LTF, regardless of the implant. We believe the differences observed were due to the

stress at the implant-block contact area. In the case of the staples there is a smaller implant-block contact area than in the 1.2 mm wire samples and, consequently, a higher stress concentration at the implant-block interface. In the 1.2 mm wire samples, the implant-block contact area is larger, so the load applied to the specimen is spread more widely, leading to lower stress concentrations at the implant-block interface, resulting in greater loads before failure of the block. The ultimate LTF measures the force that is necessary to apply to catastrophically destroy a construct (Cohen & Griffin, 2002). Evidently, for this variable, higher values are preferable. Hence, group 1.2 has shown to be the most advantageous in terms of ultimate strength of the constructs.

Because we tested constructs (block-implant-block) rather than just an implant, we were testing the properties of the blocks, of the implants, and also the structural properties of the constructs as a whole. Hence, we found some particular features in the traces of the load-displacement curves. In all the staple specimens and in the majority of the 1.2 wire, we observed a brief, frequently biphasic, loss of resistance on the first third of the straight portion of the curve. We suspect it was caused by the wire cutting into the edges of the blocks, and, similarly, by the serrated portion of the staple into the blocks. It seems, therefore, that was the point when maximal implant-block coaptation was reached. When it happened in two phases, each phase corresponded to the moment when it occurred on each block. From then on, the curve returned to its straight fashion, with each unit of force resulting in the same increment in displacement. That would be typical of the elastic phase, during which any deformation suffered by the construct under load is returned to its pre-loaded state when the load is removed (Cheng et al., 1993; Cohen & Griffin, 2002). However, as mentioned before, on our tests we were applying tension to a structure. Thus, for the wire samples, although there was a linear portion of the load-displacement curve, that coincided with steady, gradual unravelling of the wire, which is an irreversible process. If the load had been withdrawn, the construct would not have gone back to its starting point. With the staples, the curves we obtained were closer to a true material test of the implant. However, the lack of a true linear portion, which was instead a gently convex line, is probably a combination of the material elasticity of the implant with the structural characteristics of the staple legs being distracted superimposed. It is then important to highlight that the linear portion of the curve was not analogous to the usual elastic deformation part of a typical material test. This corresponded to a structure test, not a simple material test. Stiffness measures the rate at which a construct deforms when under tension load (Cross, 2012), i.e. measures the recoverable deformation under loading (Cohen & Griffin, 2002). Therefore, it is calculated by finding the slope of the straight portion

(Cheng et al., 1993; Cohen & Griffin, 2002; Cross, 2012). STIF was thus measured on the straight portion of the curve. However, it is important to mention that, on our case, deformation of a wire sample was not recoverable. In spite of that, we were still measuring stiffness, i.e. the amount of displacement per unit of load. Our results showed that the 2.0 staple constructs were significantly stiffer than the remaining constructs at 142.2 ± 19.9 N/mm. In fact, mean STIF of group 2.0 was 3.7 times that of the stiffest wire group, group 1.2 (37.6 ± 2.0 N/mm). This finding is not surprising as it is the lower stiffness that makes the wire compliant enough to be handled and twisted. When comparing STIF of the two staple groups, we can observe that an increase of 0.4 mm in staple width resulted in an increase of 44.7% in construct STIF. These results are useful to compare our findings regarding displacement and LTF. Group 1.2 had the highest LTF but was significantly more displaced at 100 and 200 N than group 2.0, meaning that, given its lower stiffness, the higher LTF was achieved at the cost of a higher displacement. The opposite appears to have occurred with samples from group 2.0, which, with their high stiffness, allowed minimal displacements, but were significantly weaker than those of group 1.2. No significant differences in STIF were found between the wire groups. Nevertheless, there was a trend for the bigger wires to be stiffer, which would be consistent with the fact that stiffness is directly related with cross-sectional area (Baumgart, 2000). However, the STIF values we obtained were related to the construct and not to a single strand of wire. Stiffness is not only related with the material properties of the wire, but also with the number of wires bearing the load and type of knot (Roe, 1997). In our case, stiffness was influenced by several other factors apart from the material properties of the wire, which included block stiffness (the same for every group), shape of construct (similar between groups), and type of knot (again, almost identical between groups). Despite the influence of an increasing wire diameter on STIF, all these factors may have contributed to the lack of significant differences between the wire groups. Therefore, a type II statistical error may have been present, and a higher number of samples might have demonstrated a significant difference between these groups. Stiffness quantifies the fixation stability of an implant (Cheng et al., 1993). In general, an implant with higher stiffness is preferable, as it is more stable, and produces less motion at each load when compared with an implant with lower stiffness (Cheng et al., 1993; Cohen & Griffin, 2002). Hence, regarding STIF, group 2.0 seems to be more advantageous than the other groups, particularly when compared with any of the wire groups.

Yield point (YP) is the point at which increasing displacement is not accompanied by increasing resistance (Blass et al., 1986). Generally, from this point, transition from elastic to plastic phase occurs, where any strain developed by the construct results in permanent deformation (Blass et al., 1986; Cheng et al., 1993; Cohen & Griffin, 2002; Cross, 2012). The Yield Load (YL) is the load registered at YP. In our case, the YP and YL are not analogous to the normal yield point and yield load at all, due to the fact that before that point the deformation was not recoverable. It appears that from that point the structure starts to fail. Nevertheless, a higher YL is preferable for both wire and staple, as it implies that the construct would need to be subjected to higher loads to start failing. The group that presented highest mean YL was group 1.2 at 324.0 ± 14.3 N, followed by group 1.0 at 264.0 ± 18.4 N. Groups 1.6 and 2.0 registered YL lower than group 1.0, and, similarly to what happened with LTF, no significant differences were found between the two groups. Mean YL was lowest for group 0.8. Therefore, as far as YL is concerned, samples from group 1.2 appear to be more advantageous, being the ones that can resist the highest loads without starting to fail. Yield Load values, respective wire diameters, and knot features found in several biomechanical studies can be found in Annex 9. Similar to what happened with LTF, we observed an increase in YL with increasing wire diameter, which is in agreement with the findings of Wilson (1988). In general, our findings regarding YL are lower than those found in the majority of the literature. This may be explained by the same reasons aforementioned for LTF. Assuming that the findings of Guadagni and Drummond (1986) regarding LTF (i.e. loss of 25% strength when using two knots instead of one) would apply to YL, it is not a surprise to observe these differences between our values and those of others, as in all of the mentioned studies only one knot was used. However, to the author's knowledge, there are no studies comparing the effect of the number of knots on YL. In addition, according to the findings of Meyer et al. (2003) (i.e. LTF is lower in knots with lower tension), we would expect that tying the figure-of-eight until a snug fit is achieved rather than compression and the possible decrease in tension caused by cutting the knot would result in lower YL, in the same way as for LTF. However, it is very important to mention once again the fact that, in our case, our YL marked the point from which the structure started to fail. In our study we identified the YP visually (Roe, 1997). Similar to what had happened with Roe (1997), we found that accurately identifying the YP proved sometimes to be a challenge, given the gradual transition from the straight portion to the curved one, particularly in the staple groups. In spite of that, we still believe it provided acceptable YL results. By using this method, some error was introduced, accounting therefore as another limitation in this study.

V. Conclusion

The MMT is a relatively new technique, having passed only 4 years since the publication of the first study describing it. It seems to be gaining popularity and being the focus of increasingly more investigations, with long-term clinical studies now starting to appear and showing promising results. The MMP was launched approximately 1 year after the first study regarding the MMT and thus far there has yet to be published a study focusing on this procedure. It shares the same rationale of the MMT but the methods differ slightly. In addition to the use of a titanium wedge for advancement of the TT, figure-of-eight orthopaedic wire or a surgical staple provide additional support to the distal TT. In this study we compared several mechanical parameters of five different types of distal TT fixation, in an attempt to assess which one provided the most advantages. We compared the implants regarding their load to failure, yield load, stiffness, and displacement, as we believe these parameters are clinically relevant.

Based on the variables investigated in our study, the ideal implant would have the highest yield load, load to failure, and stiffness, and allow the least displacement. As expected, the size of the wire influenced some of the parameters. LTF and YL were directly related to wire size, and, in contrast, displacement was inversely related. Our findings show that group 1.2 was superior to the remaining wire groups in all but one parameter, STIF. In spite of that, samples from group 1.2 allowed significantly less displacement than the remaining wire samples, at any load. Furthermore 1.2 wire specimens showed to be stronger, yielding and failing at significantly higher loads. To the author's knowledge, this was the first study to use titanium orthopaedic staples. Given their significantly higher STIF, the staple constructs allowed significantly lower D_{200} and D_{FAIL} than the wire samples. Nevertheless, the 1.2 mm wire samples failed at significantly higher loads than both the types of staple specimens. The 1.0 wire samples showed significantly higher YL, albeit showing no significant differences in LTF. Samples from groups 1.2, 1.6, and 2.0 failed by block breakage instead of implant failure. Hence, these implants proved to be more advantageous than those from groups 0.8 and 1.0, as the MOF implies that the implants were strong enough to withstand the higher loads. However, it should be noted that the wire samples were only able to resist higher loads than the staple samples at the cost of displacement, and that they allowed an irreversible displacement, even under modest loads. Thus, it appears that the staples may be more advantageous, because, even though they did not present the highest construct LTF, they

allowed the lowest displacement, resulting in minimal movement at the site. Our findings have shown that the two sizes of staples lead to similar construct properties. No significant differences were found between the means of the staple groups in four of the six parameters we investigated. The variables where we observed significant differences were D_{FAIL} and STIF, with group 2.0 showing significantly higher STIF and significantly lower D_{FAIL} than group 1.6. The lower values of D_{FAIL} are expected as a result of the higher values of STIF. An increase in width of 0.4 mm resulted in an increase of almost 50% in STIF. These results show that it would be mechanically advantageous to use the 2.0 mm staples, as they provide more stability than the 1.6 mm. Therefore, we may conclude that, despite not having achieved the best results in all the parameters, the 2.0 mm staple is the implant that proved to be the most advantageous. In addition, given the poorer performance of 0.8 mm and 1.0 mm wire, we would not recommend their use.

It has been shown that fatigue greatly reduces wire strength. However, the effect of fatigue in staple efficiency is still unknown. Because we used a static model, we did not replicate the systematic loading-unloading cycles observed *in vivo*. In addition, the true forces acting *in vivo* at the surgical site are still unknown, preventing a more accurate simulation of their action. These factors dramatically limit the transposition of these results to practice. Therefore, it would be interesting to test our assumptions in a clinical study. Only then we would be able to validate the clinical relevance of the mechanical advantages.

Our findings are a result of static *in vitro* study and should be interpreted as such, and any transposition should be done with great prudency. In spite of the inherent limitations, we believe our preliminary study has provided valid, interesting data, which may have opened doors to further investigations.

References

Albrektsson, T., & Johansson, C. (2001). Osteoinduction, osteoconduction and osseointegration. *European Spine Journal*, *10*(2), S96–S101.

Allan, R. M. (2014). A modified Maquet technique for management of cranial cruciate avulsion in a cat. *Journal of Small Animal Practice*, *55*(1), 52–56.

American Society for Testing and Materials. (2012). *ASTM F1839-08, Specification for Rigid Polyurethane Foam for Use as a Standard Material for Testing Orthopaedic Devices and Instruments*. West Conshohocken: ASTM. Retrieved October 14, 2014, from http://www.astm.org/Standards/F1839.htm

Anderst, W. J., & Tashman, S. (2009). The association between velocity of the center of closest proximity on subchondral bones and osteoarthritis progression. *Journal of Orthopaedic Research*, *27*(1), 71–77.

Apelt, D., Kowaleski, M. P., & Boudrieau, R. J. (2007). Effect of Tibial Tuberosity Advancement on Cranial Tibial Subluxation in Canine Cranial Cruciate-Deficient Stifle Joints: An In Vitro Experimental Study. *Veterinary Surgery*, *36*(2), 170–177.

Aragon, C. L., & Budsberg, S. C. (2005). Applications of evidence-based medicine: cranial cruciate ligament injury repair in the dog. *Veterinary surgery: VS*, *34*(2), 93–98.

Arcand, M. A., Rhalmi, S., & Rivard, C.-H. (2000). Quantification of mechanoreceptors in the canine anterior cruciate ligament. *International Orthopaedics*, *24*(5), 272–275.

Arnault, F., Cauvin, E., Viguier, E., Kraft, E., Sonet, J., & Carozzo, C. (2009). Diagnostic value of ultrasonography to assess stifle lesions in dogs after cranial cruciate ligament rupture: 13 cases. *Veterinary and Comparative Orthopaedics and Traumatology: V.C.O.T*, *22*(6), 479–485.

Arnoczky, S. P., & Marshall, J. L. (1977). The cruciate ligaments of the canine stifle: an anatomical and functional analysis. *American Journal of Veterinary Research*, *38*(11), 1807–1814.

Arnoczky, S. P., Rubin, R. M., & Marshall, J. L. (1979). Microvasculature of the cruciate ligaments and its response to injury. An experimental study in dogs. *The Journal of Bone & Joint Surgery*, *61*(8), 1221–1229.

Arnoczky, S. P., Tarvin, G. B., & Marshall, J. L. (1982). Anterior cruciate ligament replacement using patellar tendon. An evaluation of graft revascularization in the dog. *The Journal of Bone and Joint Surgery. American Volume*, *64*(2), 217–224.

Arnoldy, C. (2011). Rehabilitation for Dogs with Cranial Cruciate Ligament Rupture. In P. Muir (Ed.), *Advances in the Canine Cranial Cruciate Ligament* (pp. 249–253). John Wiley & Sons.

Au, K. K., Gordon-Evans, W. J., Dunning, D., O'dell-Anderson, K. J., Knap, K. E., Griffon, D., & Johnson, A. L. (2010). Comparison of Short- and Long-term Function and Radiographic Osteoarthrosis in Dogs After Postoperative Physical Rehabilitation and Tibial Plateau Leveling Osteotomy or Lateral Fabellar Suture Stabilization. *Veterinary Surgery*, *39*(2), 173–180.

Baril, E., Lefebvre, L. P., & Hacking, S. A. (2011). Direct visualization and quantification of bone growth into porous titanium implants using micro computed tomography. *Journal of Materials Science: Materials in Medicine*, *22*(5), 1321–1332.

Barthelemy, N., Ramirez, J. M., Noel, S., Claeys, S., Farnir, F., & Balligand, M. (2014). Modified maquet technique for treatment of canine cranial cruciate ligament injury: early results, complications and risk factors in 109 dogs. In S. Baines & M. Owen (Eds.), *Proceeding of the European College of Veterinary Surgeons Annual Scientific Meeting, 2014* (p. 226). Copenhagen, Denmark: ECVS.

Baumgart, E. (2000). Stiffness--an unknown world of mechanical science? *Injury*, *31 Suppl 2*, S–B14–23.

Beale, B., & Hulse, D. A. (2011). Arthroscopy versus Arthrotomy for Surgical Treatment. In P. Muir (Ed.), *Advances in the Canine Cranial Cruciate Ligament* (pp. 145–158). John Wiley & Sons.

Blass, C. E., Piermattei, D. L., Withrow, S. J., & Scott, R. J. (1986). Static and Dynamic Cerclage Wire Analysis. *Veterinary Surgery*, *15*(2), 181–184.

Bostrom, M. P., Asnis, S. E., Ernberg, J. J., Wright, T. M., Giddings, V. L., Berberian, W. S., & Missri, A. A. (1994). Fatigue testing of cerclage stainless steel wire fixation. *Journal of Orthopaedic Trauma*, *8*(5), 422–428.

Böttcher, P., & Rey, J. (2010). In vivo kinematics of the canine stifle. *Proceedings of the 15th ESVOT Congress* (pp. 58–59). Bologna, Italy: ESVOT.

Boudrieau, R. J. (2009). Tibial Plateau Leveling Osteotomy or Tibial Tuberosity Advancement? *Veterinary Surgery*, *38*(1), 1–22.

Boudrieau, R. J. (2011). Tibial Tuberosity Advancement. In P. Muir (Ed.), *Advances in the Canine Cranial Cruciate Ligament* (pp. 177–187). John Wiley & Sons.

Bragdon, C. R., Burke, D., Lowenstein, J. D., O'Connor, D. O., Ramamurti, B., Jasty, M., & Harris, W. H. (1996). Differences in stiffness of the interface between a cementless porous implant and cancellous bone in vivo in dogs due to varying amounts of implant motion. *The Journal of Arthroplasty*, *11*(8), 945–951.

Bree, H. van, Rooster, H. de, & Gielen, I. (2011). Stress Radiography of the Stifle. In P. Muir (Ed.), *Advances in the Canine Cranial Cruciate Ligament* (pp. 113–116). John Wiley & Sons.

Bruin, T. de, Rooster, H. de, Bosmans, T., Duchateau, L., Bree, H. van, & Gielen, I. (2007). Radiographic assessment of the progression of osteoarthrosis in the contralateral stifle

joint of dogs with a ruptured cranial cruciate ligament. *Veterinary Record*, *161*(22), 745–750.

De Bruin, T., de Rooster, H., van Bree, H., & Cox, E. (2007). Evaluation of anticollagen type I antibody titers in synovial fluid of both stifle joints and the left shoulder joint of dogs with unilateral cranial cruciate disease. *American Journal of Veterinary Research*, *68*(3), 283–289.

Brunel, L., Etchepareborde, S., Barthélémy, N., Farnir, F., & Balligand, M. (2013). Mechanical testing of a new osteotomy design for tibial tuberosity advancement using the Modified Maquet Technique. *Veterinary and Comparative Orthopaedics and Traumatology: V.C.O.T*, *26*(1), 47–53.

Buote, N., Fusco, J., & Radasch, R. (2009). Age, Tibial Plateau Angle, Sex, and Weight as Risk Factors for Contralateral Rupture of the Cranial Cruciate Ligament in Labradors. *Veterinary Surgery*, *38*(4), 481–489.

Butler, D. L., Hulse, D. A., Kay, M. D., Grood, E. S., Shires, P. K., D'ambrosia, R., & Shoji, H. (1983). Biomechanics of Cranial Cruciate Ligament Reconstruction in the Dog II. Mechanical Properties. *Veterinary Surgery*, *12*(3), 113–118.

Cabrera, S. Y., Owen, T. J., Mueller, M. G., & Kass, P. H. (2008). Comparison of tibial plateau angles in dogs with unilateral versus bilateral cranial cruciate ligament rupture: 150 cases (2000–2006). *Journal of the American Veterinary Medical Association*, *232*(6), 889–892.

Calvert, K. L., Trumble, K. P., Webster, T. J., & Kirkpatrick, L. A. (2010). Characterization of commercial rigid polyurethane foams used as bone analogs for implant testing. *Journal of Materials Science: Materials in Medicine*, *21*(5), 1453–1461.

Cameron, H. U., Pilliar, R. M., & Macnab, I. (1973). The effect of movement on the bonding of porous metal to bone. *Journal of Biomedical Materials Research*, *7*(4), 301–311.

Carobbi, B., & Ness, M. G. (2009). Preliminary study evaluating tests used to diagnose canine cranial cruciate ligament failure. *Journal of Small Animal Practice*, *50*(5), 224–226.

Cheng, W., Cameron, D. E., Warden, K. E., Fonger, J. D., & Gott, V. L. (1993). Biomechanical study of sternal closure techniques. *The Annals of Thoracic Surgery*, *55*(3), 737–740.

Cheung, S., Gauthier, M., Lefebvre, L.-P., Dunbar, M., & Filiaggi, M. (2007). Fibroblastic interactions with high-porosity Ti-6Al-4V metal foam. *Journal of Biomedical Materials Research Part B: Applied Biomaterials*, *82B*(2), 440–449.

Christopher, S. A., Beetem, J., & Cook, J. L. (2013). Comparison of Long-Term Outcomes Associated With Three Surgical Techniques for Treatment of Cranial Cruciate Ligament Disease in Dogs. *Veterinary Surgery*, *42*(3), 329–334.

Cohen, C. D. J., & Griffin, L. V. (2002). A biomechanical comparison of three sternotomy closure techniques. *The Annals of Thoracic Surgery*, *73*(2), 563–568.

Comerford, E. J. (2011). Stifle Morphology. In P. Muir (Ed.), *Advances in the Canine Cranial Cruciate Ligament* (pp. 65–69). John Wiley & Sons.

Comerford, E. J., Smith, K., & Hayashi, K. (2011). Update on the aetiopathogenesis of canine cranial cruciate ligament disease. *Veterinary and Comparative Orthopaedics and Traumatology: V.C.O.T*, *24*(2), 91–98.

Comerford, E. J., Tarlton, J. F., Avery, N. C., Bailey, A. J., & Innes, J. F. (2006). Distal femoral intercondylar notch dimensions and their relationship to composition and metabolism of the canine anterior cruciate ligament. *Osteoarthritis and cartilage / OARS, Osteoarthritis Research Society*, *14*(3), 273–278.

Comerford, E. J., Tarlton, J. F., Innes, J. F., Johnson, K. A., Amis, A. A., & Bailey, A. J. (2005). Metabolism and composition of the canine anterior cruciate ligament relate to differences in knee joint mechanics and predisposition to ligament rupture. *Journal of*

Orthopaedic Research: Official Publication of the Orthopaedic Research Society, *23*(1), 61–66.

Conzemius, M. G., Evans, R. B., Besancon, M. F., Gordon, W. J., Horstman, C. L., Hoefle, W. D., Nieves, M. A., et al. (2005). Effect of surgical technique on limb function after surgery for rupture of the cranial cruciate ligament in dogs. *Journal of the American Veterinary Medical Association*, *226*(2), 232–236.

Cook, C. (2011). Stifle Ultrasonography. In P. Muir (Ed.), *Advances in the Canine Cranial Cruciate Ligament* (pp. 117–121). John Wiley & Sons.

Cook, J. L. (2010). Cranial Cruciate Ligament Disease in Dogs: Biology versus Biomechanics. *Veterinary Surgery*, *39*(3), 270–277.

Cook, J. L. (2011). Extracapsular Stabilization. In P. Muir (Ed.), *Advances in the Canine Cranial Cruciate Ligament* (pp. 163–168). John Wiley & Sons.

Cook, J. L., Evans, R., Conzemius, M. G., Lascelles, B. D. X., McIlwraith, C. W., Pozzi, A., Clegg, P., et al. (2010). Proposed Definitions and Criteria for Reporting Time Frame, Outcome, and Complications For Clinical Orthopedic Studies in Veterinary Medicine. *Veterinary Surgery*, *39*(8), 905–908.

Cook, J. L., Luther, J. K., Beetem, J., Karnes, J., & Cook, C. R. (2010). Clinical Comparison of a Novel Extracapsular Stabilization Procedure and Tibial Plateau Leveling Osteotomy for Treatment of Cranial Cruciate Ligament Deficiency in Dogs. *Veterinary Surgery*, *39*(3), 315–323.

Cross, A. R. (2012). Fracture Biology and Biomechanics. In K. M. Tobias & S. A. Johnston (Eds.), *Veterinary Surgery: Small Animal* (pp. 565–571). Saint Louis: Elsevier Saunders.

DeAngelis, M., & Lau, R. E. (1970). A lateral retinacular imbrication technique for the surgical correction of anterior cruciate ligament rupture in the dog. *Journal of the American Veterinary Medical Association*, *157*(1), 79–84.

DeCamp, C. E., Riggs, C. M., Olivier, N. B., Hauptman, J. G., Hottinger, H. A., & Soutas-Little, R. W. (1996). Kinematic evaluation of gait in dogs with cranial cruciate ligament rupture. *American Journal of Veterinary Research*, *57*(1), 120–126.

Dennler, R., Kipfer, N. M., Tepic, S., Hassig, M., & Montavon, P. M. (2006). Inclination of the patellar ligament in relation to flexion angle in stifle joints of dogs without degenerative joint disease. *American Journal of Veterinary Research*, *67*(11), 1849–1854.

Denny, H., & Butterworth, S. (2000). Options in Fracture Management. *A Guide to Canine and Feline Orthopaedic Surgery* (4th ed., pp. 87–131). John Wiley & Sons.

Dickinson, C. R., & Nunamaker, D. M. (1977). Repair of ruptured anterior cruciate ligament in the dog: experience in 101 cases, using a modified fascia strip technique. *Journal of the American Veterinary Medical Association*, *170*(8), 827–830.

Drygas, K. A., Pozzi, A., Goring, R. L., Horodyski, M., & Lewis, D. D. (2010). Effect of Tibial Plateau Leveling Osteotomy on Patellar Tendon Angle: A Radiographic Cadaveric Study. *Veterinary Surgery*, *39*(4), 418–424.

Ducheyne, P., De Meester, P., Aernoudt, E., Martens, M., & Mulier, J. C. (1977). Influence of a functional dynamic loading on bone ingrowth into surface pores of orthopedic implants. *Journal of Biomedical Materials Research*, *11*(6), 811–838.

Duval, J. M., Budsberg, S. C., Flo, G. L., & Sammarco, J. L. (1999). Breed, sex, and body weight as risk factors for rupture of the cranial cruciate ligament in young dogs. *Journal of the American Veterinary Medical Association*, *215*(6), 811–814.

Etchepareborde, S., Barthelemy, N., Brunel, L., Claeys, S., & Balligand, M. (2014). Biomechanical testing of a β-tricalcium phosphate wedge for advancement of the tibial tuberosity. *Veterinary and Comparative Orthopaedics and Traumatology: V.C.O.T*, *27*(1), 14–19.

Etchepareborde, S., Barthelemy, N., Mills, J., Pascon, F., Ragetly, G. R., & Balligand, M. (2010). Mechanical testing of a modified stabilisation method for tibial tuberosity advancement. *Veterinary and Comparative Orthopaedics and Traumatology: V.C.O.T*, *23*(6), 400–405.

Etchepareborde, S., Brunel, L., Bollen, G., & Balligand, M. (2011). Preliminary experience of a modified Maquet technique for repair of cranial cruciate ligament rupture in dogs: *Veterinary and Comparative Orthopaedics and Traumatology*, *24*(3), 223–227.

Evans, H. E., & Lahunta, A. de. (2013a). Arthrology. *Miller's Anatomy of the Dog* (4th ed., pp. 158–184). Saint Louis: Elsevier Health Sciences.

Evans, H. E., & Lahunta, A. de. (2013b). The Skeleton. *Miller's Anatomy of the Dog* (4th ed., pp. 80–157). Saint Louis: Elsevier Health Sciences.

Evans, H. E., & Lahunta, A. de. (2013c). The Heart and Arteries. *Miller's Anatomy of the Dog* (4th ed., pp. 428–504). Saint Louis: Elsevier Health Sciences.

Fulkerson, J. P. (2002). Diagnosis and treatment of patients with patellofemoral pain. *The American Journal of Sports Medicine*, *30*(3), 447–456.

Gielen, I., Saunders, J., Ryssen, B. van, & Bree, H. van. (2011). Computed Tomography of the Stifle. In P. Muir (Ed.), *Advances in the Canine Cranial Cruciate Ligament* (pp. 123–133). John Wiley & Sons.

Gnudi, G., & Bertoni, G. (2001). Echographic Examination of the Stifle Joint Affected by Cranial Cruciate Ligament Rupture in the Dog. *Veterinary Radiology & Ultrasound*, *42*(3), 266–270.

Griffon, D. J. (2010). A Review of the Pathogenesis of Canine Cranial Cruciate Ligament Disease as a Basis for Future Preventive Strategies. *Veterinary Surgery*, *39*(4), 399–409.

Guadagni, J. R., & Drummond, D. S. (1986). Strength of surgical wire fixation. A laboratory study. *Clinical Orthopaedics and Related Research*, (209), 176–181.

Guastella, D. B., Fox, D. B., & Cook, J. L. (2008). Tibial plateau angle in four common canine breeds with cranial cruciate ligament rupture, and its relationship to meniscal tears. *Veterinary and Comparative Orthopaedics and Traumatology: V.C.O.T*, *21*(2), 125–128.

Gyger, O., Botteron, C., Doherr, M., Zurbriggen, A., Schawalder, P., & Spreng, D. (2007). Detection and distribution of apoptotic cell death in normal and diseased canine cranial cruciate ligaments. *Veterinary Journal (London, England: 1997)*, *174*(2), 371–377.

Harnroongroj, T. (1998). Twist knot cerclage wire: the appropriate wire tension for knot construction and fracture stability. *Clinical Biomechanics*, *13*(6), 449–451.

Hayashi, K., Frank, J. D., Dubinsky, C., Hao, Z., Markel, M. D., Manley, P. A., & Muir, P. (2003). Histologic Changes in Ruptured Canine Cranial Cruciate Ligament. *Veterinary Surgery*, *32*(3), 269–277.

Hayes, G. M., Granger, N., Langley-Hobbs, S. J., & Jeffery, N. D. (2013). Abnormal reflex activation of hamstring muscles in dogs with cranial cruciate ligament rupture. *The Veterinary Journal*, *196*(3), 345–350.

Hayes, G. M., Reynolds, D., Moens, N. M. M., Singh, A., Oblak, M., Gibson, T. W. G., Brisson, B. A., et al. (2014). Investigation of Incidence and Risk Factors for Surgical Glove Perforation in Small Animal Surgery. *Veterinary Surgery*, *43*(4), 400–404.

Heffron, L. E., & Campbell, J. R. (1978). Morphology, histology and functional anatomy of the canine cranial cruciate ligament. *The Veterinary Record*, *102*(13), 280–283.

Henderson, R. A., & Milton, J. L. (1978). The tibial compression mechanism: a diagnostic aid in stifle injuries. *Journal American Animal Hospital Association*, *14*, 474–479.

Herrenbruck, T. M., Mullen, D. J., & Parker, R. (2001). Operative Management of Patellofemoral Pain With Degenerative Arthrosis. *Sports Medicine and Arthroscopy Review*, *9*(4), 312–324.

Hoffmann, D. E., Miller, J. M., Ober, C. P., Lanz, O. I., Martin, R. A., & Shires, P. K. (2006). Tibial tuberosity advancement in 65 canine stifles. *Veterinary and Comparative Orthopaedics and Traumatology: V.C.O.T*, *19*(4), 219–227.

Hulse, D. A., Michaelson, F., Johnson, C., & Abdelbaki, Y. Z. (1980). A Technique for Reconstruction of the Anterior Cruciate Ligament in the Dog: Preliminary Report. *Veterinary Surgery*, *9*(4), 135–140.

Imwinkelried, T. (2007). Mechanical properties of open-pore titanium foam. *Journal of Biomedical Materials Research Part A*, *81A*(4), 964–970.

Inauen, R., Koch, D., Bass, M., & Haessig, M. (2009). Tibial tuberosity conformation as a risk factor for cranial cruciate ligament rupture in the dog. *Veterinary and Comparative Orthopaedics and Traumatology: V.C.O.T*, *22*(1), 16–20.

Jaegger, G., & Budsberg, S. C. (2011). Medical Therapy for Stifle Arthritis. In P. Muir (Ed.), *Advances in the Canine Cranial Cruciate Ligament* (pp. 241–245). John Wiley & Sons.

Jaegger, G., Marcellin-Little, D. J., & Levine, D. (2002). Reliability of goniometry in Labrador Retrievers. *American Journal of Veterinary Research*, *63*(7), 979–986.

Jasty, M., Bragdon, C., Burke, D., O'connor, D., Lowenstein, J., & Harris, W. H. (1997). In Vivo Skeletal Responses to Porous-Surfaced Implants Subjected to Small Induced Motions*. *The Journal of Bone & Joint Surgery*, *79*(5), 707–14.

Jasty, M., Bragdon, C. R., Zalenski, E., O'Connor, D., Page, A., & Harris, W. H. (1997). Enhanced stability of uncemented canine femoral components by bone ingrowth into the porous coatings. *The Journal of Arthroplasty*, *12*(1), 106–113.

Johnston, S. A., von Pfeil, D. J. F., Déjardin, L., Weh, M., & Roe, S. C. (2012). Internal Fracture Fixation. In K. M. Tobias & S. A. Johnston (Eds.), *Veterinary Surgery: Small Animal* (pp. 576–607). Saint Louis: Elsevier Saunders.

Jones, S. C., Kim, S. E., Banks, S. A., Conrad, B. P., Abbasi, A. Z., Tremolada, G., Lewis, D. D., et al. (2014). Accuracy of noninvasive, single-plane fluoroscopic analysis for measurement of three-dimensional femorotibial joint poses in dogs. *American Journal of Veterinary Research*, *75*(5), 477–485.

Kienapfel, H., Sprey, C., Wilke, A., & Griss, P. (1999). Implant fixation by bone ingrowth. *The Journal of Arthroplasty*, *14*(3), 355–368.

Kim, S. E., Pozzi, A., Banks, S. A., Conrad, B. P., & Lewis, D. D. (2009). Effect of Tibial Plateau Leveling Osteotomy on Femorotibial Contact Mechanics and Stifle Kinematics. *Veterinary Surgery*, *38*(1), 23–32.

Kim, S. E., Pozzi, A., Kowaleski, M. P., & Lewis, D. D. (2008). Tibial Osteotomies for Cranial Cruciate Ligament Insufficiency in Dogs. *Veterinary Surgery*, *37*(2), 111–125.

Kobayashi, S., Baba, H., Uchida, K., Negoro, K., Sato, M., Miyazaki, T., Nomura, E., et al. (2006). Microvascular system of anterior cruciate ligament in dogs. *Journal of Orthopaedic Research*, *24*(7), 1509–1520.

Korvick, D. L., Pijanowski, G. J., & Schaeffer, D. J. (1994). Three-dimensional kinematics of the intact and cranial cruciate ligament-deficient stifle of dogs. *Journal of Biomechanics*, *27*(1), 77–87.

Kowaleski, M. P., Boudrieau, R. J., & Pozzi, A. (2012). Stifle Joint. In K. M. Tobias & S. A. Johnston (Eds.), *Veterinary Surgery: Small Animal* (pp. 906–998). Saint Louis: Elsevier Saunders.

Krayer, M., Rytz, U., Oevermann, A., Doherr, M. G., Forterre, F., Zurbriggen, A., & Spreng, D. E. (2008). Apoptosis of ligamentous cells of the cranial cruciate ligament from stable stifle joints of dogs with partial cranial cruciate ligament rupture. *American Journal of Veterinary Research*, *69*(5), 625–630.

Lafaver, S., Miller, N. A., Stubbs, W. P., Taylor, R. A., & Boudrieau, R. J. (2007). Tibial Tuberosity Advancement for Stabilization of the Canine Cranial Cruciate Ligament-

Deficient Stifle Joint: Surgical Technique, Early Results, and Complications in 101 Dogs. *Veterinary Surgery*, *36*(6), 573–586.

Lazar, T. P., Berry, C. R., Dehaan, J. J., Peck, J. N., & Correa, M. (2005). Long-Term Radiographic Comparison of Tibial Plateau Leveling Osteotomy Versus Extracapsular Stabilization for Cranial Cruciate Ligament Rupture in the Dog. *Veterinary Surgery*, *34*(2), 133–141.

Lewis, B. A., Allen, D. A., Henrikson, T. D., & Lehenbauer, T. W. (2008). Computed tomographic evaluation of the canine intercondylar notch in normal and cruciate deficient stifles. *Veterinary and Comparative Orthopaedics and Traumatology: V.C.O.T*, *21*(2), 119–124.

Lim, L., Bobyn, J. D., Bobyn, K. M., Lefebvre, L.-P., & Tanzer, M. (2012). The Otto Aufranc Award: Demineralized Bone Matrix Around Porous Implants Promotes Rapid Gap Healing and Bone Ingrowth. *Clinical Orthopaedics and Related Research®*, *470*(2), 357–365.

Lorenz, N. D., & Pettitt, R. (2014). Cranial tibial plating in the management of failed tibial tuberosity advancement in four large breed dogs. *Veterinary and Comparative Orthopaedics and Traumatology: V.C.O.T*, *27*(3), 236–242.

Manley, P. A. (2011). Intra-articular Stabilization. In P. Muir (Ed.), *Advances in the Canine Cranial Cruciate Ligament* (pp. 189–193). John Wiley & Sons.

Maquet, P. (1976). Advancement of the tibial tuberosity. *Clinical Orthopaedics and Related Research*, (115), 225–230.

Maquet, P. (1979). Mechanics and osteoarthritis of the patellofemoral joint. *Clinical Orthopaedics and Related Research*, (144), 70–73.

Mendes, D. G., Soudry, M., & Iusim, M. (1987). Clinical assessment of Maquet tibial tuberosity advancement. *Clinical Orthopaedics and Related Research*, (222), 228–238.

Meyer, D. C., Ramseier, L. E., Lajtai, G., & Nötzli, H. (2003). A new method for cerclage wire fixation to maximal pre-tension with minimal elongation to failure. *Clinical Biomechanics*, *18*(10), 975–980.

Miyatsu, M., Atsuta, Y., & Watakabe, M. (1993). The physiology of mechanoreceptors in the anterior cruciate ligament. An experimental study in decerebrate-spinalised animals. *Journal of Bone & Joint Surgery, British Volume*, *75-B*(4), 653–657.

Montavon, P., Damur, D., & Tepic, S. (2002). Advancement of the tibial tuberosity for the treatment of cranial cruciate deficient canine stifle. *Proceedings of the 1st World Orthopaedic Veterinary Congress* (p. 152). Munich, Germany.

Moore, K., & Read, R. (1995). Cranial cruciate ligament rupture in the dog—a retrospective study comparing surgical techniques. *Australian Veterinary Journal*, *72*(8), 281–285.

Morris, E., & Lipowitz, A. J. (2001). Comparison of tibial plateau angles in dogs with and without cranial cruciate ligament injuries. *Journal of the American Veterinary Medical Association*, *218*(3), 363–366.

Mostafa, A. A., Griffon, D. J., Thomas, M. W., & Constable, P. D. (2009). Morphometric characteristics of the pelvic limbs of Labrador Retrievers with and without cranial cruciate ligament deficiency. *American Journal of Veterinary Research*, *70*(4), 498–507.

Mostafa, A. A., Griffon, D. J., Thomas, M. W., & Constable, P. D. (2010). Morphometric Characteristics of the Pelvic Limb Musculature of Labrador Retrievers with and without Cranial Cruciate Ligament Deficiency. *Veterinary Surgery*, *39*(3), 380–389.

Muir, P. (2011). History and Clinical Signs of Cruciate Ligament Rupture. In P. Muir (Ed.), *Advances in the Canine Cranial Cruciate Ligament* (pp. 101–104). John Wiley & Sons.

Ness, M. G. (2011). *OrthoFoam MMP Wedge For Canine Cruciate Disease*. Huddersfield: Orthomed UK.

Ness, M. G. (2012). *Modified Maquet Procedure, MMP. User Update*. Huddersfield: Orthomed UK.

Ness, M. G. (2013). *MMP Staple Technique For Canine Cruciate Disease*. Huddersfield: Orthomed UK.

Niebauer, G. W., Wolf, B., Bashey, R. I., & Newton, C. D. (1987). Antibodies to canine collagen types i and II in dogs with spontaneous cruciate ligament rupture and osteoarthritis. *Arthritis & Rheumatism*, *30*(3), 319–327.

Noyes, F. R., Delucas, J. L., & Torvik, P. J. (1974). Biomechanics of Anterior Cruciate Ligament Failure: An Analysis of Strain-Rate Sensitivity and Mechanisms of Failure in Primates. *The Journal of Bone & Joint Surgery*, *56*(2), 236–253.

O'Connor, B. L., & Woodbury, P. (1982). The primary articular nerves to the dog knee. *Journal of Anatomy*, *134*(Pt 3), 563–572.

O'donoghue, D. H., Charles a. Rockwood, J., Frank, G. R., Jack, S. C., & Kenyon, R. (1966). Repair of the Anterior Cruciate Ligament in Dogs. *The Journal of Bone & Joint Surgery*, *48*(3), 503–519.

Paatsama, S. (1988). Long-Standing and Traumatic Ligament Injuries and Meniscal Ruptures of the Canine Stifle. *Veterinary Radiology*, *29*(2), 54–56.

Pacchiana, P. D., Morris, E., Gillings, S. L., Jessen, C. R., & Lipowitz, A. J. (2003). Surgical and postoperative complications associated with tibial plateau leveling osteotomy in dogs with cranial cruciate ligament rupture: 397 cases (1998–2001). *Journal of the American Veterinary Medical Association*, *222*(2), 184–193.

Palissery, V., Taylor, M., & Browne, M. (2004). Fatigue characterization of a polymer foam to use as a cancellous bone analog material in the assessment of orthopaedic devices. *Journal of Materials Science: Materials in Medicine*, *15*(1), 61–67.

Patel, P. S., Shepherd, D. E., & Hukins, D. W. (2008). Compressive properties of commercially available polyurethane foams as mechanical models for osteoporotic human cancellous bone. *BMC Musculoskeletal Disorders*, *9*(1), 137.

Piermattei, D. L., Flo, G. L., DeCamp, C. E., & Brinker, W. O. (2006a). The Stifle Joint. *Brinker, Piermattei, and Flo's Handbook of Small Animal Orthopedics and Fracture Repair* (4th ed., pp. 562–632). Saint Louis: Elsevier Saunders.

Piermattei, D. L., Flo, G. L., DeCamp, C. E., & Brinker, W. O. (2006b). Fractures: Classification, Diagnosis, and Treatment. *Brinker, Piermattei, and Flo's Handbook of Small Animal Orthopedics and Fracture Repair* (4th ed., pp. 25–159). Saint Louis: Elsevier Saunders.

Pilliar, R. M., Lee, J. M., & Maniatopoulos, C. (1986). Observations on the effect of movement on bone ingrowth into porous-surfaced implants. *Clinical Orthopaedics and Related Research*, (208), 108–113.

Pond, M. J., & Campbell, J. R. (1972). The canine stifle joint I. Rupture of the anterior cruciate ligament. *Journal of Small Animal Practice*, *13*(1), 1–10.

Pozzi, A., & Cook, J. L. (2011). Meniscal Structure and Function. In P. Muir (Ed.), *Advances in the Canine Cranial Cruciate Ligament* (pp. 29–35). John Wiley & Sons.

Pozzi, A., & Kim, S. E. (2011). Biomechanics of the Normal and Cranial Cruciate Ligament-deficient Stifle. In P. Muir (Ed.), *Advances in the Canine Cranial Cruciate Ligament* (pp. 37–42). John Wiley & Sons.

Pozzi, A., Kowaleski, M. P., Apelt, D., Meadows, C., Andrews, C. M., & Johnson, K. A. (2006). Effect of Medial Meniscal Release on Tibial Translation After Tibial Plateau Leveling Osteotomy. *Veterinary Surgery*, *35*(5), 486–494.

Priddy, N. H., Tomlinson, J. L., Dodam, J. R., & Hornbostel, J. E. (2003). Complications with and owner assessment of the outcome of tibial plateau leveling osteotomy for

treatment of cranial cruciate ligament rupture in dogs: 193 cases (1997–2001). *Journal of the American Veterinary Medical Association*, *222*(12), 1726–1732.

Ragetly, C. A., Griffon, D. J., Mostafa, A. A., Thomas, J. E., & Hsiao-Wecksler, E. T. (2010). Inverse Dynamics Analysis of the Pelvic Limbs in Labrador Retrievers With and Without Cranial Cruciate Ligament Disease. *Veterinary Surgery*, *39*(4), 513–522.

Read, R. A., & Robins, G. M. (1982). Deformity of the proximal tibia in dogs. *The Veterinary Record*, *111*(13), 295–298.

Reif, U., Hulse, D. A., & Hauptman, J. G. (2002). Effect of Tibial Plateau Leveling on Stability of the Canine Cranial Cruciate–Deficient Stifle Joint: An In Vitro Study. *Veterinary Surgery*, *31*(2), 147–154.

Reif, U., & Probst, C. W. (2003). Comparison of tibial plateau angles in normal and cranial cruciate deficient stifles of Labrador retrievers. *Veterinary surgery: VS*, *32*(4), 385–389.

Rey, J., Fischer, M. S., & Böttcher, P. (2014). Sagittal joint instability in the cranial cruciate ligament insufficient canine stifle. Caudal slippage of the femur and not cranial tibial subluxation. *Tierärztliche Praxis. Ausgabe K, Kleintiere/Heimtiere*, *42*(3), 151–156.

Robinson, D. A., Mason, D. R., Evans, R., & Conzemius, M. G. (2006). The Effect of Tibial Plateau Angle on Ground Reaction Forces 4–17 Months After Tibial Plateau Leveling Osteotomy in Labrador Retrievers. *Veterinary Surgery*, *35*(3), 294–299.

Roe, S. C. (1997). Mechanical Characteristics and Comparisons of Cerclage Wires: Introduction of the Double-Wrap and Loop/Twist Tying Methods. *Veterinary Surgery*, *26*(4), 310–316.

Roe, S. C. (2002). Evaluation of tension obtained by use of three knots for tying cerclage wires by surgeons of various abilities and experience. *Journal of the American Veterinary Medical Association*, *220*(3), 334–336.

Roe, S. C. (2003). Internal Fracture Fixation. In D. H. Slatter (Ed.), *Textbook of Small Animal Surgery* (pp. 1798–1818). Elsevier Health Sciences.

Rooks, R. L., Tarvin, G. B., Pijanowski, G. J., & Daly, W. B. (1982). In Vitro Cerclage Wiring Analysis. *Veterinary Surgery*, *11*(2), 39–43.

De Rooster, H., Cox, E., & Bree, H. van. (2000). Prevalence and relevance of antibodies to type-I and -II collagen in synovial fluid of dogs with cranial cruciate ligament damage. *American Journal of Veterinary Research*, *61*(11), 1456–1461.

Rosa, A. L., Crippa, G. E., De Oliveira, P. T., Taba Jr, M., Lefebvre, L.-P., & Beloti, M. M. (2009). Human alveolar bone cell proliferation, expression of osteoblastic phenotype, and matrix mineralization on porous titanium produced by powder metallurgy. *Clinical Oral Implants Research*, *20*(5), 472–481.

Sample, S., Vanderby, R., & Muir, P. (2011). Biomechanics of the Cruciate Ligaments. In P. Muir (Ed.), *Advances in the Canine Cranial Cruciate Ligament* (pp. 13–20). John Wiley & Sons.

Scavelli, T. D., Schrader, S. C., Matthiesen, D. T., & Skorup, D. E. (1990). Partial rupture of the cranial cruciate ligament of the stifle in dogs: 25 cases (1982-1988). *Journal of the American Veterinary Medical Association*, *196*(7), 1135–1138.

Schultz, R. S., Boger, J. W., & Dunn, H. K. (1985). Strength of stainless steel surgical wire in various fixation modes. *Clinical Orthopaedics and Related Research*, (198), 304–307.

Schwandt, C. S., Bohorquez-Vanelli, A., Tepic, S., Hassig, M., Dennler, R., Vezzoni, A., & Montavon, P. M. (2006). Angle between the patellar ligament and tibial plateau in dogs with partial rupture of the cranial cruciate ligament. *American Journal of Veterinary Research*, *67*(11), 1855–1860.

Scrivani, P. (2011). Magnetic Resonance Imaging of the Stifle. In P. Muir (Ed.), *Advances in the Canine Cranial Cruciate Ligament* (pp. 135–142). John Wiley & Sons.

Shirazi-Adl, A., & Mesfar, W. (2007). Effect of tibial tubercle elevation on biomechanics of the entire knee joint under muscle loads. *Clinical Biomechanics*, *22*(3), 344–351.

Simmons, C. A., Valiquette, N., & Pilliar, R. M. (1999). Osseointegration of sintered porous-surfaced and plasma spray-coated implants: An animal model study of early postimplantation healing response and mechanical stability. *Journal of Biomedical Materials Research*, *47*(2), 127–138.

Slocum, B., & Devine, T. (1983). Cranial tibial thrust: a primary force in the canine stifle. *Journal of the American Veterinary Medical Association*, *183*(4), 456–459.

Slocum, B., & Devine, T. (1984). Cranial tibial wedge osteotomy: a technique for eliminating cranial tibial thrust in cranial cruciate ligament repair. *Journal of the American Veterinary Medical Association*, *184*(5), 564–569.

Smith, G. K., & Torg, J. S. (1985). Fibular head transposition for repair of cruciate-deficient stifle in the dog. *Journal of the American Veterinary Medical Association*, *187*(4), 375–383.

Søballe, K., Brockstedt-Rasmussen, H., Hansen, E. S., & Bünger, C. (1992). Hydroxyapatite coating modifies implant membrane formation. *Acta Orthopaedica*, *63*(2), 128–140.

Søballe, K., Hansen, E. S., B.-Rasmussen, H., Jørgensen, P. H., & Bünger, C. (1992). Tissue ingrowth into titanium and hydroxyapatite-coated implants during stable and unstable mechanical conditions. *Journal of Orthopaedic Research*, *10*(2), 285–299.

Stauffer, K. D., Tuttle, T. A., Elkins, A. D., Wehrenberg, A. P., & Character, B. J. (2006). Complications associated with 696 tibial plateau leveling osteotomies (2001-2003). *Journal of the American Animal Hospital Association*, *42*(1), 44–50.

Stein, S., & Schmoekel, H. (2008). Short-term and eight to 12 months results of a tibial tuberosity advancement as treatment of canine cranial cruciate ligament damage. *The Journal of Small Animal Practice*, *49*(8), 398–404.

St-Pierre, J.-P., Gauthier, M., Lefebvre, L.-P., & Tabrizian, M. (2005). Three-dimensional growth of differentiating MC3T3-E1 pre-osteoblasts on porous titanium scaffolds. *Biomaterials*, Dedicated to Canadian Biomaterials Research Dedicated to Canadian Biomaterials Research, *26*(35), 7319–7328.

Szivek, J. A., Thomas, M., & Benjamin, J. B. (1993). Characterization of a synthetic foam as a model for human cancellous bone. *Journal of Applied Biomaterials: An Official Journal of the Society for Biomaterials*, *4*(3), 269–272.

Szivek, J. A., Thompson, J. D., & Benjamin, J. B. (1995). Characterization of three formulations of a synthetic foam as models for a range of human cancellous bone types. *Journal of Applied Biomaterials: An Official Journal of the Society for Biomaterials*, *6*(2), 125–128.

Talaat, M. B., Kowaleski, M. P., & Boudrieau, R. J. (2006). Combination Tibial Plateau Leveling Osteotomy and Cranial Closing Wedge Osteotomy of the Tibia for the Treatment of Cranial Cruciate Ligament-Deficient Stifles with Excessive Tibial Plateau Angle. *Veterinary Surgery*, *35*(8), 729–739.

Tashman, S., Anderst, W., Kolowich, P., Havstad, S., & Arnoczky, S. (2004). Kinematics of the ACL-deficient canine knee during gait: Serial changes over two years. *Journal of Orthopaedic Research*, *22*(5), 931–941.

Tepic, S., Damur, D., & Montavon, P. (2002). Biomechanics of the stifle joint. *Proceedings of the 1st World Orthopaedic Veterinary Congress* (pp. 189–190). Munich, Germany.

Thompson, M. S., McCarthy, I. D., Lidgren, L., & Ryd, L. (2003). Compressive and Shear Properties of Commercially Available Polyurethane Foams. *Journal of Biomechanical Engineering*, *125*(5), 732–734.

Tirgari, M. (1978). The surgical significance of the blood supply of the canine stifle joint. *Journal of Small Animal Practice*, *19*(1-12), 451–462.

Tonks, C. A., Lewis, D. D., & Pozzi, A. (2011). A review of extra-articular prosthetic stabilization of the cranial cruciate ligament-deficient stifle. *Veterinary and Comparative Orthopaedics and Traumatology: V.C.O.T*, *24*(3), 167–177.

Vasseur, P. B. (1984). Clinical Results Following Nonoperative Management for Rupture of the Cranial Cruciate Ligament in Dogs. *Veterinary Surgery*, *13*(4), 243–246.

Vasseur, P. B. (2003). Stifle Joint. In D. H. Slatter (Ed.), *Textbook of Small Animal Surgery* (pp. 2090–2133). Elsevier Health Sciences.

Vasseur, P. B., & Arnoczky, S. P. (1981). Collateral ligaments of the canine stifle joint: anatomic and functional analysis. *American Journal of Veterinary Research*, *42*(7), 1133–1137.

Vasseur, P. B., Pool, R. R., Arnoczky, S. P., & Lau, R. E. (1985). Correlative biomechanical and histologic study of the cranial cruciate ligament in dogs. *American Journal of Veterinary Research*, *46*(9), 1842–1854.

Wähnert, D., Lenz, M., Schlegel, U., Perren, S., & Windolf, M. (2011). Cerclage handling for improved fracture treatment. A biomechanical study on the twisting procedure. *Acta Chirurgiae Orthopaedicae Et Traumatologiae Cechoslovaca*, *78*(3), 208–214.

Warzee, C. C., Dejardin, L. M., Arnoczky, S. P., & Perry, R. L. (2001). Effect of Tibial Plateau Leveling on Cranial and Caudal Tibial Thrusts in Canine Cranial Cruciate–Deficient Stifles: An In Vitro Experimental Study. *Veterinary Surgery*, *30*(3), 278–286.

Wazen, R. M., Lefebvre, L.-P., Baril, E., & Nanci, A. (2010). Initial evaluation of bone ingrowth into a novel porous titanium coating. *Journal of Biomedical Materials Research Part B: Applied Biomaterials*, *94B*(1), 64–71.

Whitehair, J. G., Vasseur, P. B., & Willits, N. H. (1993). Epidemiology of cranial cruciate ligament rupture in dogs. *Journal of the American Veterinary Medical Association*, *203*(7), 1016–1019.

Wilke, V. L., Conzemius, M. G., Besancon, M. F., Evans, R. B., & Ritter, M. (2002). Comparison of tibial plateau angle between clinically normal Greyhounds and Labrador Retrievers with and without rupture of the cranial cruciate ligament. *Journal of the American Veterinary Medical Association*, *221*(10), 1426–1429.

Wilke, V. L., Conzemius, M. G., Kinghorn, B. P., Macrossan, P. E., Cai, W., & Rothschild, M. F. (2006). Inheritance of rupture of the cranial cruciate ligament in Newfoundlands. *Journal of the American Veterinary Medical Association*, *228*(1), 61–64.

Wilke, V. L., Robinson, D. A., Evans, R. B., Rothschild, M. F., & Conzemius, M. G. (2005). Estimate of the annual economic impact of treatment of cranial cruciate ligament injury in dogs in the United States. *Journal of the American Veterinary Medical Association*, *227*(10), 1604–1607.

Wilson, J. W. (1988). Knot strength of cerclage bands and wires. *Acta Orthopaedica*, *59*(5), 545–547.

Wilson, J. W., Belloli, D. M., & Robbins, T. (1985). Resistance of cerclage to knot failure. *Journal of the American Veterinary Medical Association*, *187*(4), 389–391.

Wingfield, C., Amis, A. A., Stead, A. C., & Law, H. T. (2000a). Comparison of the biornechanical properties of rottweiler and racing greyhound cranial cruciate ligaments. *Journal of Small Animal Practice*, *41*(7), 303–307.

Wingfield, C., Amis, A. A., Stead, A. C., & Law, H. T. (2000b). Cranial cruciate stabilitv in the rottweiler and racing greyhound: an in vitro study. *Journal of Small Animal Practice*, *41*(5), 193–197.

Witsberger, T. H., Villamil, J. A., Schultz, L. G., Hahn, A. W., & Cook, J. L. (2008). Prevalence of and risk factors for hip dysplasia and cranial cruciate ligament deficiency in dogs. *Journal of the American Veterinary Medical Association*, *232*(12), 1818–1824.

Yahia, L. H., Newman, N. M., & St-Georges, M. (1992). Innervation of the Canine Cruciate Ligaments. *Anatomia, Histologia, Embryologia*, *21*(1), 1–8.

Yahia, L.-H., & Drouin, G. (1989). Microscopical investigation of canine anterior cruciate ligament and patellar tendon: Collagen fascicle morphology and architecture. *Journal of Orthopaedic Research*, *7*(2), 243–251.

Yakacki, C. M., Griffis, J., Poukalova, M., & Gall, K. (2009). Bearing area: A new indication for suture anchor pullout strength? *Journal of Orthopaedic Research*, *27*(8), 1048–1054.

Annex

Annex 1: Descriptive statistics, one-way ANOVA, and Bonferroni adjustments for the "Displacement at 100 N (mm)" variable

Descriptive

Group	N	Mean	SD	Min	Max
0.8	10	2.866810	0.50517453	1.88475	3.83856
1.0	10	1.432123	0.59658352	0.80425	2.34156
1.2	10	0.758286	0.16887977	0.50425	1.117
1.6	10	0.664737	0.11966465	0.45312	0.84775
2.0	10	0.591187	0.06783312	0.497	0.70369

One-way ANOVA

	Df	Sum Sq	Mean Sq	F value	Pr (>F)
Group	4	36.65	9.162	69.56	<2e-16 ***
Residuals	45	5.93	0.132		

*Signif. codes: 0 '***' 0.001 '**' 0.01 '*' 0.05 '.' 0.1 ' ' 1*

P value adjustment method: bonferroni

	0.8	1.0	1.2	1.6
1.0	2.1e-10	---	---	---
1.2	7.9e-16	0.00145	---	---
1.6	< 2e-16	0.00023	1.00000	---
2.0	< 2e-16	5.0e-05	1.00000	1.00000

Annex 2: Descriptive statistics, one-way ANOVA, and Bonferroni adjustments for the "Displacement at 200 N (mm)" variable

Descriptive

Group	N	N/A	Mean	SD	Min	Max
0.8	4	6	6.896718	0.6709364	5.993	7.56306
1.0	10	0	4.852999	1.0132206	3.4545	6.42494
1.2	10	0	3.031592	0.5944479	1.92925	4.00862
1.6	10	0	1.689780	0.1234661	1.41125	1.87337
2.0	10	0	1.299462	0.1140184	1.07844	1.45375

One-way ANOVA

	Df	Sum Sq	Mean Sq	F value	Pr (>F)
Group	4	140.74	35.19	97.85	<2e-16 ***
Residuals	39	14.02	0.36		

*Signif. codes: 0 '***' 0.001 '**' 0.01 '*' 0.05 '.' 0.1 ' ' 1*

6 observations deleted due to missingness

P value adjustment method: bonferroni

	0.8	1.0	1.2	1.6
1.0	1.1e-05	---	---	---
1.2	2.1e-12	4.1e-07	---	---
1.6	< 2e-16	2.0e-13	0.00012	---
2.0	< 2e-16	5.1e-15	1.2e-06	1.00000

Annex 3: Descriptive statistics, one-way ANOVA, and Bonferroni adjustments for the “Displacement at Failure (mm)” variable

Descriptive

Group	N	Mean	SD	Min	Max
0.8	10	8.110579	0.8647642	6.79187	9.78794
1.0	10	10.944774	0.9623359	9.25444	12.60012
1.2	10	9.741619	0.7342581	8.826	11.25869
1.6	10	3.930449	0.4765045	2.828	4.54131
2.0	10	2.617781	0.2732077	2.09194	2.97875

One-way ANOVA

	Df	Sum Sq	Mean Sq	F value	Pr (>F)
Group	4	529.1	132.3	263	<2e-16 ***
Residuals	45	22.6	0.5		

*Signif. codes: 0 '***' 0.001 '**' 0.01 '*' 0.05 '.' 0.1 ' ' 1*

P value adjustment method: bonferroni

	0.8	1.0	1.2	1.6
1.0	1.6e-10	---	---	---
1.2	5.7e-05	0.0044	---	---
1.6	4.7e-16	< 2e-16	< 2e-16	---
2.0	< 2e-16	< 2e-16	< 2e-16	0.0015

Annex 4: Descriptive statistics, one-way ANOVA, and Bonferroni adjustments for the "Load to Failure (N)" variable

Descriptive

Group	N	Mean	SD	Min	Max
0.8	10	195.8664	15.80165	172.87823	218.90951
1.0	10	319.1573	21.30404	274.7857	342.00237
1.2	10	401.0640	19.50268	360.47273	427.76866
1.6	10	312.4103	15.24895	290.65872	333.85137
2.0	10	314.8144	26.29905	260.14964	339.14526

One-way ANOVA

	Df	Sum Sq	Mean Sq	F value	Pr (>F)
Group	4	214230	53558	133.4	<2e-16 ***
Residuals	45	18073	402		

*Signif. codes: 0 '***' 0.001 '**' 0.01 '*' 0.05 '.' 0.1 ' ' 1*

P value adjustment method: bonferroni

	0.8	1.0	1.2	1.6
1.0	< 2e-16	---	---	---
1.2	< 2e-16	8.1e-11	---	---
1.6	7.6e-16	1	7.3e-12	---
2.0	3.6e-16	1	1.7e-11	1

Annex 5: Descriptive statistics, one-way ANOVA, and Bonferroni adjustments for the "Stiffness (N/mm)" variable

Descriptive

Group	N	Mean	SD	Min	Max
0.8	10	23.92107	2.102791	20.28687104	26.27832047
1.0	10	28.77093	2.385709	24.47027648	31.75475905
1.2	10	37.63954	2.037289	33.26454449	39.70063744
1.6	10	98.26363	13.488184	80.79000097	121.6933683
2.0	10	142.23256	19.933041	120.3381306	187.6040218

One-way ANOVA

	Df	Sum Sq	Mean Sq	F value	Pr (>F)
Group	4	108132	27033	227.7	<2e-16 ***
Residuals	45	5342	119		

*Signif. codes: 0 '***' 0.001 '**' 0.01 '*' 0.05 '.' 0.1 ' ' 1*

P value adjustment method: bonferroni

	0.8	1.0	1.2	1.6
1.0	1.000	---	---	---
1.2	0.072	0.754	---	---
1.6	< 2e-16	< 2e-16	3.6e-15	---
2.0	< 2e-16	< 2e-16	< 2e-16	1.2e-10

Annex 6: Descriptive statistics, one-way ANOVA, and Bonferroni adjustments for the "Yield Load (N)" variable

Descriptive

Group	N	Mean	SD	Min	Max
0.8	10	158	16.865481	130	180
1.0	10	264	18.378732	230	290
1.2	10	324	14.298407	310	350
1.6	10	213	4.830459	210	220
2.0	10	216	12.649111	200	230

One-way ANOVA

	Df	Sum Sq	Mean Sq	F value	Pr (>F)
Group	4	155360	38840	192.3	<2e-16 ***
Residuals	45	9090	202		

*Signif. codes: 0 '***' 0.001 '**' 0.01 '*' 0.05 '.' 0.1 ' ' 1*

P value adjustment method: bonferroni

	0.8	1.0	1.2	1.6
1.0	< 2e-16	---	---	---
1.2	< 2e-16	3.1e-11	---	---
1.6	3.9e-10	3.2e-09	< 2e-16	---
2.0	8.4e-11	1.6e-08	< 2e-16	1

Annex 7: Samples after testing

Group 0.8 (left) and group 1.0 (right), implant failure occurred in every case.

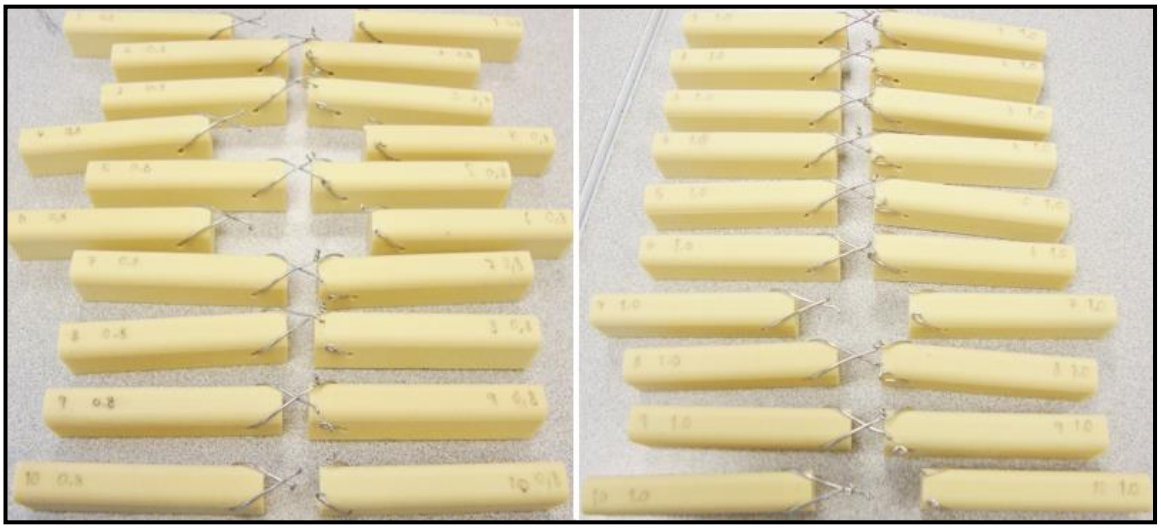

Group 1.2 (left), group 1.6 middle, and group 2.0 (right), block failure occurred in every case.

Annex 8: Load to failure values, respective wire diameters, and knot features reported in several biomechanical studies using unbent twist knots.

	No. knots	*Pattern*	*No. Twists*	*Cut*	*Ø (mm)*	*LTF (N)*	*LTF×0.75*
Wilson et al., 1985	Single	No loop	Three or approx. 5 mm length	Yes	0.8	311 ± 13.8	≈ 233
					1.0	478 ± 19.3	≈ 359
					1.2	711 ± 16.3	≈ 533
Guadgani and Drummond, 1986	Single	Loop	Two	Yes	1.0	516 ± 6	≈ 387
					1.2	≈ 700	≈ 525
	Two		**N/A**	**N/A**	**1.0**	**396 ± 9**	**-**
Bostrom et al., 1994	Single	Loop	N/A	N/A	1.0	480 ± 18	≈ 360
Meyer et al., 2003	Single	No loop	Six	By twisting	1.0	≈ 200	≈ 150
					1.2	≈ 300	≈ 225
Etchepareborde et al., 2010	**Two**	**Figure-of-eight**	**Two**	**Yes**	**1.0**	**613 ± 77**	**-**

Annex 9: Yield load values, respective wire diameters, and knot features reported in several biomechanical studies using unbent twist knots.

	No. knots	*Pattern*	*No. Twists*	*Cut*	*Ø (mm)*	*LTF (N)*
Schultz et al., 1985	Single	Figure-of-eight	Five	Yes	0.8	≈ 225
					1.0	≈ 325
Wilson, 1988	Single	No loop	Three or approx. 5 mm length	Yes	0.8	224 ± 23
					1.0	323 ± 24
					1.2	550 ± 17
Guadgani and Drummond, 1986	Single	Loop	N/A	N/A	1.0	400-450
Blass et al., 1986	Single	Loop	Three	Yes	1.0	≈ 546
Roe, 1997	Single	Loop	Two to Three	Yes	1.0	189.2 ± 22